

# **Lignin in Suspended Particulate Matter in the Albemarle-Pamlico Estuarine System During the 2018 Hurricane Season**

By:

Ariana A. Donini Rivera

July 2022

Director of Thesis: Dr. Siddhartha Mitra

Major Department: Geological Sciences

## **ABSTRACT**

During the 2018 Atlantic hurricane season, North Carolina (NC) was adversely impacted by two major storms: Hurricanes Florence and Michael. Combined, these storms dropped more than 900 mm of precipitation across the entire state and caused flooding along the coast. While both Florence and Michael impacted North Carolina, Hurricane Florence had the greatest impact on coastal NC, which is the focus of this study.

This study quantifies particulate lignin, a marker for vascular plants, in water samples collected within the Albemarle Pamlico Estuary System (APES) and coastal ocean adjacent to North Carolina to determine if precipitation during the 2018 hurricane season increased suspended sediments and terrigenous organic matter concentrations in the APES system. Lignin monomers were quantified on glass fiber filters (GFF) using cupric oxide oxidation on samples collected from the APES and the coastal ocean during two time periods: October and November

2018 (~ 6 – 11 weeks post-Florence), and again in July of 2019 (no storm activity). This research allowed for an understanding of the impact of Hurricane Florence, which was one of the largest storms during the 2018 Hurricane Season, on mobilization of terrigenous organic matter into the Albemarle-Pamlico Estuary system.

Lignin concentrations in estuarine and coastal suspended sediments in October and November 2018 ( $14.34 \pm 32.40 \text{ mg g}^{-1}$ ) were considerably higher than estuarine and coastal lignin concentrations in July 2019 ( $0.34 \pm 0.36 \text{ mg g}^{-1}$ ). Estuarine samples generally had higher lignin concentrations compared to coastal NC samples. Lignin monomer ratios [acid : aldehyde (Ad/Al), syringyl to vanillyl (S/V), and cinnamyl to vanillyl (C/V)] were used to determine the sources of terrestrial organic matter into the system as well as the extent of degradation. Based on these, suspended sediments in the 2018 samples consisted of both angiosperm and gymnosperm sources. In contrast, the 2019 suspended sediment samples were solely derived from non-woody angiosperm sources. Generally, lignin on suspended sediments in 2018 was a combination of fresh and highly degraded plant material while in 2019, it was degraded. Samples elevated in the gymnosperm signal only occurred in 2018 and were “fresh” as indicated by lignin acid-aldehyde ratios  $< 0.8$ , while samples elevated in angiosperm tissue, found in both 2018 and 2019, were degraded, indicating that the input is coming from both the erosional deposition of gymnosperm vascular plants and the resuspension of already-present sediments. This study suggests that flooding, erosion, and resuspension associated with the 2018 hurricane season did directly affect the concentration of lignin in North Carolina estuarine and coastal systems.



Quantifying Lignin in Suspended Particulate Matter in the Albemarle-  
Pamlico Estuarine System During the 2018 Hurricane Season

A Thesis

Presented to the Faculty of the Department of Geological Sciences  
East Carolina University

In Partial Fulfillment of the Requirements for the Degree  
Masters of Science in Geology

By

Ariana A. Donini Rivera

July 2022

© Ariana A. Donini Rivera, 2022

Quantifying Lignin in Suspended Particulate Matter in the Albemarle-  
Pamlico Estuarine System During the 2018 Hurricane Season

By

Ariana A Donini Rivera

APPROVED BY: \_\_\_\_\_

DIRECTOR OF THESIS: \_\_\_\_\_  
Siddhartha Mitra, Ph. D.

COMMITTEE MEMBER: \_\_\_\_\_  
David Mallinson, Ph. D.

COMMITTEE MEMBER: \_\_\_\_\_  
Stephen Moysey, Ph. D.

COMMITTEE MEMBER: \_\_\_\_\_  
Reide Corbett, Ph. D.

CHAIR OF THE DEPARTMENT  
OF GEOLOGICAL SCIENCES: \_\_\_\_\_  
Eric Horsman, Ph. D.

INTERIM DEAN OF  
THE GRADUATE SCHOOL: \_\_\_\_\_  
Kathleen T Cox, Ph. D.

## **DEDICATION**

To my mother, Claudia, my grandparents, Carole, and Frank Donini, and my stepfather Donald Callahan. You have never failed to support me in everything that I've ever wanted to do. Thank you for your consistent encouragement.

## Table of Contents

LIST OF TABLES	vi
LIST OF FIGURES	vii
I. INTRODUCTION	1
II. BACKGROUND	5
1. The 2018 Hurricane Season	5
2. The Albemarle Pamlico Estuary System	6
3. Outer Banks and Inlets	10
4. Lignin	12
5. Wave Driven Resuspension	14
6. Storm Derived Disturbances	16
6.1 Indicators of Storm Derived Disturbances	17
III. METHODS	22
1. Sample Collection and Preparation	22
2. Lignin Isolation	24
IV. RESULTS	28
1. Salinity and Suspended Sediment	28
2. Lignin Concentration	33
3. Lignin Monomers in Suspended Sediment	38

4. Lignin Interclass Ratios	44
4.1 S/V and C/V Ratios	44
4.2 Acid – Aldehyde Ratios	44
V. DISCUSSION	48
1. Salinity and Suspended Sediment	48
2. Pre- and Post-storm Lignin Abundances	54
3. Lignin Monomers in Suspended Sediment	57
3.1 Monomer Subclass	57
3.2 Interclass Ratios	58
4. Limitations and Future Directions	60
VI. CONCLUSION	61
VII. CITATIONS	63
Appendix A. L <sub>8</sub> , V, S and C concentrations	75
Appendix B. Sample Filtration Data	77
Appendix C. Percent difference in similar stations	83
Appendix D. Conceptual Model	84

## List of Tables

1	2018 Atlantic Hurricanes	5
2	Table from Simmons (1976) Basin Data	19
3	Monomers, Retention Time, Target & Reference Ions	25
4	2018 Salinity and TSS	31
5	2019 Salinity and TSS	32
6	2018 L <sub>8</sub> , S/V, C/V & Ad/Al	35
7	2019 L <sub>8</sub> , S/V, C/V & Ad/Al	36
8	Data Similar to this study	56

## List of Figures

1	Map showing Albemarle-Pamlico Estuary and inlets	2
2	NASA satellite image showing flooding from Florence	3
3	River basins that flow into APES	7
4	Proximity of Capes Henry, Hatteras, and Lookout	10
5	Lignin phenylpropane units	12
6	Lignin products of cupric oxide oxidation	13
7	Cathelot <i>et al.</i> S/V to C/V ratios	15
8	Station locations	23
9	TSS and salinity graph	29
10	TSS and salinity graph showing individual filter sizes	30
11	L <sub>8</sub> and salinity graph	34
12	L <sub>8</sub> and TSS	37
13	Vanillyl Phenol Concentrations	41
14	Syringyl Phenol Concentrations	42
15	Cinnamyl Phenol Concentrations	43
16	S/V and C/V ratios	46
17	Acid-aldehyde ratios	47
18	Average daily wind speeds	50
19	Fort Barnwell discharge	51
20	Barrier island vegetation zone	53

## I. INTRODUCTION

Extreme weather events (EWE) have topped the list of the World Economic Forum's most significant risks facing humanity since 2015 (World Economic Forum: The global risks report 2021). The World Meteorological Organization's Atlas of Mortality and Economic Losses from Weather, Climate and Water Extremes (2021) shows that disasters related to weather, water, or climatic hazards account for 50% of all disasters, 45% of reported deaths and 74% of reported economic losses. This equates to a little over 2 million deaths and \$3.6 trillion in economic loss, worldwide between 1970 and 2019 (World Meteorological Organization, 2021).

In the United States, Hurricane season spans six months – June through November. Between 1851 and 2019, 298 hurricanes and over 362 tropical storms have made landfall on mainland USA (NOAA, 2020). Since 1965, there have been 56 storms, ranging from tropical storms to category 5 hurricanes, that have each caused over \$1 billion in damages (NOAA, 2021). From 1851 to 2021, 387 hurricanes and tropical storms have impacted North Carolina, and of those 84 storms have made landfall (North Carolina Climate Office, 2022.).

Excess organic material contributes to changes in water quality, carbon budgets, and heterotrophic bioavailability within coastal ecosystems (Paerl et al., 2018). EWE, including tropical storms and hurricanes, can contribute much of the annual organic carbon loading in coastal watersheds. Moreover, they can transmit massive amounts of terrestrial organic matter into coastal and marine ecosystems in relatively short amounts of time (Yan *et al.*, 2020). Such events are expected to intensify in the coming years due to climate change (Knutson et al., 2015; Trenberth et al., 2018), with recent models showing that the frequency of very intense hurricanes (Category 4 and 5) in the western Atlantic between 20° – 40° N are expected to double by the turn of the century (Bender *et al.*, 2010). Across the globe, there has been a 12% increase in

record breaking rainfall between 1981 – 2010, which correlates with rising temperatures (Lehmann, *et al.*, 2015). Coastal storm events cause flooding, and subsequent soil erosion leading to an influx of nutrients and allochthonous organic material into the estuary (Paerl *et al.*, 2001).

Hurricane Florence (2018) was one of the wettest storms on record for the United States (Erdman, 2018). In September of 2018, Hurricane Florence (Category 1 on the Saffir-Simpson scale) deposited  $\sim 3.0 \times 10^{13}$  L of water on the Carolinas (Moody, 2018), with some areas receiving more than 90 cm of rain (Kunkel & Champion, 2019), and wind gusts reaching up to 106 mph (National Weather Service, 2018). Extreme precipitation, flooding, and storm surges along the coast can cause

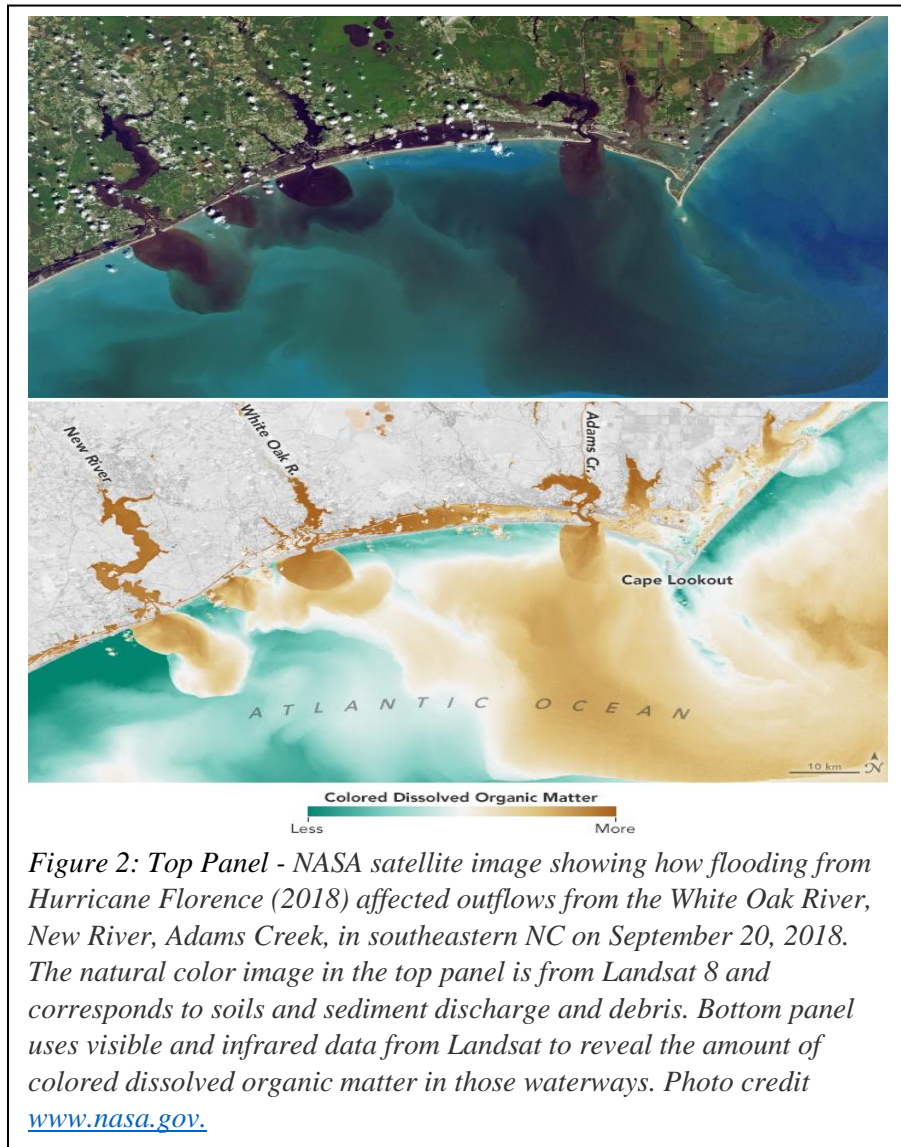
the shoreline to erode, and deposit large amounts of sediment into the estuary and ocean (Paerl *et al.* 2006). The excessive rainfall from the hurricane initially mobilized suspended sediments and colored dissolved organic matter (CDOM) into the Atlantic Ocean from rivers and streams in



Figure 1: Map showing Albemarle-Pamlico Sound and the Oregon Inlet, Hatteras Inlet, and Ocracoke Inlet which connects the Sound to the open ocean. Photo credit [www.nasa.gov](http://www.nasa.gov).

southeastern NC (NASA.gov, 2018). Consequently, Hurricane Florence may have also caused a pulse of suspended sediment from coastal NC soils into the Albemarle-Pamlico Estuary System (APES) and ultimately into the Atlantic Ocean via the Ocracoke, Oregon, or Hatteras inlets (Figure 1). Soil-derived nutrient loads from flooding may contain contaminants and runoff from agricultural and urban land (Osburn *et al.*, 2016). These contaminants may be harmful to aquatic life as they can accelerate primary production, which can lead to an increase in algal blooms, followed by hypoxia, and fish kills. Consequently, excess nutrients from runoff may cause an overall decline in habitat quality and estuarine condition (Paerl *et al.*, 2006). Determining how pulses of storm-driven organic matter (Figure 2) impact estuarine waters is critical to understanding how current and future climate change may affect the coastal carbon cycle.

One component of terrestrial organic matter found in soil-derived suspended sediments is lignin. Lignin is a stable,



complex phenolic polymer that is crucial for vascular plant life (Hedges & Mann, 1979). Lignin is a fundamental component of the tissues of vascular plants and is the second most abundant terrestrial biopolymer, making up nearly one-third of the biosphere's organic carbon (Hedges & Mann, 1979; Boerjan *et al.*, 2003). Lignin decomposes at a slower rate than other organic macromolecules found in plants (e.g., cellulose, hemi-cellulose), which makes it abundant in terrestrial soils (Killops and Killops, 1993). The high quantity of lignin in terrestrial soils makes it a reliable biomarker for terrestrial organic matter entering the ocean (Hedges *et al.*, 1997).

The primary goal of this research is to gain a better understanding of the impacts of storms on organic matter transport into the estuary and coastal ocean by analyzing and quantifying lignin in storm-derived suspended sediments, specifically associated with the 2018 Hurricane Season. *I hypothesized that in contrast to non-storm periods (i.e., July 2019 precipitation conditions), precipitation caused by Hurricane Florence led to an increased concentration of suspended sediments and associated terrigenous organic matter into the APES and adjacent continental shelf that can be seen within the immediate two months after the storm season. No other studies have examined both estuarine and coastal samples during storm and non-storm periods within this system.*

## II. BACKGROUND

### 1. The 2018 Hurricane Season

The 2018 Hurricane Season consisted of 37 tropical storms and hurricanes between the Atlantic and Eastern Pacific oceans (NOAA, 2020). The Atlantic Basin experienced 15 storms in 2018, eight of these being hurricanes, making the 2018 hurricane season busier than an average hurricane season which yields 14 named storms per year (NCDC NOAA, 2019). The total damage from the 2018 storm season is estimated to be around \$91 billion (NOAA, 2021). Nearly half of these damages stemmed from four Atlantic hurricanes that made landfall in 2018 (Table 1). These four storms totaled over \$40.3 billion in damages, with damage from Hurricane Florence causing >50% of these total costs (Table 1).

At its strongest, Hurricane Florence was a Category 4 hurricane, but decreased to a Category 1 before making landfall on September 14, 2018, near Wrightsville Beach, NC. Wind gusts associated with the storm were as high as 105 mph, with sustained winds reaching up to 90 mph upon landfall (Paul *et al.*, 2019). The storm's movement slowed significantly upon landfall, moving ~6 mph and causing record-breaking regional rainfall (Table 1) as it travelled a southwest across the southeastern US (Kunkel & Champion, 2019 & Paul *et al.*, 2019). Over 900 mm of rain fell in the four-day period following landfall (Kunkel & Champion, 2019). Hurricane Florence caused massive amounts of flooding on North Carolina's coasts (NC DEQ, 2019), and

*Table 1. Atlantic Hurricanes During the 2018 Hurricane Season*

Storm Name	Saffir-Simpson Category	Amount of Rainfall (mm)	State in which storm made landfall	Cost of Damages (USD)	Total Deaths
Alberto	TS	313	FL	\$125 million	12
Florence	4	912	NC	\$24 billion	53
Gordon	TS	323	FL	≥ \$200 million	3
Michael	5	330	FL	\$16 billion	16

along the Cape Fear, Neuse, and Lumberton Rivers where industrial waste sites such as hog lagoons and coal ash pits are located (Paul *et al.*, 2019). The North Carolina Department of Environmental Quality indicated that 32 lagoons released waste due to flooding, and five lagoons experienced structural damage specifically due to Hurricane Florence (Paul *et al.*, 2019). This abundance of rainfall and the subsequent flooding, leading to soil erosion, likely contributed to increased suspended sediment discharge within the APES (Figure 3).

The severity of coastal erosion depends on the magnitude of the storm event, the sequence and timing of storms as well as the initial conditions of the shoreline (Phillips, 1999). Excessive coastal erosion associated with these storms can introduce terrestrial organic matter into the system. Terrestrial organic matter may change the quantity of light within the system and may also lead to eutrophication due to an excess input of nutrients within the system (Deininger & Frigstad, 2019).

## **2. The Albemarle-Pamlico Estuary System**

In North Carolina, there are more than 17,000 km of estuarine shoreline, consisting primarily of marsh and swamp forest (NC DEQ, 2015). The shorelines of an estuary are dynamic, with accretion and erosion being impacted by sea-level rise, shoreline orientation, wind energy, storms, tides, and waves (Eulie *et al.*, 2015). The Albemarle-Pamlico Estuarine system is the largest lagoonal estuary and second largest estuary in the United States. The system is a drowned river estuary that is relatively shallow, with an average depth of ~5 m, a maximum depth of 7.3 m, and a total surface area of ~6,500 km<sup>2</sup> (Giese *et al.*, 1979, Wells & Kim, 1989). The watershed is ~73,000 km<sup>2</sup> spanning from the Piedmont to the Coastal Plain of North Carolina and Virginia (Giese *et al.*, 1979). It consists of six river basins, the Pasquotank,

Chowan, and Roanoke that flow through swampy, forested plains into the Albemarle Sound, the Tar-Pamlico and Neuse Basins that flow into the Pamlico Sound, and the White Oak basin (Figure 4) that flows into the southernmost portion of the Sound (“The Albemarle Pamlico Region”, n.d.). The Roanoke River makes up more than half of the Albemarle Estuarine systems’ drainage, with an average flow of  $238 \text{ m}^3 \text{ s}^{-1} \text{ d}^{-1}$  (Riggs, 1996). The Albemarle and Pamlico Sounds are connected by two smaller sounds, the Croatan, and Roanoke (Roelofs & Bumpus, 1952, Giese *et al.*, 1979).

The APES is separated from the Atlantic Ocean by the Outer Banks barrier-island chain (Figure 3) and is connected to the ocean via Ocracoke, Hatteras, and Oregon inlets (Figure 1). The system has an average flushing time of 11 months (Giese *et al.*, 1979), high primary productivity, low tidal activity and salinities ranging from 3 ppt in portions of the Currituck

Sound and around 20 ppt closest to the inlets in the Pamlico Sound (Giese *et al.*, 1979).

The system is a key contributor to North Carolina’s economy: the APES is an ideal nursery for crabs, shrimp, and many

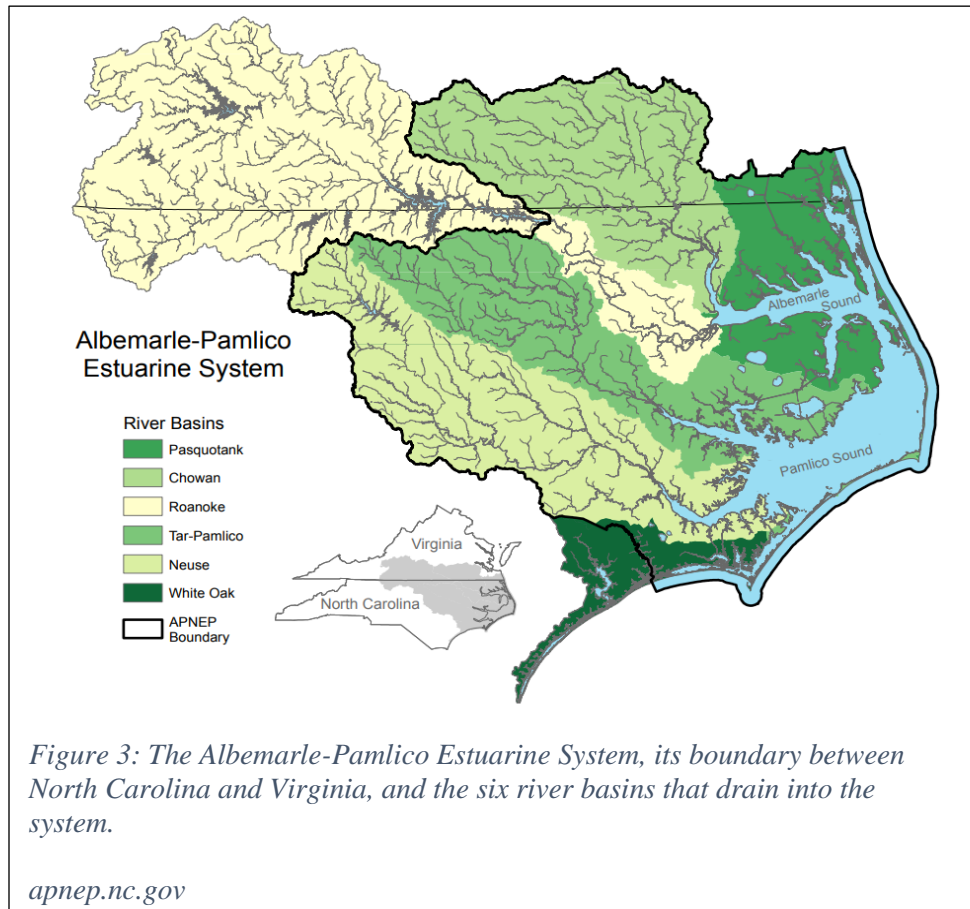


Figure 3: The Albemarle-Pamlico Estuarine System, its boundary between North Carolina and Virginia, and the six river basins that drain into the system.

[apnep.nc.gov](http://apnep.nc.gov)

fish species and make it an important location for both recreational and commercial fishing (Giese *et al.*, 1979).

Samples within this study were taken within the northern portion of the Pamlico Sound and the southernmost portion of the Albemarle Sound. These sounds, and their surrounding estuaries, are drowned river valleys, with low velocities of freshwater inflow (Giese *et al.*, 1985). The Pamlico Sound is the largest sound on the east coast, covering ~3,315 km<sup>2</sup> and containing 26 million m<sup>3</sup> of water (Giese *et al.*, 1985). The Tar-Pamlico River system drains a total of 11,137 km<sup>2</sup> with an average annual discharge of 153 m<sup>3</sup> s<sup>-1</sup> (Giese *et al.*, 1985). The lack of connection to the ocean leads to an astronomical tidal influence <10 cm (Giese *et al.*, 1985). Research by Jia and Li (2012) show that circulation within the Albemarle and northern Pamlico Sounds are driven by winds, while circulation in the southern Pamlico Sound is driven by both wind and gravitational force.

Organic and inorganic material enter the Pamlico Sound via river discharge, coastal or riverine erosion, nearby marshes, *in situ* production, or erosion and transport from the continental shelf. Much of the land within the watershed is either urban, forested, or used for crops including corn, tobacco, and soybeans (Mattson *et al.*, 1983). Surrounding saltmarshes contain cordgrasses, and black needlerush. Muddy sediments are found in > 90% of the system while sandy sediments within the system are found in areas where water is less than 2 – 3 m deep (Mattson *et al.*, 1983). The most common types of shorelines surrounding the Pamlico Sound are sediment bank (33.9%), marsh (31.4%), modified shoreline (27.4%) and swamp forest (7.3%) (Eulie *et al.*, 2018). Research done by Eulie *et al.* (2018) found that over a ten-year period, a change in shore type has occurred over more than one-quarter of the Tar-Pamlico shoreline. During the one decade measuring period, approximately 70% of shorelines that had

not been modified were eroding while ~28% of shorelines were accumulating sediment. All wetland shorelines were eroding to some extent. Wetland erosion sediment contribution is estimated to be  $6.3 \times 10^4$  tons per year coming from ~219 km of shoreline, while river input accounts for  $9.6 \times 10^4$  tons of sediment per year (~43% and ~57% of sediment, respectively) (Eulie *et al.*, 2018). Total fine sediment (grain-size  $<63 \mu\text{m}$ ) storage is  $1.6 \times 10^5$  tons per year, which is ~93% of the total sediment contributed to the system, with a remaining  $3.0 \times 10^3$  tons of sediment per year (~7%) transported from the Tar-Pamlico estuary to the adjoining Pamlico Sound (Eulie *et al.*, 2018).

The Albemarle estuarine system (AES) consists of the Albemarle Sound and three tributaries: the Alligator River, the North River, and the Pasquotank River, as well as the Currituck, Croatan, and Roanoke Sounds (Giese *et al.*, 1985). The Albemarle Sound is ~1,250  $\text{km}^2$ , with a total drainage area of ~46,000  $\text{km}^2$  (Giese *et al.*, 1985). The system is dominated by the inflow of fresh water and has no connection to the Atlantic Ocean (Riggs *et al.*, 1993). Salinity within the sound ranges from fresh water to ~7, with minimal stratification (Corbett *et al.*, 2007) with the lowest salinity occurring during spring when runoff is at a maximum, and highest in winter due to a lack of freshwater inflow (Riggs *et al.*, 1993). The average sediment accumulation rate in the AES is roughly  $0.13 \text{ cm yr}^{-1}$ , with sediments being resuspended by wind-driven waves and likely pulsed into the Pamlico Sound (Corbett *et al.*, 2007). Protected portions of the estuary accumulate sediments at a faster rate of between  $0.25 - 0.57 \text{ cm yr}^{-1}$  (Corbett *et al.*, 2007). Short-term sediment accumulation is controlled by wave-base, while long-term sediment accumulation is controlled by sea-level rise and basin subsidence (Corbett *et al.*, 2007).

### 3. Outer Banks and Inlets

The Outer Banks are a microtidal, wave-dominated, barrier-island chain that formed between 6,000 and 4,500 years ago (Smith *et al.*, 2008; Mallinson *et al.*, 2018). The island chain spans 320 km from Cape Henry in southern Virginia, to Cape Lookout, North Carolina (Figure 4), and separate the Atlantic Ocean from five back-barrier estuaries (Albemarle, Core, Croatan, Currituck, Pamlico, and Roanoke) (Smith *et al.*, 2008). These estuaries have widths of up to 45 km and separate the Outer Banks from mainland

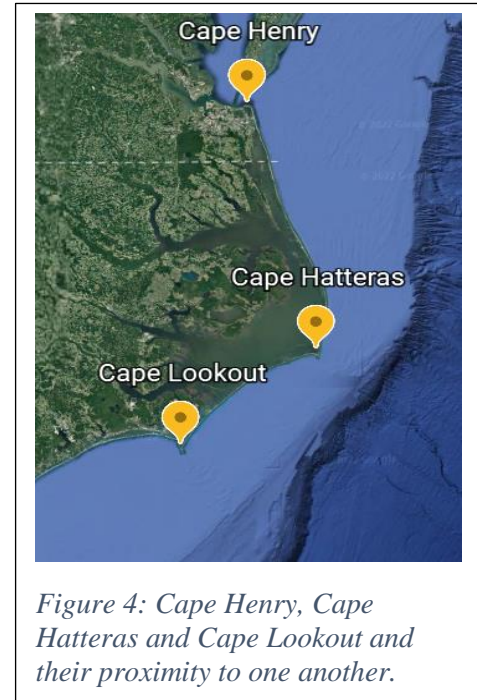


Figure 4: Cape Henry, Cape Hatteras and Cape Lookout and their proximity to one another.

NC (Moore *et al.*, 2010). Estuarine astronomical tidal ranges are around 0.1 m, with water-level changes propelled by wind-forcing. The coastal side of the barriers experience tidal ranges spanning from 0.3 – 1 m, dependent upon location (Mallinson, *et al.*, 2018). The islands display both local and regional variability in width and morphology, with barrier widths ranging from 0.2 – 3 km, and dune heights ranging from 0.5 – 12 m (Moore *et al.*, 2010). The system is constantly changing due to ocean currents, wave action, sea-level rise, and sediment flux (Inman & Dolan, 1989; Mallinson *et al.*, 2011), which contributes to barrier island transgression and tidal inlet migration (Hayes, 1980; Inman & Dolan., 1989; Mallinson *et al.*, 2010; 2011). The shoreline changes between  $-4 - 2 \text{ m yr}^{-1}$  due to sea-level rise, overwash processes, longshore transport, transport of windblown sands, inlet dredging, and inlet deposits (Inman & Dolan., 1989; Miller *et al.*, 2005; Moore *et al.*, 2010). Outer Banks sediments consist mainly of sand, shells, and skeletal remnants (Inman & Dolan., 1989). Barrier and shallow shelf sediments come

from three sources: river sediments, remnants of marine life or old sediment remaining from a previous environment (Inman & Dolan., 1989).

Tidal inlets are major tidal channels, often more than 5 – 10 m deep, that separate barrier islands (or barrier spits), and create a connection between the coastal ocean, and the Albemarle Pamlico estuary (Hayes and Fitzgerald, 2013). Wave action keeps the inlets open (Hayes & Fitzgerald, 2013). The size of the inlet is dependent upon its tidal prism, and the quantity of sand delivered by-way-of longshore transport (Hayes and Fitzgerald, 2013). The size of the channel is dependent upon the amount of water coming through. Sand is constantly moving through the inlet. During flood tide, sediments are pushed into the estuary and during ebb tide sediments are pushed out into the coastal ocean (Mallinson *et al.*, 2008). The Hatteras, Ocracoke, and Oregon Inlets that have been active for more than 100 years (Smith *et al.*, 2008; Mallinson *et al.*, 2018) , with the Oregon Inlet having the greatest impact on this studies' sample sites. The rate of inlet migration varies, depending on inlet depth and longshore sediment transport, some inlets migrate up to dozens of meters each year (Hayes, 1980). The Oregon Inlet was formed in 1846 and migrated two miles southward over ~150 years (Mallinson *et al.*, 2008). The Hatteras Inlet formed during the same storm that created the Oregon Inlet, and the Ocracoke inlet has been around since at least the 16<sup>th</sup> century (Mallinson *et al.*, 2008). The tidal range for these three inlets ranges from ~ 0.58 – 0.61 m (Giese *et al.*, 1979). Flow measurements show that the tidal exchange through the inlets is ~ 6,850 m<sup>3</sup> s<sup>-1</sup> to the Pamlico Sound while freshwater input is ~ 539 m<sup>3</sup> s<sup>-1</sup> (Inman & Dolan., 1989). The inlets contribute to the high residence time within the estuary, allow for the exchange of water between the estuary and the coastal ocean, as well as the transfer of TSS from the estuary into coastal waters.

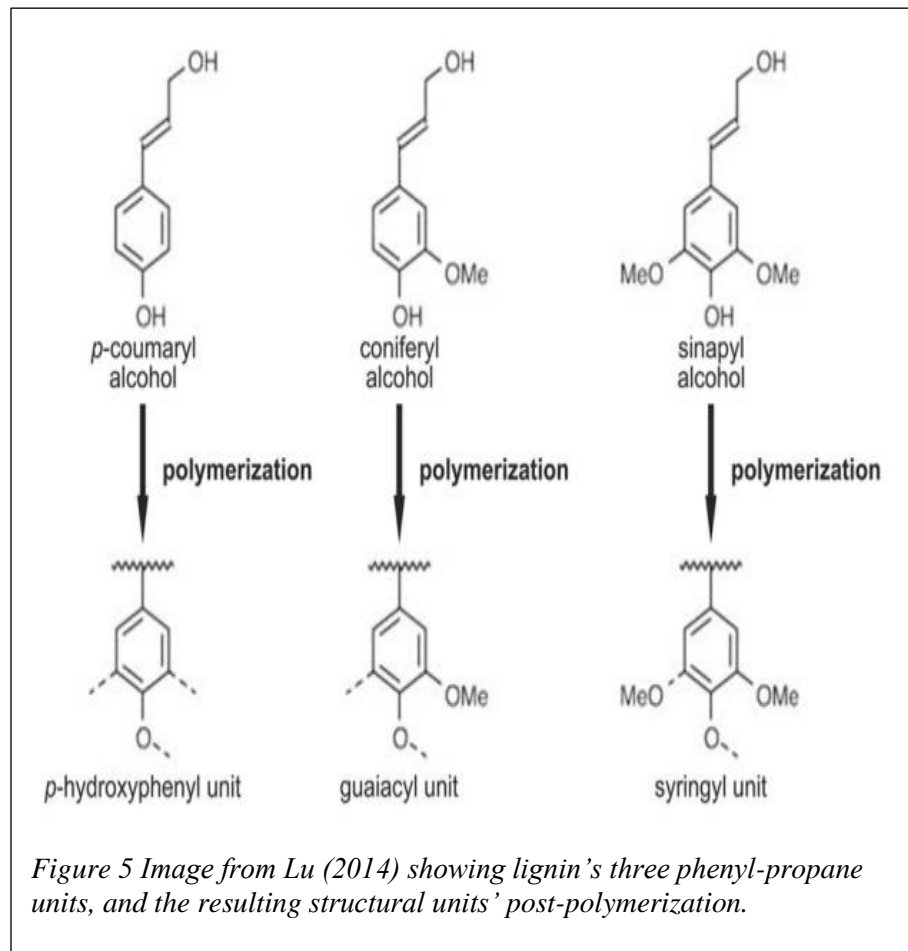
## 4. Lignin

Lignin is a relatively stable, complex polyphenolic organic compound found in the cell walls of vascular plants (Hedges & Mann, 1979). Thus, it can be used as a tracer for terrestrial organic matter (Hedges & Mann, 1979). The macromolecule provides rigidity and structure, while also allowing for the transport of water and nutrients through the tissues of the plant (Katahira *et al.*, 2018). Lignin also creates a barrier against microbes and other external threats (Liu, 2018). Lignin makes up around 15-35% of plant biomass (Katahira *et al.*, 2018), and is the second most abundant biopolymer, making up 20-30% of vascular plant tissue (Killops & Killops, 1993).

Lignin consists of three types of phenylpropane units: coniferyl alcohol, sinapyl alcohol, and *p*-coumaryl alcohol (Figure 5) (Chakar & Ragauskas, 2004). These building blocks correlate

with *p*-hydroxyphenyl (H-unit), Guaiacyl (G-unit), and syringyl (S-unit) structures in lignin (Katahira *et al.*, 2018).

Different types of lignin have different combinations of these H-, G- and S-unit structures (Katahira *et al.*, 2018). Herbaceous plant lignin contain all three structures, while



hardwood lignin (angiosperms) contains G- and S- structures, and softwood lignin (gymnosperms) contains mainly G-structures with a lesser quantity of the H-structures (Katahira *et al.*, 2018).

In a lab setting, the large polymer is typically oxidized into characteristic monomers (Figure 6) with cupric oxide. Controlled cupric oxide oxidation produces eight main reaction products (Hedges & Mann, 1979). Reaction products can be divided into four phenol groups: p-hydroxy, vanillyl, syringyl and cinnamyl (Yamamoto *et al.*, 2005), each with an aldehyde, ketone, or acid substitution (Thevenot *et al.*, 2010). Ratios of the p-hydroxyl, vanillyl, syringyl and

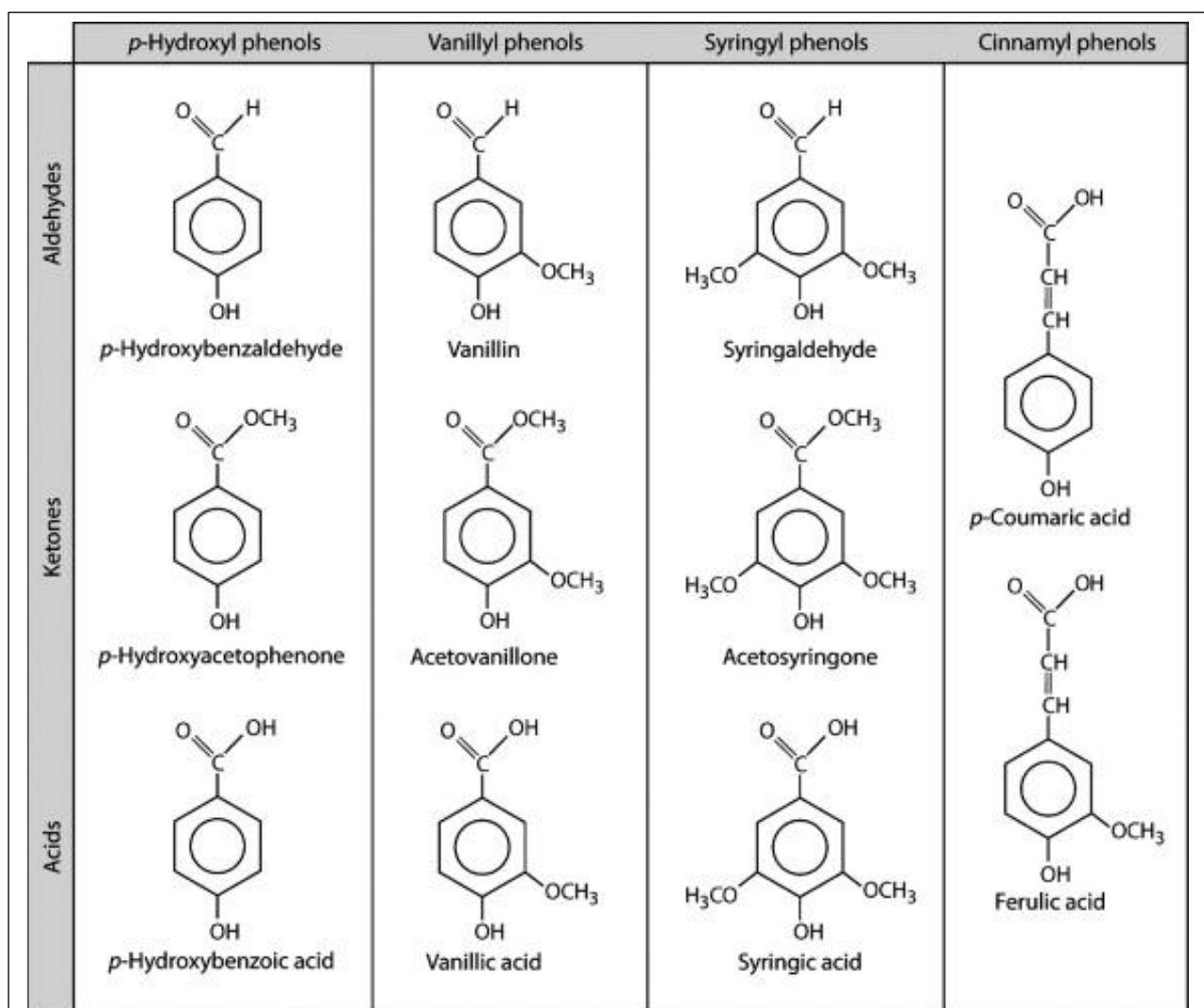


Figure 6: Figure from Thevenot *et al.* (2010) showing the lignin monomers that are a product of cupric oxide oxidation. Each set of phenols; p-hydroxyl, vanillyl, and syringyl are made up of an acid, aldehyde, and ketone. Cinnamyl phenols consist of two acids.

cinnamyl phenols (Figure 6) allow for the characterization of plant type and abundance. The ratios of aldehydes, ketones and acids can indicate state of soil degradation, with a higher ratio indicating a higher level of degradation (Thevenot *et al.*, 2010).

Angiosperms and gymnosperms, the two most common classifications of land plant, contain differing phenol ratios (Hedges & Mann, 1979). Due to these compositional differences, lignin can be used to determine if the source of vascular plant material is woody or non-woody. All vascular plants yield vanillin during oxidation. Angiosperms yield syringyl phenols while non-woody vascular plant tissue yields cinnamyl phenols (Hedges & Mann, 1979). The ratios of these oxidation products can determine the source of organic matter, with ratios of syringyl to vanillyl (S/V) yielding angiosperms and ratios of (C/V) yielding non-woody plant materials (Figure 7) (Wotton, 1994). The ratio of acid to aldehyde (Ad/Al) of V and S can determine the decomposition level of the soil. Increased (Ad/Al) ratios are indicative of a lower lignin concentration within the sample (Hedges *et al.*, 1988). vanillyl (S/V) yielding angiosperms and ratios of (C/V) yielding non-woody plant materials (Figure 7) (Wotton, 1994). The ratio of acid to aldehyde (Ad/Al) of V and S can determine the decomposition level of the soil. Increased (Ad/Al) ratios are indicative of a lower lignin concentration within the sample (Hedges *et al.*, 1988).

## **5. Wave Driven Resuspension**

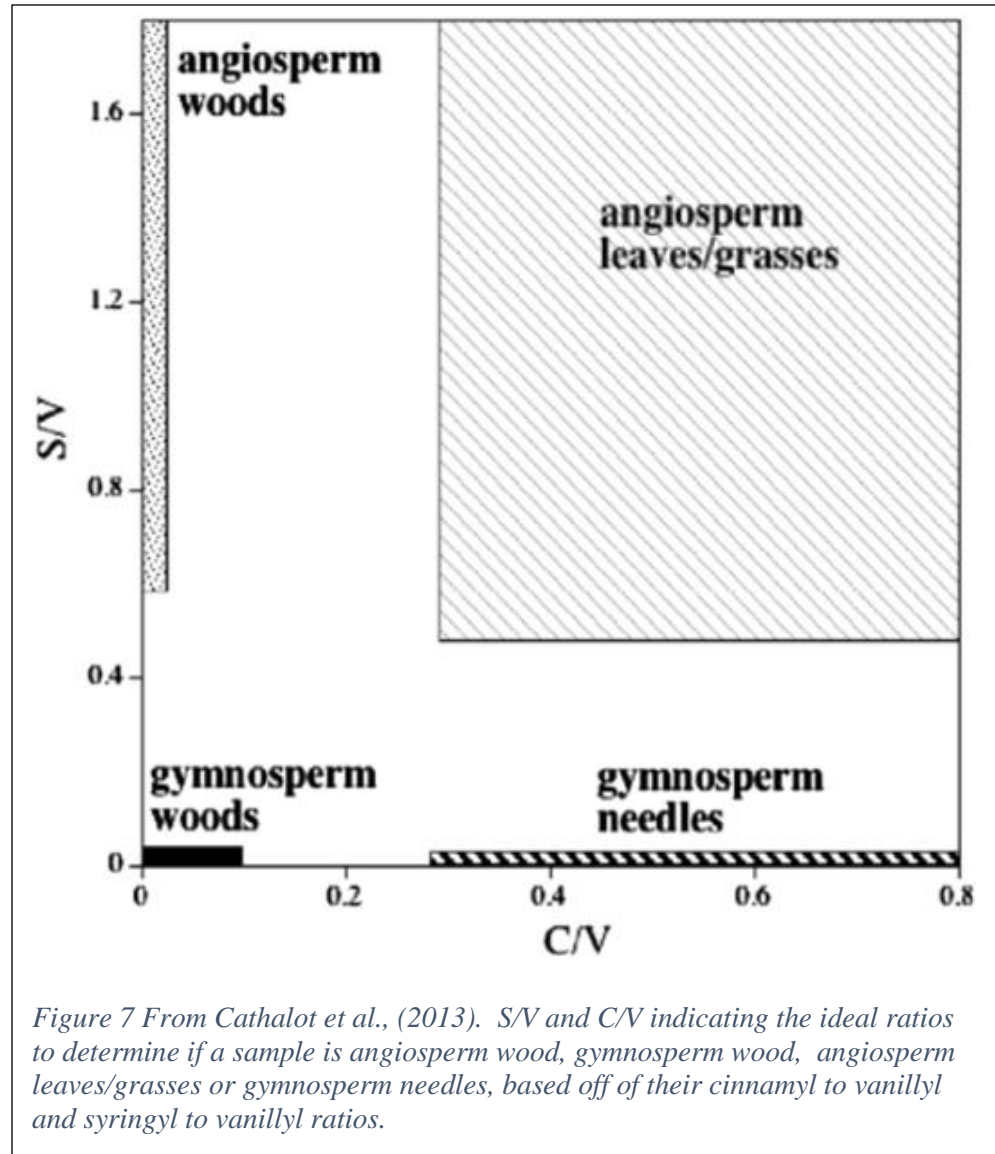
Waves play an important role in the functioning of estuarine systems, with waves being the main method of sediment resuspension within these systems (Green & Coco, 2013). Waves within the APES are generated locally; wind acts on the fetch to create the wave. Waves may also generate within the coastal ocean and then make their way into the sound through the inlets

(Shi *et al.*, 2006).

Currents within the system are caused by winds, tides, and density changes (Shi *et al.*, 2006). Short-period wind-driven waves tend to have orbital motions, which reach the bottom of the seabed and cause

resuspension

(Green & Coco,



2013). Near the mouth of the estuary, wave action along with outflows lead to higher suspended sediment concentrations (Xie *et al.*, 2018). Research conducted by Gong and Shen (2009) found that during storms, waves play a crucial role when it comes to mixing seabed sediments, while storm surge increase sediment transport flux by a factor of 100. Strong winds created by storms also play a role in resuspension, and transport of TSS, but these effects within estuarine systems still need further research to be better understood (Gong & Shen, 2009).

## 6. Storm Derived Disturbances

Several researchers have quantified the results of storms as episodic events along coastal North Carolina. For example, Paerl *et al.* (2001) did an in-depth study focusing on Hurricanes Dennis, Floyd, and Irene and their impacts on the APES. Together, the three hurricanes brought ~ 1 m of rainfall within a six-week period between 4 September 1999 and 17 October 1999 (Paerl *et al.*, 2001). Fresh water inflow created vertical stratification, salinity in the sound was depressed by 70%, and hypoxic and anoxic conditions occurred killing shrimp and crabs (Paerl *et al.*, 2006). Hypoxic conditions lasted for three weeks, until Hurricane Irene destratified the Sound, but then returned when freshwater inflows from Irene caused the area to restratify. Dissolved organic carbon abundance tripled, and primary production and the phytoplankton community showed signs of stimulation for the next 6 months (Paerl *et al.*, 2006).

Five years later, more comprehensive research was conducted by Paerl *et al.* (2006) examining the impacts of landfalling hurricanes between 1996 – 2005 on the Pamlico Sound. That study looked at eight storms that impacted the NC coast over the nine-year period: Hurricanes Bertha and Fran (1996), Bonnie (1998), Irene, Dennis, and Floyd (1999), Isabel (2003) and Ophelia (2005). Hurricanes Bertha and Bonnie both had high wind speeds and low precipitation. Bonnie's windspeeds reached over 160 km/h, downing trees, and causing structural damage, but there were no fish kills, and no detectable change in seasonal or annual nitrogen within the estuary (Paerl *et al.*, 2006). Hurricane Isabel brought strong winds, and low precipitation. Storm surges associated with the hurricane caused shoreline erosion that led coastal sediments to be eroded into the Sound. Ophelia was also a high wind, low precipitation storm, causing beach erosion and structural damage but did not deliver excessive nutrient loads into the Sound (Paerl *et al.*, 2006). Hurricane Fran brought over 50 cm of precipitation which

caused high freshwater discharge, low dissolved oxygen concentration, and increased nitrogen loading throughout the Neuse River Estuary. Flooding from Fran doubled the annual nitrogen load to the estuary (Paerl *et al.*, 2006). Finfish and shellfish kills lasted for weeks after the storm. Flood events allow for the exchange of organic matter and nutrients between the land and adjacent coast including estuarine systems and may eventually impact the adjacent ocean (Kandasami and Nath, 2016; Bianchi *et al.*, 2013). Paerl *et al.* (2006) concluded that storms bringing high amounts of rainfall impacted nutrient loads the most. High rainfall, flood-producing hurricanes led to increased nutrient loading, low oxygen conditions, and increased spatial coverage of phytoplankton blooms, while low rainfall hurricanes yield lower nutrient inputs (Paerl *et al.*, 2006).

Recent research by Kossin (2018) noted a decrease in hurricane translation speed by ~ 10% over the past ~ 70 years which is likely related to anthropogenic warming. As the climate continues to change, we may not only be seeing an increase in strength and frequency of hurricanes, but a slowdown in their translation speed.

### **6.1 Indicators of Storm Derived Disturbances**

A five-year study done by Simmons (1976), lasting from 1969 to 1973, observed the sediment-transport characteristics of rivers in a 15,500 km<sup>2</sup> area of the Piedmont and Coastal Plain regions of North Carolina. Four major river basins were examined: the Roanoke, Pamlico, Neuse, and Cape Fear. Their sediment yield and average annual suspended sediment discharge are listed in Table 2. The Roanoke, Pamlico, and Neuse rivers all eventually discharge into the Albemarle-Pamlico Sound, while the Cape Fear discharges directly into the Atlantic Ocean. The study shows that erodibility, topography, precipitation intensity, runoff and the presence of man-

made structures are all major contributing factors which affect sediment yields in streams (Simmons, 1976).

Typically, there is a positive correlation between carbon flux and riverine discharge (Bauer *et al.*, 2013). Annual precipitation, temperature, and hydrologic events all play a role in OC transport, with hydrologic events accounting for a disproportionate quantity of transported OC (Bauer *et al.*, 2013). Heavy precipitation from these events can lead to erosion, thus increasing export of particulates from the river out into the coast; one intense storm can account for upwards of two-fifths of a rivers yearly export of OC (Bauer *et al.*, 2013). Climate change only stands to further impact these riverine carbon fluxes (Bauer *et al.*, 2013).

The biogeochemical properties of an estuary vary based on type of estuary and its location (Bauer *et al.*, 2013). Geomorphology and nutrient input magnitude both influence the fluxes and carbon cycling within an estuary which ultimately alters the quantity and properties of OC and IC that move between the land and sea (Cai, 2011). Estuarine DOC and POC stems from estuarine, marine, and terrestrial primary production (Bianchi & Bauer, 2011). *In situ* OC production in some estuarine systems can be equaled to or surpass the supply coming from marine or riverine sources (Raymond & Bauer, 2001). Photochemical oxidation, microbial degradation, sedimentation, scavenging and flocculation all contribute to OC reduction within the estuary (Moran *et al.*, 2000; Sholkovitz, 1976). Unfortunately, there are not enough accurate measurements from enough systems to create regional estimates of the direction of magnitude of carbon flux within an individual estuarine system (Bauer *et al.*, 2013).

Basin	USGS station No.	Station name	Drainage area (mi <sup>2</sup> )	Average water discharge (ft <sup>3</sup> /s)	Average annual suspended-sediment discharge 1969-73 (tons)	Average annual sediment yield 1969-73 (tons/mi <sup>2</sup> )	Suspended-sediment concentration equaled or exceeded 1 percent of the time (mg/l)	Suspended sediment concentration equaled or exceeded 95 percent of the time (mg/l)
Roanoke ----	02077200	Hyc Creek near Leasburg.....	44.0	39.2	4,320	98	218	7
	02077240	Double Creek near Roseville.....	7.47	5.71	2,490	333	237	0
	02077250	South Hyc Creek near Roseville.....	55	48.9	7,320	133	248	10
	02077300	Hyc River at McGehees Mill.....	191	126	2,380	12	34	5
Pamlico ----	02081500	Tar River near Tar River.....	167	152	28,800	172	292	10
	02081800	Cedar Creek near Louisburg.....	47.8	50.1	3,860	81	133	18
	02082770	Swift Creek at Hilliardston.....	163	136	7,430	46	135	4
	02082950	Little Fishing Creek near White Oak.....	175	165	9,980	57	124	9
Neuse -----	02085000	Eno River at Hillsborough.....	66.5	61.8	7,416	112	272	7
	02085070	Eno River near Durham.....	141	123	17,700	126	263	23
	02085220	Little River near Orange Factory.....	81.6	71.7	6,960	85	181	5
	02086000	Dial Creek near Bahama.....	4.71	4.16	512	109	333	0
	02087000	Neuse River near Northside.....	526	517	52,300	99	151	36
	02087182	Neuse River at Falls.....	770		120,300	156	345	27
	02087500	Neuse River near Clayton.....	1,140	1,190	189,700	166	490	5
	02088000	Middle Creek near Clayton.....	80.7	93.9	4,580	57	66	4
	02088470	Little River near Kenly.....	190	179	5,530	29	59	10
	02088500	Little River near Princeton.....	229	253	7,360	32	57	9
	02089000	Neuse River near Goldsboro.....	2,390	2,525	134,300	56	93	27
	02090380	Contentnea Creek near Lucama.....	156	154	6,230	40	68	16
	02091000	Nahunta Swamp near Shine.....	77.6	88.1	4,640	60	97	18
Cape Fear --	02096500	Haw River at Haw River.....	599	561	128,400	214	521	27
	02096850	Cane Creek near Teer.....	31.3	30.9	3,931	126	210	0
	02097000	Haw River near Pittsboro.....	1,310	1,220	300,200	229	690	11
	02098000	New Hope River near Pittsboro.....	285	281	25,700	90	135	37
	02098200	Haw River near Haywood.....	1,700	1,395	305,200	180	557	5
	02102000	Deep River at Moncure.....	1,410	1,444	168,400	119	135	8
	02102500	Cape Fear River at Lillington.....	3,440	3,339	510,300	148	284	12

Table 2: Table from Simmons (1976) showing the Roanoke, Pamlico, Neuse and Cape Fear basins, station numbers, associated drainage area, average water discharge, suspended sediment discharge, suspended sediment yield, and suspended sediment concentrations.

In 2013, Bianchi *et al.* conducted research, examining sites along the lower Atchafalaya and Mississippi rivers during pre-flood, flood, and post-flood conditions. Samples were primarily analyzed for dissolved lignin, dissolved organic carbon (DOC) and dissolved inorganic carbon (DIC), and surface water dissolved pCO<sub>2</sub>. Rivers are usually a source of CO<sub>2</sub> to the atmosphere, while continental shelves act as a sink (Bianchi *et al.*, 2013). Before the flood (April), high dissolved pCO<sub>2</sub> concentrations (max = 1,875 ppm) and fluxes (max = 1,948 mmol m<sup>-2</sup>d<sup>-1</sup>) to the atmosphere were seen in the mouth of the Atchafalaya River. Shelf surface waters showed low concentrations of dissolved pCO<sub>2</sub> (min = 66 ppm) with large CO<sub>2</sub> fluxes (-368 mmol m<sup>-2</sup>d<sup>-1</sup>) into the water from the atmosphere due to increased net autotrophy. During the flood (June 2011), pCO<sub>2</sub> concentrations were higher in the river reaching 4,382 ppm (max flux = 669 mmol m<sup>-2</sup>d<sup>-1</sup>) while August river pCO<sub>2</sub> concentrations declined (max = 2,132 ppm) (Bianchi *et al.*, 2013). In May and June 2011, total fluxes of DOC from the Atchafalaya and Mississippi rivers to the coast were 33% and 58% of the overall DOC flux estimates to the Gulf of Mexico per year. Before the flood, shelf DOC was 12,237 mM, lower than during the flood (22,739 mM; June 2011) and post-flood 2011 (22,345 mM, August 2011) (Bianchi *et al.*, 2013).

Characterization of DOC and active bacteria populations showed a biological link to the shift between CO<sub>2</sub> source river water and the CO<sub>2</sub> sink shelf water. Due to the nature of the organic matter leading to respiration, Bianchi *et al.* (2013) shows that CO<sub>2</sub> released into the atmosphere likely came from the oxidation of terrestrial DOC. Flooding causes a transfer of soil carbon into the atmosphere via rivers and coastal water. Terrestrial DOC was broken down faster when derived from leached litter in flood waters as opposed to surface soil. This may be indicative of enhanced oxidation, photochemical breakdown, and priming mechanisms may be working to augment the breakdown of terrestrial DOC. Increased flooding associated with

global warming, may allow for an increased exchange between soil and litter derived OC and coastal environments (Bianchi *et al.*, 2015). Rapid conversion to CO<sub>2</sub> in coastal versus terrestrial systems indicates that there will be an inevitable increase in the transfer of stored organic carbon in terrestrial systems to the atmosphere eventually, creating a positive feedback loop (Bianchi *et al.*, 2013).

Hurricane Harvey generated 500 mm of precipitation over five days. Yan *et al.* (2020) found that precipitation, groundwater, runoff and flooding from San Jacinto and Trinity Rivers during Hurricane Harvey released  $14 - 17 \times 10^9$  m<sup>3</sup> of water into the Galveston Bay, which is four times the total volume of the bay. Looking at tDOC, they found that ~ 87 Gg of DOC was transferred from land to the Bay, and 95% of this was transported during the first week. Analysis of syringyl to vanillyl (S/V) and cinnamyl to vanillyl (C/V) ratios using dissolved lignin phenols determined that most of the storm-derived organic material came from non-woody angiosperm tissue.

### III. METHODS

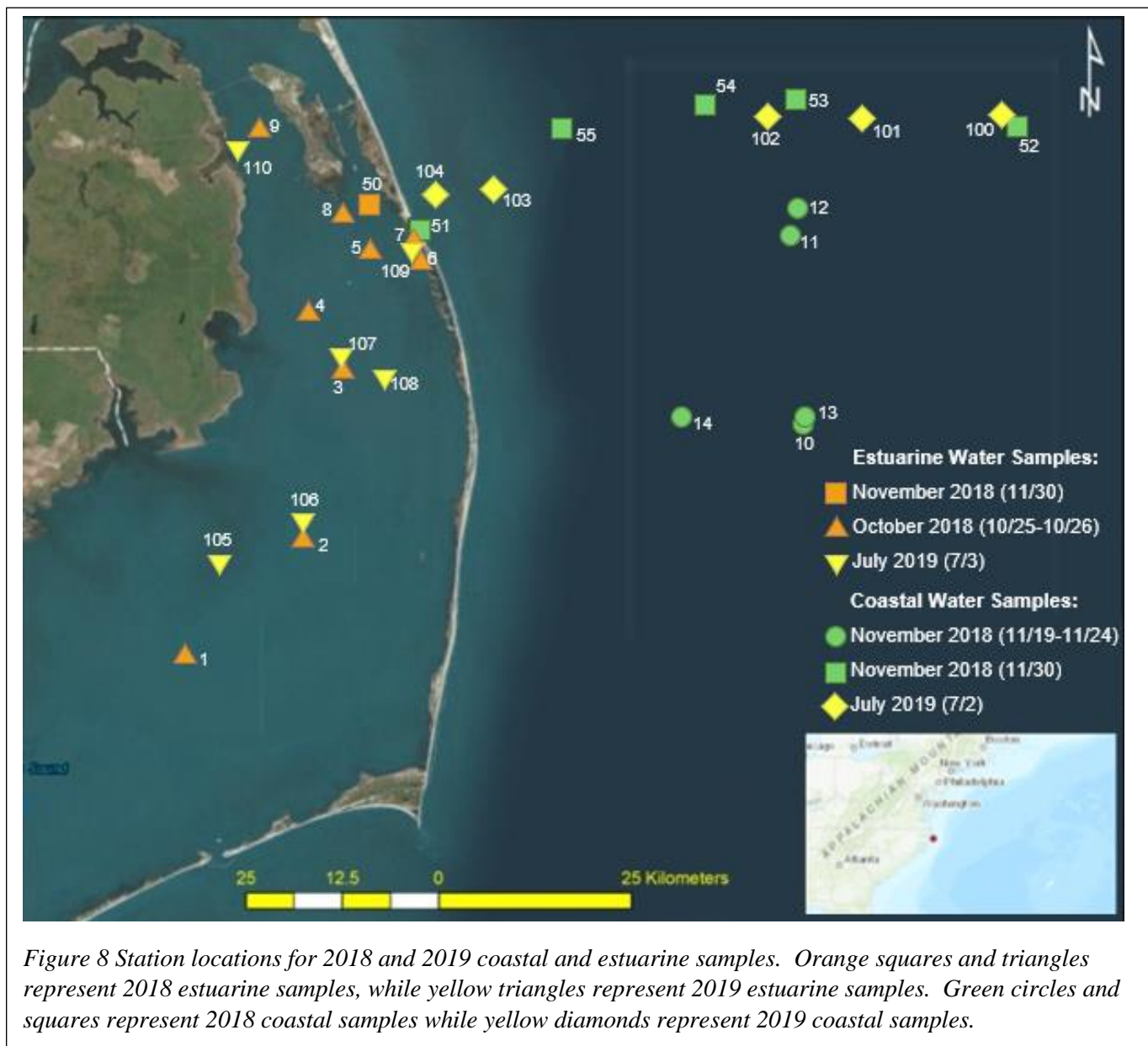
#### 1. Sample Collection and Preparation

Post-storm surface water samples were collected from twenty different locations in the APES and portions of a cross-shelf transect, Oregon Inlet and the Gulf Stream (Figure 8). Due to adverse weather conditions, the earliest that a post Florence sample could be collected was October 25, 2018. Sampling was conducted again between 11/19-11/24 and the final set of 2018 samples was collected on November 30, 2018, 41 to 77 days after Hurricane Florence made landfall in coastal NC. A second set of samples was taken 07/02-07/03/2019 as a “non-storm” period at 11 different stations (Figure 8). Samples were taken ~10 cm below the water’s surface by filling clean Nalgene 1 L and 4 L high density polyethylene water bottles. All samples were collected while wearing nitrile gloves. All collection vessels were cleaned by rinsing with a dilute solution of Alconox and distilled deionized water (DDI), and then triple rinsing with DDI water. Collection bottles were conditioned in the field by rinsing with water at the sampling station prior to sample retrieval. Two to five replicates were collected for each sample. Samples were placed in coolers with ice immediately after collection.

Each 2018 sample was filtered through 47 mm diameter pre-combusted (450° C for 4 h), 1.5 µm and 0.7 µm pore size glass fiber filters (GFF). Each 2019 sample was filtered through pre-combusted (450° C for 4 h) 0.7 µm GFF. Filters from 2018 and 2019 were air-dried at room temperature until there was no further change in dry weight (Equation 1). These filters were used for lignin extraction from total suspended solids using stainless steel pressure vessels in a Lindberg/Blue M 3.5 kW oven.

$$\text{TSS} = \frac{(\text{Filter dry weight including sediment (g)}) - (\text{Tare weight of filter (g)})}{\text{Volume of water filtered (L)}} \quad (\text{Equation 1})$$

Filter tare weight, volume of water filtered, total mass of filter and mass of total suspended sediments (TSS) are noted in the Appendix (Tables 11, 12, 13).



## 2. Lignin Isolation

Hedges and Ertel (1982) described a reproducible method (via controlled thermal oxidation in mini bombs), that allows for the characterization of lignin in sediment samples containing a minimum of 10 mg of organic material. Goñi and Montgomery (2000) modified the methodology of Hedges and Ertel (1982), to streamline the procedure. Lignin was extracted from TSS on GFFs using the modified methodology of Goñi and Montgomery (2000). The following monomers were quantified in this study: vanillin (VAL), acetovanillone (VON), vanillic acid (VAD), syringaldehyde (SAL), acetosyringone (SON), syringic acid (SAD), p-coumaric acid (CAD), and ferulic acid (FAD) (Table 3). Total lignin ( $L_8$ ) can be calculated by adding all individual monomer concentrations together.

Roughly 100 mg of ferrous ammonium sulfate and, 1 g of cupric oxide, and the glass fiber filter were placed inside scintillation vials. The scintillation vials that contained the samples were emptied into metal pressure vessels. These vessels had Teflon tape wrapped tightly around the threads of each side, one side was sealed, and the other was left open for sample transfer. The pressure vessels were placed into an argon filled glove box, and then they were sparged three times with argon gas, ensuring anoxic conditions as required for controlled oxidation.

Approximately 25 mL of 2N NaOH was added to each vessel and capped while in the glove box. Vessels were removed from the glove box and the ends were further tightened using an adjustable wrench. The sealed pressure vessels were placed in a pre-heated oven where the temperature was set to 150°C and samples were placed inside for 90 min (5.6kW). Following oxidation, each vessel was cooled to room temperature, for subsequent acidification and organic solvent extraction of lignin oxidation products.

Samples were transferred to 50 mL Teflon tubes. Ethylvanillin was added as an internal standard to each Teflon centrifuge tube at a concentration of 1 mg mL<sup>-1</sup> NaOH. Tubes were then capped and shaken. The tubes were then centrifuged at 3,000 rpm for 5 minutes to separate the solid residue from the base extract containing the lignin oxidation product. The supernatant was decanted into a clean 30 mL Pyrex centrifuge tubes. An additional 5 mL of sodium hydroxide was added to the residue in the Teflon tube and shaken once again. This process was repeated once more for a total of two rinses plus the original sample. Concentrated HCL (~ 5 mL) was added to each Pyrex tube to acidify the lignin oxidation products (LOPs). The Pyrex tube was sealed and shaken. Litmus paper was used to verify acidification. After acidification,

*Table 3 Each of the nine monomers analyzed via GC/MS, the abbreviation, retention time, and both target and reference ions.*

<b>Compound</b>	<b>Abbreviation</b>	<b>Retention Time (min)</b>	<b>Target Ion (m/z)</b>	<b>Reference Ions</b>
Vanillin	VAL	9.098	194.00	209.15, 193.15, 224.10
Acetovanillone	VON	10.155	223.05	193.00, 208.00, 238.10
Vanillic Acid	VAD	12.150	297.10	267.05, 312.10, 223.05
Syringaldehyde	SAL	11.256	224.05	239.10, 254.10, 223.05
Acetosyringone	SON	12.236	238.05	223.00, 253.10, 268.10
Syringic Acid	SAD	14.119	312.10	312.10, 342.15, 297.05
<i>p</i> -Coumaric Acid	CAD	14.787	293.10	219.05, 308.10, 249.10
Ferulic Acid	FAD	17.034	338.15	323.10, 308.05, 249.10
Ethylvanillin	Eval	9.852	167.05	195.00, 238.10, 179.00

8-10 mL of ethyl acetate was added to each tube and shaken (~ 2 minutes). Tubes were then centrifuged at 2,000 rpm (~ 2 minutes) to separate the organic from aqueous layer. The organic phase (top layer) was transferred to a Rotovap flask. The aqueous layer was re-extracted with 8 – 10 ml of ethyl acetate two more times and all three organic layers combined.

The ethyl acetate extract was slowly evaporated in a rotary evaporator water bath held at ~ 50° C until only a dime-sized portion of sample remained. A 0.5 mL aliquot of pyridine was added to the Rotovap flask to redissolve the residue. This rinse step was repeated two more times to maximize the transfer of the ligninaceous residue, with the final content of the vial being 1.5 mL of lignin phenol. Pyridine extracts were transferred into a pre-cleaned 4 mL glass vial for storage until derivatization and analysis.

To quantify lignin via gas chromatography-mass spectrometry (GC-MS), subsamples of pyridine were placed in GC vials containing a 200 µL glass insert and weighed. N,O-Bis(trimethylsilyl)trifluoroacetamide (BSTFA) was added at a ratio of 1:1 (pyridine:BSTFA). Hexane was added to fill the remainder of the insert and then the vial was capped. Trimethylsilyl derivatives of each monomer were obtained by heating the crimped vial for 45-minutes at 70° C in a water bath.

Upon cooling, the samples, a mixed LOP standard of known concentration, and bakeouts containing hexane were injected onto a Shimadzu GC-2010 with a 30 m long DB-5 MS column having a 0.25 µm thickness and a 0.25 µm diameter. The 1 µL derivatized samples were injected at a flowrate of 53 mL/min with a pressure of 52.8 kPa and column flow of 0.99 mL/min using Helium as a carrier gas. Column oven temperature begins at 50° C and samples are injected once the temperature reaches 250° C with a total run time of 50 minutes per each sample vial.

Peak areas associated with the mixed LOP standard were used to determine the relative response factor (RRF) for each day's injections. The RRF was used to confirm compound retention times and qualifying ions (Table 3) and to adjust for daily GC response.

This method was also applied to standard reference materials to confirm accuracy.

Although total aquatic lignin concentrations were able to be quantified on GFFs, particulate organic carbon and nitrogen were unable to be quantified. Thus, values of lignin in this study are represented as the sum of the individual phenol yields in  $\text{mg g}^{-1}$ .

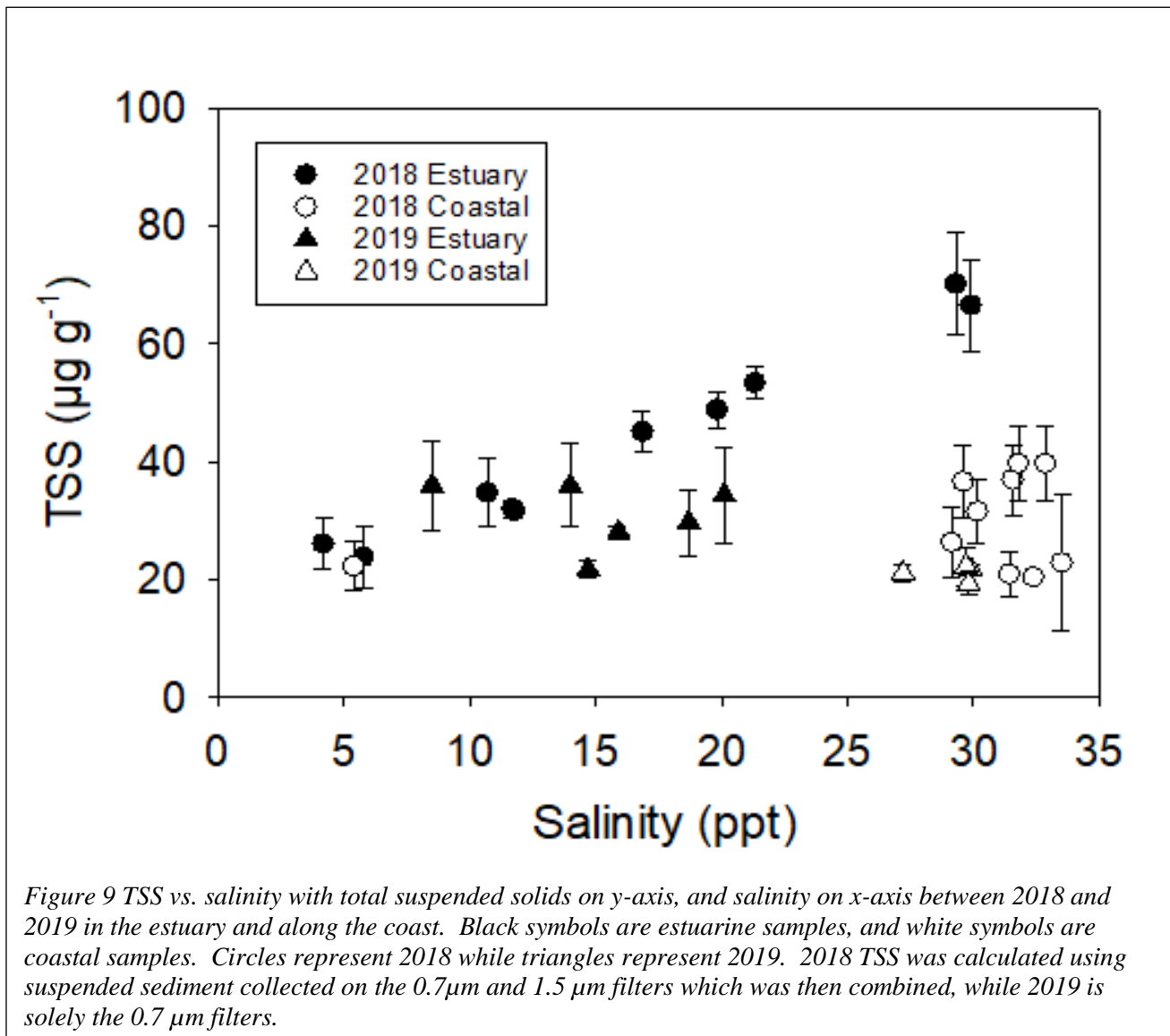
## IV. RESULTS

### 1. Salinity and Suspended Sediment

In 2018, during the storm period, estuarine salinity varied from 4.2 – 29.9 ppt (Stations 1 – 9, 50; n = 10), while salinity in the coastal stations (Stations 10 – 14, 51 – 54; n = 10) varied from 5.4 – 33.51 ppt. Note, that in 2018, there were several stations near the Gulf Stream that were sampled using the R/V Neil Armstrong, while those stations were not accessible in 2019. In 2019, salinity within the estuarine stations varied from 8.5 – 20.1 ppt (Stations 105 – 110; n = 6), while salinity ranged from 26.7 – 29.9 ppt in the coastal stations (Stations 100 – 104; n = 5) (Figure 9, 10; Table 4).

Since the 2018 samples were filtered using both the 0.7 and 1.5  $\mu\text{m}$  GFF's, their individual values were combined into a total TSS value for each station for comparison to the 2019 samples (Table 4) that were only filtered using 0.7  $\mu\text{m}$  GFF. In 2018, TSS collected on combined 0.7  $\mu\text{m}$  and 1.5  $\mu\text{m}$  filters ranged from 23.75 – 70.16  $\mu\text{g g}^{-1}$  ( $43.19 \pm 16.38 \mu\text{g g}^{-1}$ ) in estuarine samples, and 20.37 – 39.64  $\mu\text{g g}^{-1}$  ( $29.67 \pm 8.03 \mu\text{g g}^{-1}$ ) in coastal samples.

In 2019, TSS in estuarine samples ranged from 21.66 – 35.96  $\mu\text{g g}^{-1}$  ( $30.91 \pm 5.60 \mu\text{g g}^{-1}$ ), and in coastal samples ranged from 19.26 – 22.21  $\mu\text{g g}^{-1}$  ( $21.01 \pm 1.28 \mu\text{g g}^{-1}$ ) (Table 5; Figure 9, 10). Overall, the highest TSS concentrations occur in 2018 at five different locations across the estuary (Stations 1, 2, 5, 6 and 7), while the lowest TSS concentrations occur at the Stations 53 in 2018, and 100, 102 and 104 in 2019, all coastal stations that are located east of Oregon Inlet (Figure 8).



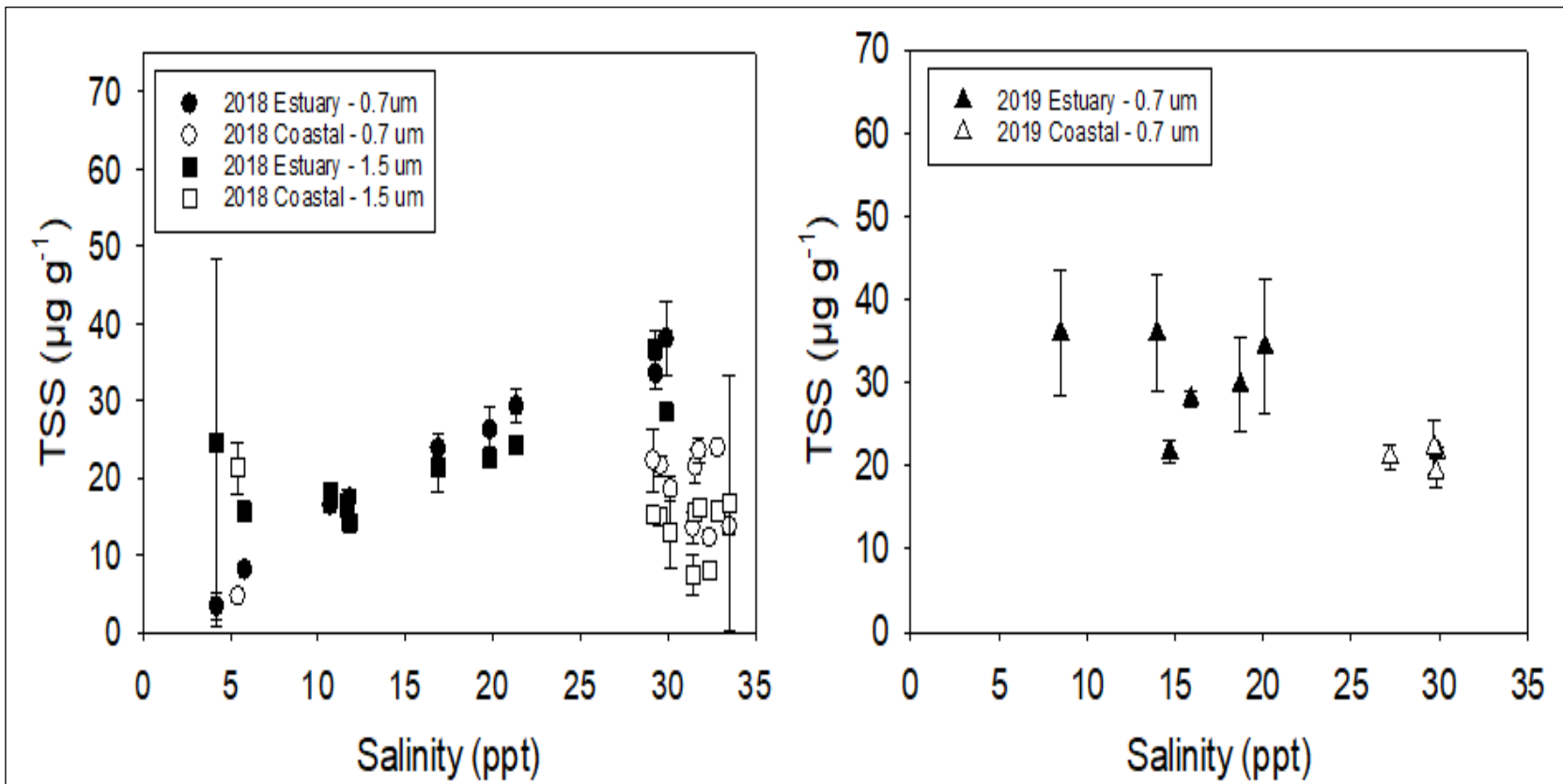


Figure 10 TSS vs. salinity looking at the different filter size classes. 2018 samples were filtered using 0.7 and 1.5 µm GFF, while 2019 samples were filtered using 0.7 GFF.

*Table 4 Total suspended sediment (0.7 and 1.5  $\mu\text{m}$  filters and combined) and salinity at stations occupied in 2018. Table also includes Station ID, date that sample was taken, collection vessel used to obtain the sample, and whether the sample was located within the estuary or along the coast. Note that three sample stations are very close to Hatteras Inlet, but they are still labeled as estuarine or coastal depending upon the side of the inlet in which the samples were taken.*

Station ID	Date	Collection Vessel	Location	Salinity	Combined 0.7 + 1.5 $\mu\text{m}$ TSS ( $\mu\text{g g}^{-1}$ )	0.7 $\mu\text{m}$ TSS ( $\mu\text{g g}^{-1}$ )	1.5 $\mu\text{m}$ TSS ( $\mu\text{g g}^{-1}$ )
GSPS-18 Station 1	10/25/2018	R/V Blackbeard	Estuary	21.33	(53.36 $\pm$ 2.81)	(29.24 $\pm$ 2.23)	(24.13 $\pm$ 1.15)
GSPS-18 Station 2	10/25/2018	R/V Blackbeard	Estuary	16.87	(45.06 $\pm$ 3.47)	(23.78 $\pm$ 1.85)	(21.28 $\pm$ 3.16)
GSPS-18 Station 3	10/25/2018	R/V Blackbeard	Estuary	11.70	(31.97 $\pm$ 1.39)	(15.22 $\pm$ 2.03)	(16.75 $\pm$ 1.57)
GSPS-18 Station 4	10/26/2018	R/V Blackbeard	Estuary	11.80	(31.54 $\pm$ 0.750)	(17.34 $\pm$ 0.960)	(14.20 $\pm$ 1.08)
GSPS-18 Station 5	10/26/2018	R/V Blackbeard	Estuary	19.83	(48.80 $\pm$ 3.18)	(26.20 $\pm$ 2.87)	(22.60 $\pm$ 1.31)
GSPS-18 Station 6	10/26/2018	R/V Blackbeard	Estuary (Inlet)	29.90	(66.50 $\pm$ 7.71)	(38.04 $\pm$ 4.67)	(28.46 $\pm$ 0.980)
GSPS-18 Station 7	10/26/2018	R/V Blackbeard	Estuary (Inlet)	29.30	(70.16 $\pm$ 8.73)	(33.48 $\pm$ 1.86)	(36.68 $\pm$ 2.49)
GSPS-18 Station 8	10/26/2018	R/V Blackbeard	Estuary	10.70	(34.71 $\pm$ 5.87)	(16.46 $\pm$ 0.870)	(18.25 $\pm$ 1.04)
GSPS-18 Station 9	10/26/2018	R/V Blackbeard	Estuary	5.790	(23.75 $\pm$ 5.10)	(8.090 $\pm$ 0.810)	(15.66 $\pm$ 1.33)
GSPS-18 Station 10	11/19/2018	R/V Neil Armstrong	Coastal	31.57	(36.90 $\pm$ 5.95)	(21.45 $\pm$ 2.21)	(15.45 $\pm$ 0.390)
GSPS-18 Station 11	11/20/2018	R/V Neil Armstrong	Coastal	32.85	(39.61 $\pm$ 6.26)	(23.93 $\pm$ 0.860)	(15.68 $\pm$ 0.700)
GSPS-18 Station 12	11/20/2018	R/V Neil Armstrong	Coastal	31.79	(39.64 $\pm$ 6.36)	(23.51 $\pm$ 1.62)	(16.13 $\pm$ 1.19)
GSPS-18 Station 13	11/23/2018	R/V Neil Armstrong	Coastal	29.60	(36.59 $\pm$ 6.19)	(21.58 $\pm$ 1.33)	(15.00 $\pm$ 0.350)
GSPS-18 Station 14	11/24/2018	R/V Neil Armstrong	Coastal	29.14	(26.25 $\pm$ 5.85)	(22.27 $\pm$ 4.06)	(15.12 $\pm$ 0.860)
GSPS-18 Station 50	11/30/2018	R/V Blackbeard	Estuary	4.200	(26.02 $\pm$ 4.29)	(3.360 $\pm$ 1.71)	(24.58 $\pm$ 23.8)
GSPS-18 Station 51	11/30/2018	R/V Blackbeard	Coastal (inlet)	5.400	(22.20 $\pm$ 4.16)	(4.630 $\pm$ 0.450)	(21.23 $\pm$ 3.37)
GSPS-18 Station 52	11/30/2018	R/V Blackbeard	Coastal	33.51	(22.82 $\pm$ 11.5)	(13.68 $\pm$ 1.03)	(16.73 $\pm$ 16.5)
GSPS-18 Station 53	11/30/2018	R/V Blackbeard	Coastal	32.38	(20.37 $\pm$ 0.420)	(8.120 $\pm$ 0.350)	(8.120 $\pm$ 0.350)
GSPS-18 Station 54	11/30/2018	R/V Blackbeard	Coastal	31.42	(20.86 $\pm$ 3.64)	(13.52 $\pm$ 1.95)	(7.340 $\pm$ 2.58)
GSPS-18 Station 55	11/30/2018	R/V Blackbeard	Coastal	30.16	(31.49 $\pm$ 5.34)	(18.54 $\pm$ 1.60)	(12.95 $\pm$ 4.56)

Table 5 Total suspended sediment (0.7  $\mu\text{m}$  filters) and salinity at stations occupied in 2019. Table also includes Station ID, date that sample was taken, collection vessel used to obtain the sample, and whether the sample was located within the estuary or along the coast. Note that one sample station is very close to Hatteras Inlet, but they are still labeled as estuarine or coastal depending upon the side of the inlet in which the samples were taken.

\*Insufficient water available for chemical analyses at Station 103.

Station ID	Date	Collection Vessel	Location	Salinity	TSS ( $\mu\text{g g}^{-1}$ )
GSPS-19 Station 100	7/2/2019	R/V Blackbeard	Coastal	29.90	(21.68 $\pm$ 0.640)
GSPS-19 Station 101	7/2/2019	R/V Blackbeard	Coastal	29.70	(22.21 $\pm$ 3.33)
GSPS-19 Station 102	7/2/2019	R/V Blackbeard	Coastal	29.80	(19.26 $\pm$ 1.99)
GSPS-19 Station 103*	7/2/2019	R/V Blackbeard	Coastal	26.70	-
GSPS-19 Station 104	7/2/2019	R/V Blackbeard	Coastal	27.20	(21.07 $\pm$ 1.45)
GSPS-19 Station 105	7/3/2019	R/V Blackbeard	Estuary	20.10	(34.10 $\pm$ 8.06)
GSPS-19 Station 106	7/3/2019	R/V Blackbeard	Estuary	18.70	(29.65 $\pm$ 5.68)
GSPS-19 Station 107	7/3/2019	R/V Blackbeard	Estuary	15.90	(28.02 $\pm$ 1.02)
GSPS-19 Station 108	7/3/2019	R/V Blackbeard	Estuary	14.70	(21.66 $\pm$ 1.41)
GSPS-19 Station 109	7/3/2019	R/V Blackbeard	Estuary (Inlet)	13.98	(35.89 $\pm$ 7.06)
GSPS-19 Station 110	7/3/2019	R/V Blackbeard	Estuary	8.500	(35.96 $\pm$ 7.59)

## 2. Lignin Concentration

Values of  $L_8$  from this study are compared to salinity at each sampling station (Figure 11). Lignin concentrations varied between 2018 and 2019 at both the estuarine and coastal stations (Table 6 and 7). Detectable estuarine  $L_8$  values ranged from 0.09 – 53.23 mg g<sup>-1</sup> and 0.06 – 1.20 mg g<sup>-1</sup> in 2018 and 2019, respectively. Detectable coastal  $L_8$  values ranged from 0.27 – 138.74 mg g<sup>-1</sup> and 0.03 – 0.23 mg g<sup>-1</sup> in 2018 and 2019, respectively (Figure 12, Table 6).

The greatest lignin concentration range occurs in 2018 coastal samples, but the average is lower ( $24.04 \pm 56.21$  mg g<sup>-1</sup>) than the outlying highest value (strong outliers are anything over 3.0 x IQR added to the third quartile). Station 11 is an outlier, with an  $L_8$  value 13x higher than the second highest sample value within the coastal stations. The 2018 estuarine samples have an average  $L_8$  value of  $15.74 \pm 17.53$  mg g<sup>-1</sup> (Table 6). Average  $L_8$  values for 2019 are  $0.47 \pm 0.42$  mg g<sup>-1</sup> and  $0.14 \pm 0.08$  mg g<sup>-1</sup> for estuarine and coastal samples, respectively.  $L_8$  average values for estuarine samples are roughly four-times greater than coastal lignin concentrations. Average  $L_8$  values from 2019 are small compared to samples collected in 2018 (Figure 12), with lignin values being ~33 times and ~170 times greater in 2018 than 2019 in both estuarine and coastal samples, respectively.

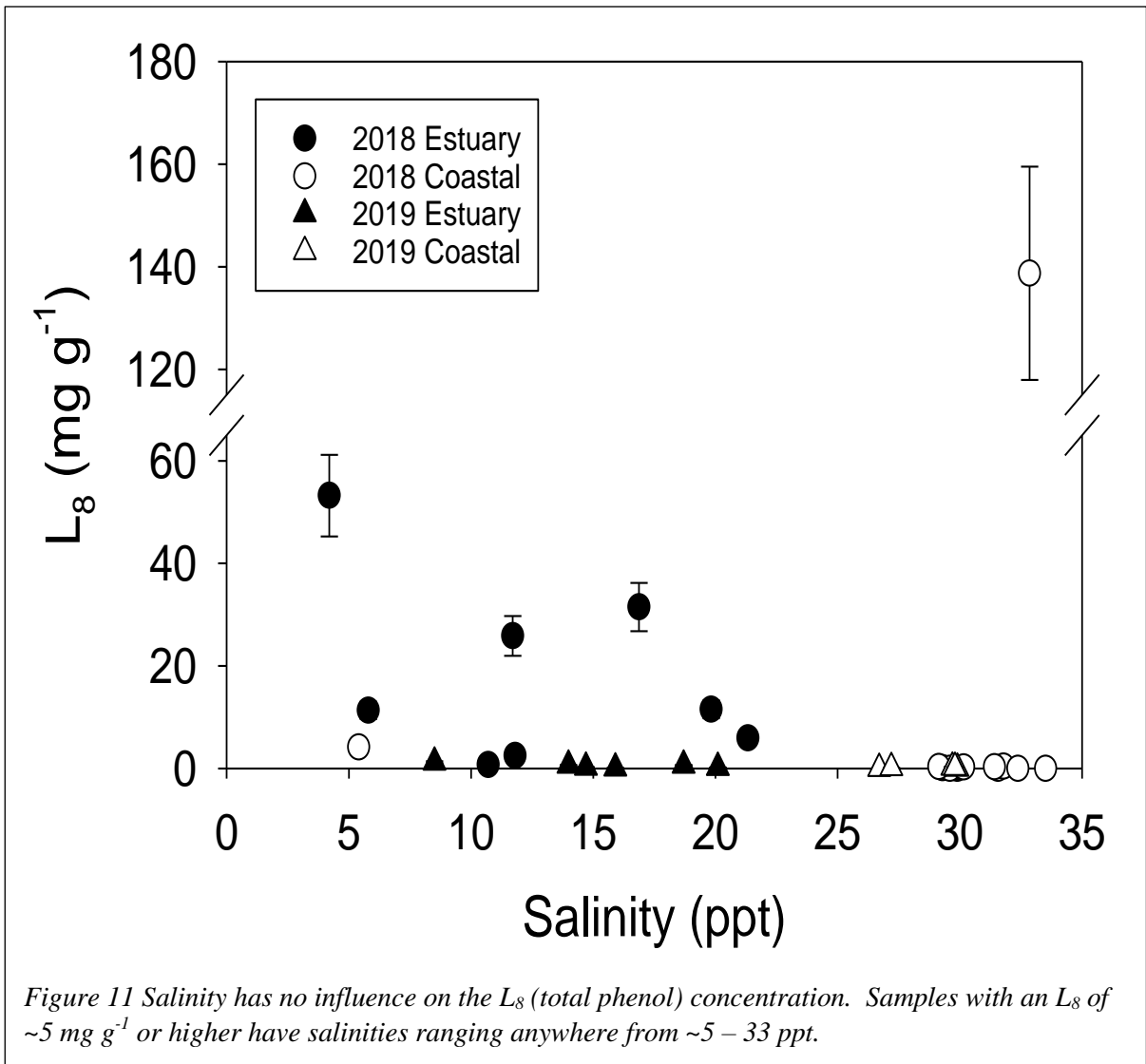


Table 6 Table showing 2018 station name,  $L_8$  values in  $\text{mg g}^{-1}$ , syringyl: vanillyl ratios (S/V), cinnamyl: vanillyl ratios (C/V), and acid to aldehyde ratios for vanillyl ( $\text{Ad/Al}_v$ ) and syringyl ( $\text{Ad/Al}_s$ ) phenols. *n.d.* indicates that a phenol is non-detectable, thus there are no possible V, S or C values to create the ratios listed below.

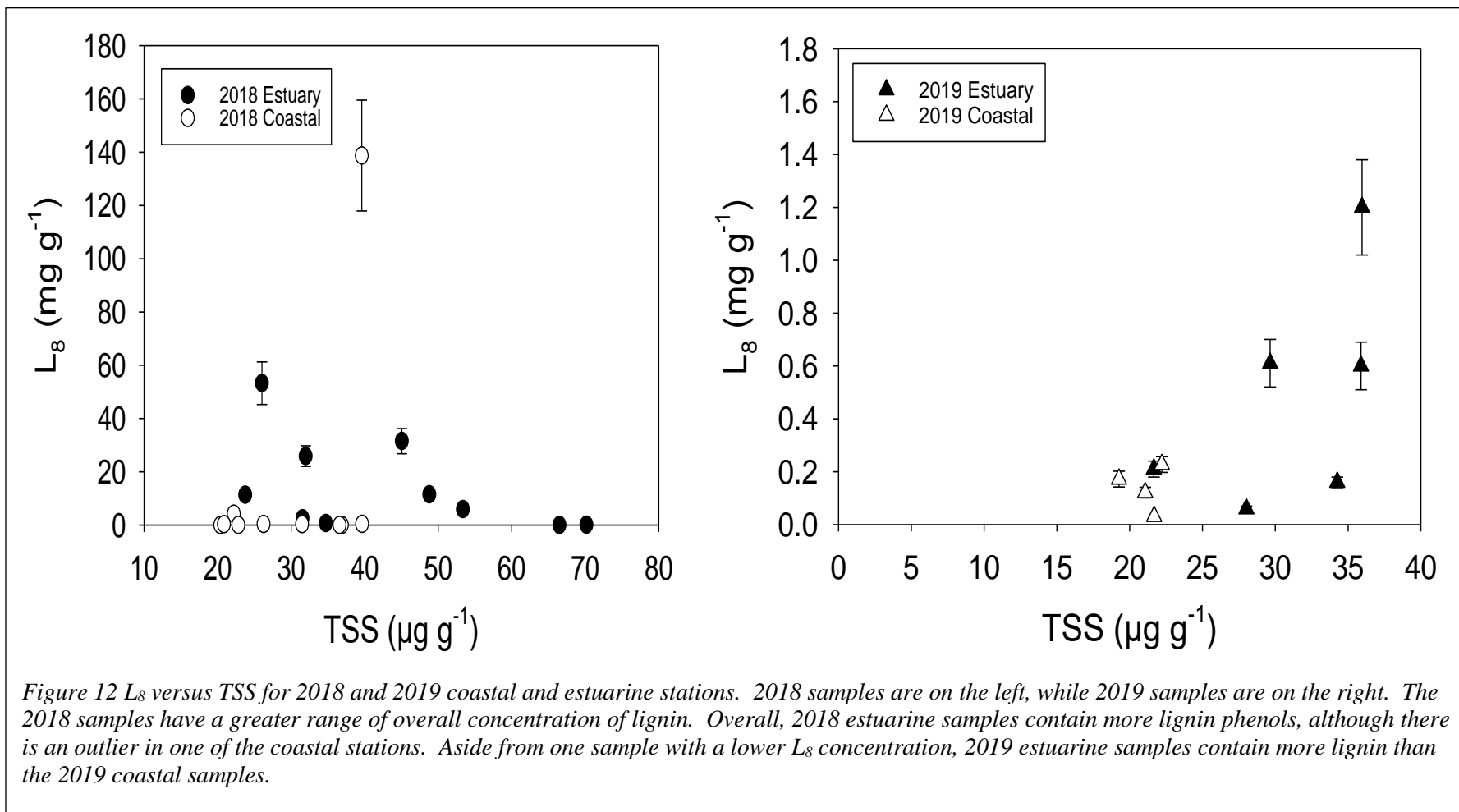
Station ID	$L_8$	S/V	C/V	$[\text{Ad/Al}]_v$	$[\text{Ad/Al}]_s$
GSPS-18 Station 1	$5.9 \pm 0.89$	1.1	2.3	6.2	<i>n.d.</i>
GSPS-18 Station 2	$32 \pm 4.7$	0.88	1.1	11	0.62
GSPS-18 Station 3	$26 \pm 3.9$	<i>n.d.</i>	<i>n.d.</i>	3.9	<i>n.d.</i>
GSPS-18 Station 4	$2.5 \pm 0.37$	<i>n.d.</i>	<i>n.d.</i>	<i>n.d.</i>	<i>n.d.</i>
GSPS-18 Station 5	$12 \pm 1.7$	<i>n.d.</i>	<i>n.d.</i>	2.2	<i>n.d.</i>
GSPS-18 Station 6	<i>n.d.</i>	<i>n.d.</i>	<i>n.d.</i>	<i>n.d.</i>	<i>n.d.</i>
GSPS-18 Station 7	$0.09 \pm 0.01$	<i>n.d.</i>	<i>n.d.</i>	0.00	<i>n.d.</i>
GSPS-18 Station 8	$0.72 \pm 0.11$	0.00	0.49	0.76	<i>n.d.</i>
GSPS-18 Station 9	$11 \pm 1.7$	0.98	0.32	1.1	2.8
GSPS-18 Station 10	<i>n.d.</i>	<i>n.d.</i>	<i>n.d.</i>	<i>n.d.</i>	<i>n.d.</i>
GSPS-18 Station 11	$140 \pm 21$	1.2	1.7	<i>n.d.</i>	<i>n.d.</i>
GSPS-18 Station 12	$0.41 \pm 0.06$	0.00	0.00	<i>n.d.</i>	<i>n.d.</i>
GSPS-18 Station 13	<i>n.d.</i>	<i>n.d.</i>	<i>n.d.</i>	<i>n.d.</i>	<i>n.d.</i>
GSPS-18 Station 14	$0.33 \pm 0.05$	0.32	<i>n.d.</i>	2.4	<i>n.d.</i>
GSPS-18 Station 50	$53 \pm 8.0$	0.78	0.97	4.3	<i>n.d.</i>
GSPS-18 Station 51	$4.2 \pm 0.63$	0.13	0.57	0.89	<i>n.d.</i>
GSPS-18 Station 52	<i>n.d.</i>	<i>n.d.</i>	<i>n.d.</i>	<i>n.d.</i>	<i>n.d.</i>
GSPS-18 Station 53	<i>n.d.</i>	<i>n.d.</i>	<i>n.d.</i>	<i>n.d.</i>	<i>n.d.</i>
GSPS-18 Station 54	$0.29 \pm 0.04$	0.00	0.00	0.00	<i>n.d.</i>
GSPS-18 Station 55	$0.27 \pm 0.04$	0.00	0.00	0.00	<i>n.d.</i>

Table 7 2019 station name,  $L_8$  values in  $\text{mg g}^{-1}$ , syringyl: vanillyl ratios (S/V), cinnamyl: vanillyl ratios (C/V), and acid to aldehyde ratios for vanillyl ( $\text{Ad/Al}_v$ ) and syringyl ( $\text{Ad/Al}_s$ ) phenols.

*n.d.* indicates that a phenol is non-detectable, thus there are no possible V, S or C values to create the ratios listed below.

Station ID	$L_8$	S/V	C/V	$[\text{Ad/Al}]_v$	$[\text{Ad/Al}]_s$
GSPS-19 Station 100	$0.03 \pm 0.01$	0.66	2.8	2.2	<i>n.d.</i>
GSPS-19 Station 101	$0.23 \pm 0.03$	0.88	1.3	3.0	<i>n.d.</i>
GSPS-19 Station 102	$0.17 \pm 0.03$	<i>n.d.</i>	<i>n.d.</i>	3.6	<i>n.d.</i>
GSPS-19 Station 103*	-	-	-	-	-
GSPS-19 Station 104	$0.12 \pm 0.02$	<i>n.d.</i>	<i>n.d.</i>	3.0	19
GSPS-19 Station 105	$0.16 \pm 0.02$	<i>n.d.</i>	<i>n.d.</i>	3.3	<i>n.d.</i>
GSPS-19 Station 106	$0.61 \pm 0.09$	0.21	0.69	1.1	<i>n.d.</i>
GSPS-19 Station 107	$0.06 \pm 0.01$	0.33	0.54	1.3	<i>n.d.</i>
GSPS-19 Station 108	$0.21 \pm 0.03$	<i>n.d.</i>	<i>n.d.</i>	1.6	3.1
GSPS-19 Station 109	$0.60 \pm 0.09$	<i>n.d.</i>	<i>n.d.</i>	<i>n.d.</i>	<i>n.d.</i>
GSPS-19 Station 110	$1.20 \pm 0.18$	<i>n.d.</i>	<i>n.d.</i>	1.6	0.77

\*Insufficient water available for chemical analyses at Station 103.



### 3. Lignin Monomers in Suspended Sediments

Detectable vanillyl phenol concentration range in 2018 ( $0.09 - 35.66 \text{ mg g}^{-1}$ ) was substantially higher than the detectable concentrations in 2019 ( $0.01 - 0.69 \text{ mg g}^{-1}$ ). Detectable phenol concentrations in 2018 range from  $0.09 - 19.33 \text{ mg g}^{-1}$  and  $0.25 - 35.66 \text{ mg g}^{-1}$  in estuarine and coastal samples, respectively. Detectable phenol concentration in 2019 range from  $0.03 - 0.69$  and  $0.01 - 0.15 \text{ mg g}^{-1}$  in estuarine and coastal samples, respectively.

A comparison of vanillyl phenol concentrations (VAL + VON + VAD) in the estuary between 2018 and 2019, suggests that phenol concentrations are at some points full orders of magnitude higher post-storm than they are during the non-storm period (Appendix Table 10, 11; Figure 13). In 2018, there was an overall greater amount of vanillyl phenols in both the estuary and coastal system compared to the following year. The highest estuarine vanillyl phenol concentration in 2018 is ~45-times greater than the highest estuarine vanillyl phenol concentration in 2019. The highest coastal vanillyl phenol concentration in 2018 is ~238-times higher than the highest coastal vanillyl phenol concentration in 2019. Station 1 and 105 are relatively close to one another but were sampled in 2018 and 2019, respectively. Samples from both stations contain VAL and VAD but not VON with quantities for the two vanillyl group monomers in 2018 being greater than those in 2019. Station 2 and 106 are in roughly the same location – in 2018 there is roughly 10-times more vanillin, and 35-times more vanillic acid than in 2019. There is no acetovanillone in estuarine samples in 2018, but it is found in one 2019 sample. Samples from Station 110 have the greatest quantity of both vanillin and vanillic acid for the 2019 samples. Plots C and D in Figure 13 show coastal vanillyl phenol concentrations for 2018 and 2019. Four samples, from Stations 10, 13, 52 and 53 in 2018 did not contain any vanillyl phenols. Samples 10 and 13 are directly next to each other, Station 53 is ~50 km away

from the Outer Banks, and Station 52 is the farthest Station from the Outer Banks. There were lower overall phenol concentrations in 2019, but each of the samples contained multiple vanillyl phenols.

Figure 14 shows the estuarine syringyl (SAL + SON + SAD) phenol concentrations in 2018 (A) and 2019 (B). In both graphs, syringaldehyde is the most common monomer, while acetosyringone is not found at any of the sample sites. Syringaldehyde is found in four samples: 2, 9, 108, and 110. Stations 9 and 110 are in the same location, while Stations 2 and 108 are ~20 km from each other. The 2018 samples have the greatest range of syringyl phenols, with detectable values ranging from 0.70 – 15.15 mg g<sup>-1</sup>, and 0.08 – 41.32 mg g<sup>-1</sup> for estuarine and coastal samples, respectively. The 2019 samples have phenol concentrations ranging from 0.01 – 0.27 mg g<sup>-1</sup> and 0.001 – 0.005 mg g<sup>-1</sup> for estuarine and coastal samples, respectively. Greater quantities of syringyl phenols occur in 2018 at all stations except the one instance of SAD in sample 109 in 2019. Figure 14 also shows coastal syringyl phenol concentrations for 2018 (C) and 2019 (D). There are no instances of syringaldehyde or acetosyringone in 2018, and only three instances of syringic acid. There are seven samples that do not contain any syringyl phenols, two that have relatively low phenol concentrations (~ 0.1 – 0.25 mg g<sup>-1</sup>) and only one sample contains a high phenol concentration (~40 mg g<sup>-1</sup>). There is also no acetosyringone in 2019 coastal samples and only one of these contained syringaldehyde. Stations 100-104 occur in a nearly straight line. Some samples that had no syringic acid in 2018 contained syringic acid in 2019. Even if we were to remove the outlier value located at Station 11, there would still be almost an order of magnitude difference between syringyl concentrations between 2018 and 2019 in the stations where it is present.

Figure 15 shows estuarine cinnamyl (CAD + FAD) phenol concentrations in 2018 (A) and 2019 (B), and coastal phenol concentrations in 2018 (C) and 2019 (D). The stations closest to Oregon Inlet (6 and 7) do not contain cinnamyl phenols. Samples 1, 105, 2, 106, 4, 107, 50 and 108 all have both CAD and FAD. Stations 9 and 110 only have CAD, while stations 5 and 109 only have FAD. Overall, cinnamyl phenol concentrations are greater in 2018 estuarine ( $5.61 \pm 6.27 \text{ mg g}^{-1}$ ) and coastal ( $31.48 \pm 42.82 \text{ mg g}^{-1}$ ) samples, than in 2019 estuarine ( $0.11 \pm 0.08 \text{ mg g}^{-1}$ ) and coastal ( $0.04 \pm 0.02 \text{ mg g}^{-1}$ ) samples. Cinnamyl phenols in 2018 ranged from  $0.27 - 61.76 \text{ mg g}^{-1}$ , while 2019 samples ranged from  $0.01 - 0.06 \text{ mg g}^{-1}$ . Concentration differences also varied between estuarine and coastal sample stations. Detectable cinnamyl phenol concentrations range from  $0.17 - 18.75 \text{ mg g}^{-1}$  and  $1.20 - 61.76 \text{ mg g}^{-1}$  in estuarine and coastal samples, respectively. Detectable cinnamyl phenol concentrations range from  $0.06 - 0.24 \text{ mg g}^{-1}$  and  $0.01 - 0.05 \text{ mg g}^{-1}$  in estuarine and coastal samples, respectively. Of the two samples that contained cinnamyl phenols, only one contained both CAD and FAD monomers. In 2019, all samples contained cinnamyl phenols, although the concentrations were lower than those of the two samples in 2018. Samples 101, 102 and 104 contain both CAD and FAD, while sample 100 contained only CAD.

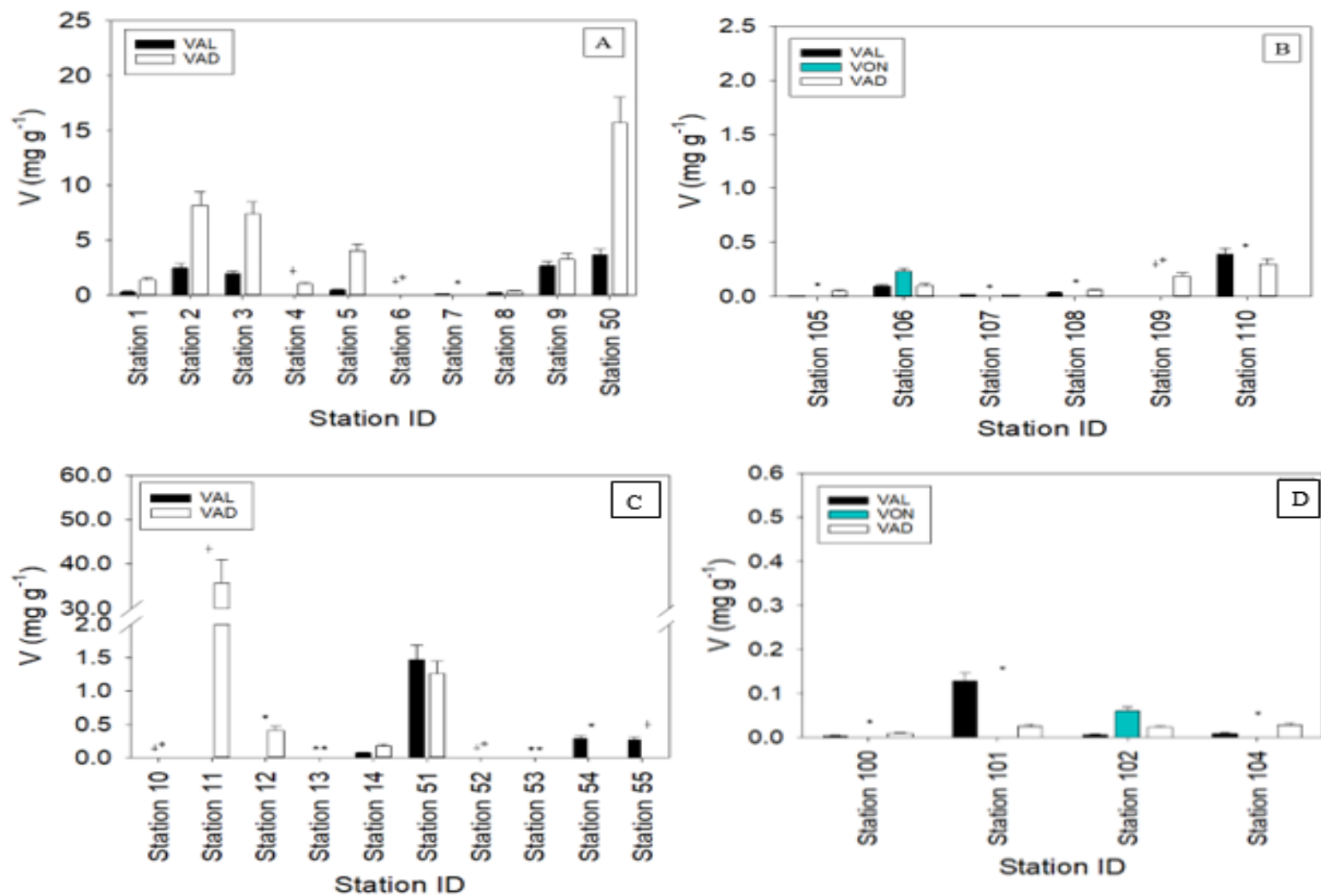


Figure 13 Vanillyl phenol (VAL, VON, VAD) concentrations for 2018 (A) and 2019 (B) estuarine and 2018 (C) and 2019 (D) coastal stations. Note the decrease in magnitude of vanillyl concentrations between the 2018 and 2019 samples. The x-axis is station ID. The y-axis is phenol concentration expressed as milligram per gram of suspended particulates isolated on glass fiber filters (GFF); see Methodology for details. Vanillin concentrations are in black, acetovanillone concentrations in blue, and vanillic acid concentrations in white. Symbols are in the same order as the monomers listed in the legend.

\* indicates that a phenol is not detectable (ND)

† indicates that a phenol is not quantifiable (NQ).

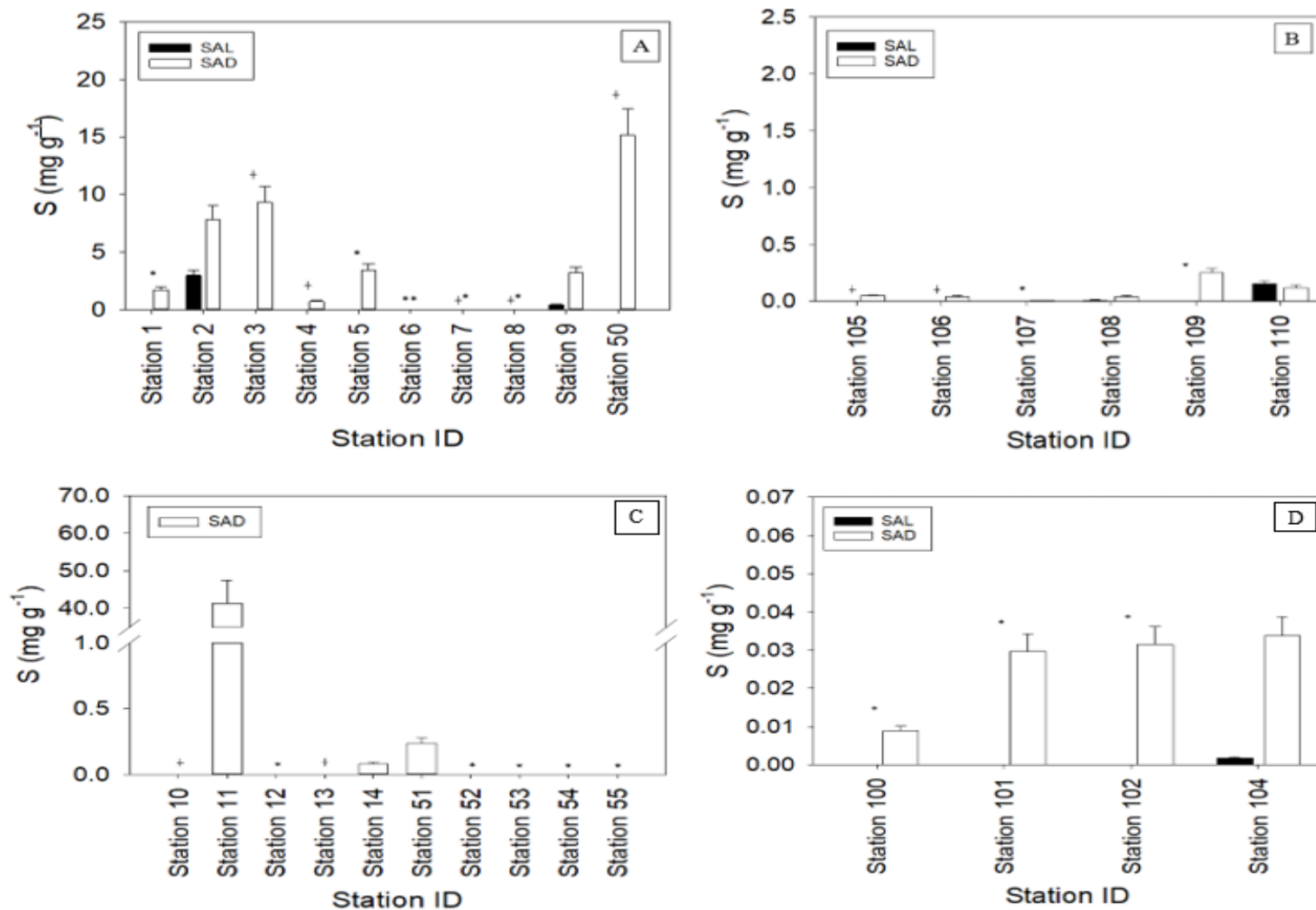


Figure 14 Syringyl phenol (SAL, SON, SAD) concentrations for 2018 (A) and 2019 (B) estuarine stations and 2018 (C) and 2019 (D) coastal stations. Note the decrease in magnitude of syringyl concentrations between the 2018 and 2019 samples. The x-axis is station ID. The y-axis is phenol concentration expressed as milligram per gram of suspended particulates isolated on glass fiber filters (GFF); see Methodology for details. Syringaldehyde is in black and syringic acid is white. There is no acetosyringone in these samples

Symbols are in the same order as the monomers listed in the legend.

\* indicates that a phenol is not detectable (ND)

† indicates that a phenol is not quantifiable (NQ).

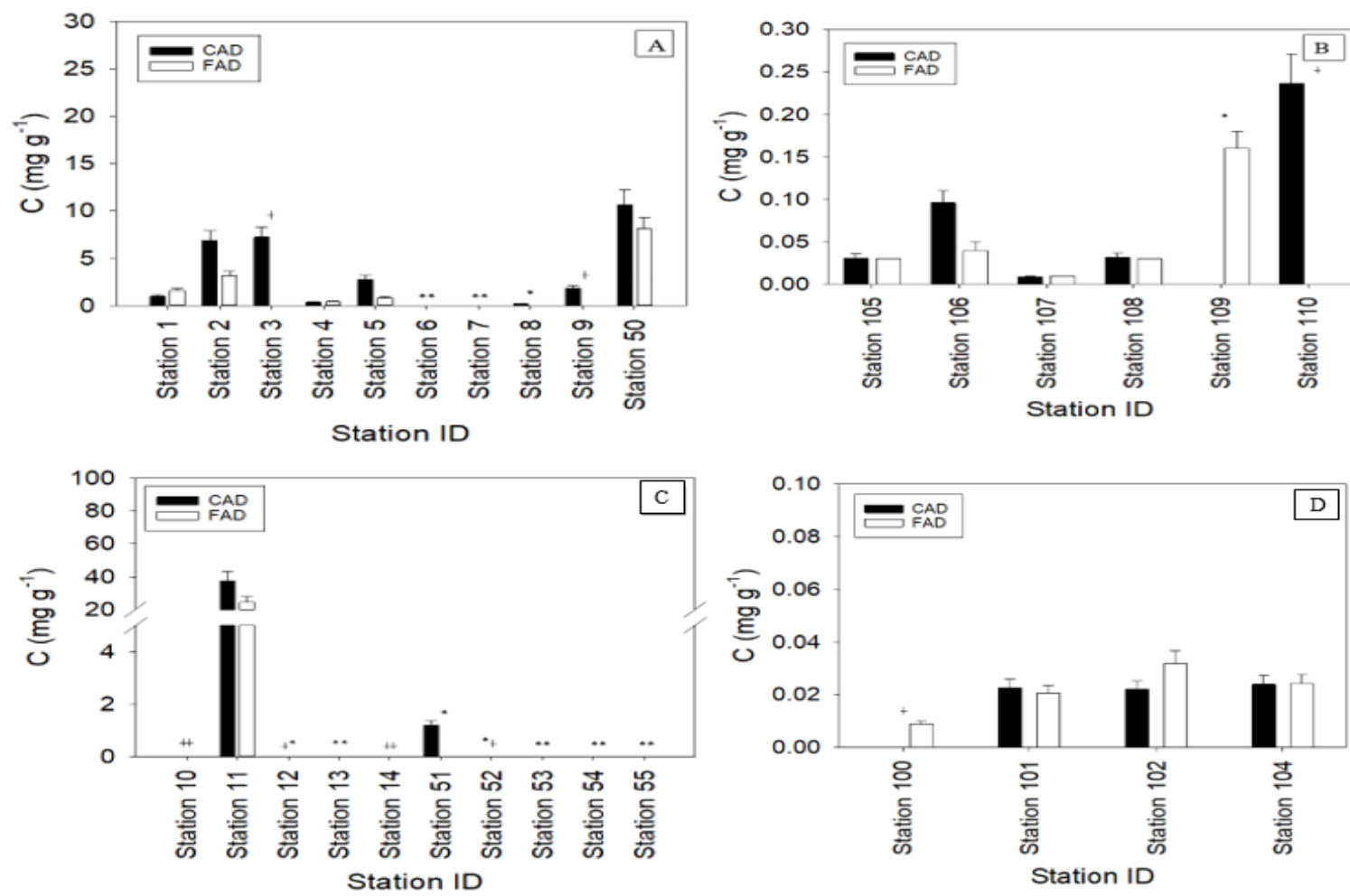


Figure 15 Cinnamyl phenol (CAD, FAD) concentrations for 2018 (A) and 2019 (B) estuarine sample stations and 2018 (C) and 2019 (D) coastal samples. Note the decrease in magnitude of syringyl concentrations between the 2018 and 2019 samples. The x-axis is station ID. The y-axis is phenol concentration expressed as milligram per gram of suspended particulates isolated on glass fiber filters (GFF); see Methodology for details. *P*-coumaric acid is in black, and ferulic acid is white.

Symbols are in the same order as the monomers listed in the legend.

\* indicates that a phenol is not detectable (ND)  
 † indicates that a phenol is not quantifiable (NQ).

## 4. Lignin Interclass Ratios

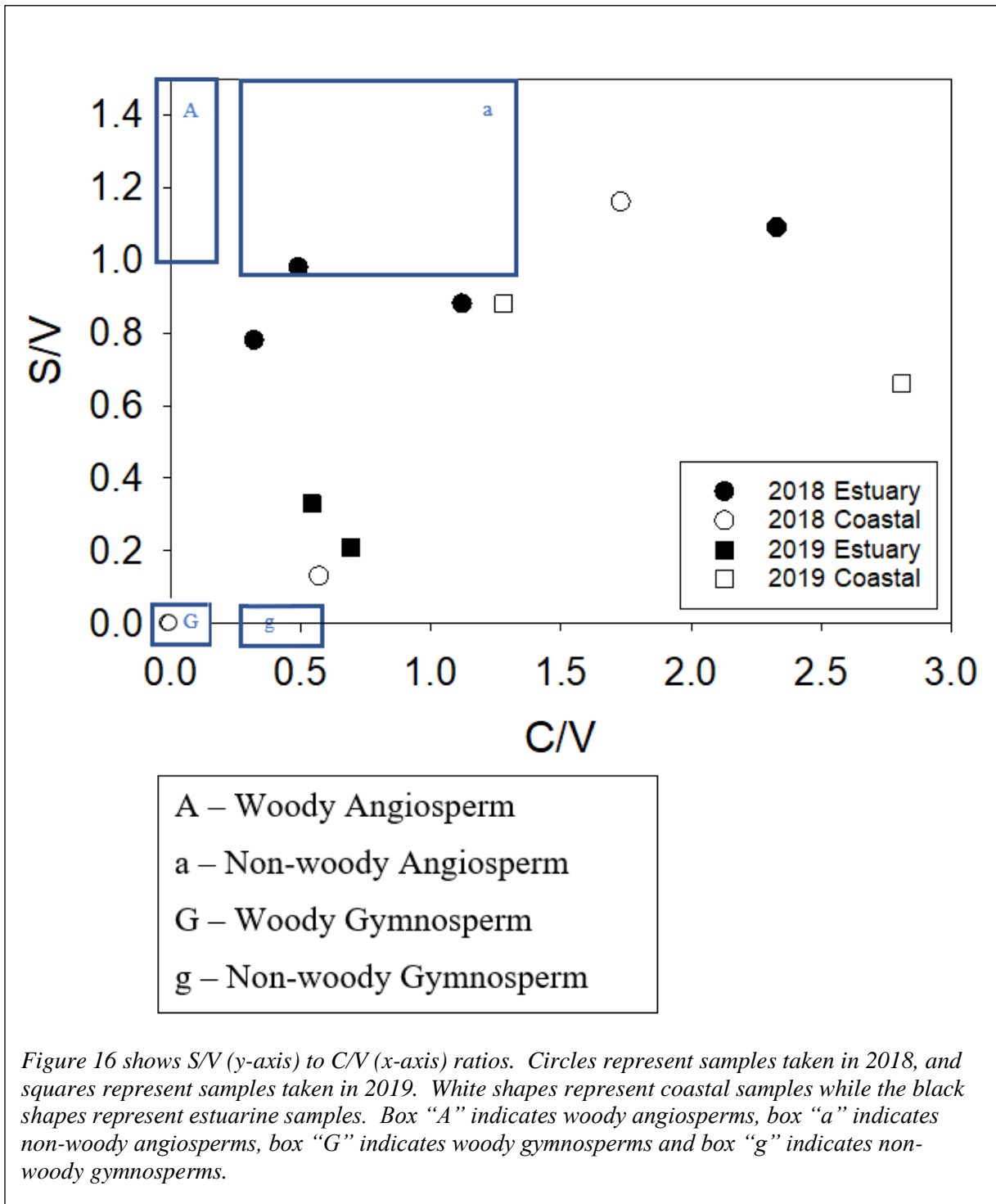
### 4.1 S/V and C/V Ratios

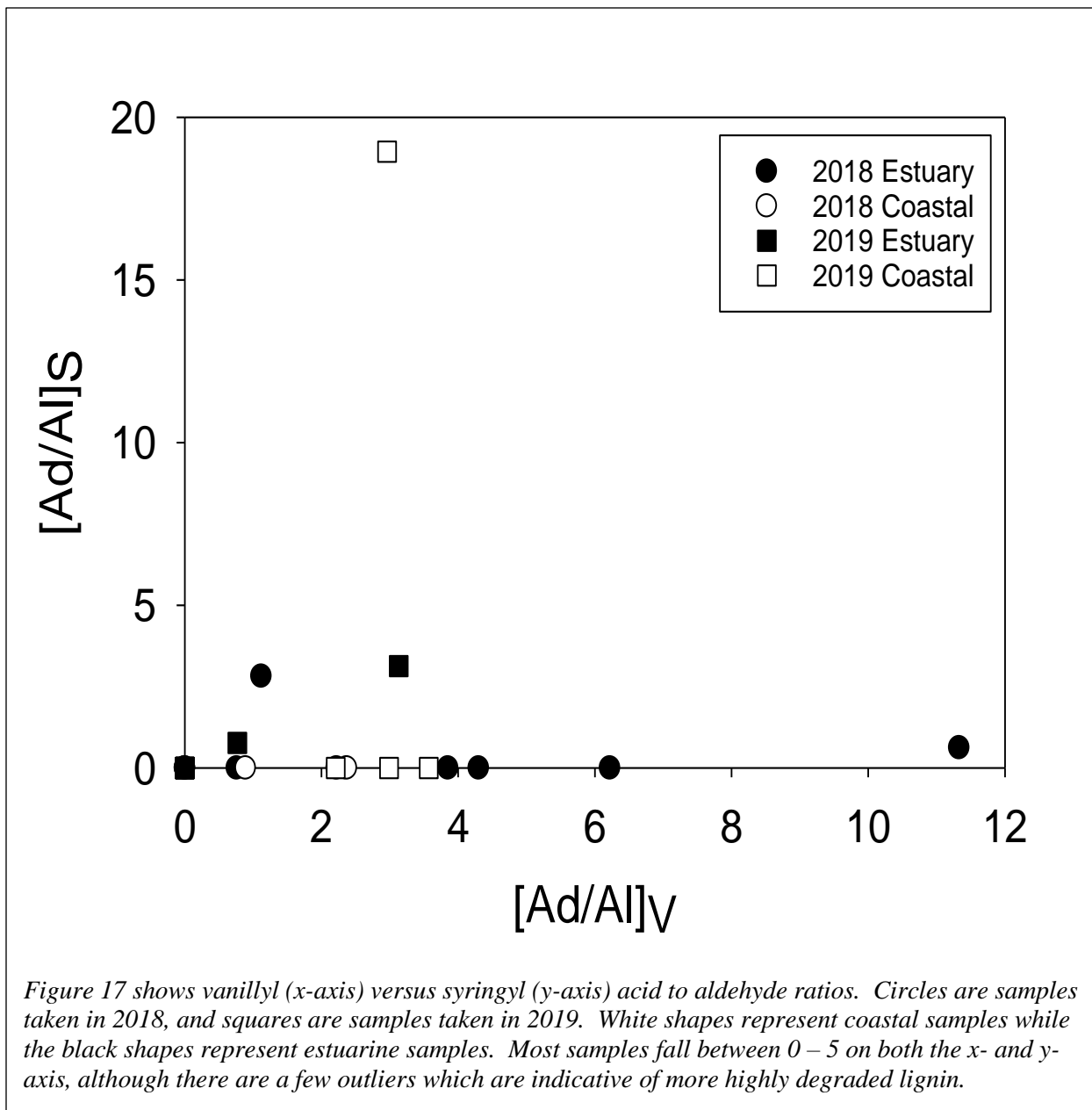
As mentioned before,  $V > 0$  indicates vascular plant tissue,  $S > 0$  is indicative of angiosperm plant tissue, while  $C > 0$  indicates that the plant tissue is non-woody. Figure 16 shows S/V (y-axis) to C/V (x-axis) ratios. The blue boxes within each image indicate whether the sample is derived from a woody or non-woody angiosperm or gymnosperm (Cathalot *et al.*, 2013). Most sample ratios fall outside of these boxes. All samples fall between 0 – 1.2 for their S/V ratio, and ~0 – 2.8 for their C/V ratio. By looking at Figure 16, one estuarine sample can be directly categorized as a non-woody angiosperm, while one coastal sample can be identified as a woody gymnosperm. In 2018, seven samples have a  $C > 0$ , and an  $S > 0$  which indicates that these samples are derived from non-woody angiosperm plant tissue (Table 6; Figure 16). Four samples have an  $S/V = 0$  and three of these have a  $C/V = 0$ , indicating that there are four samples containing gymnosperm tissue, three of which are woody and one of which is non-woody. Of the seven samples containing angiosperm plant tissue, four were found in the estuary while three came from coastal samples. Of the four samples containing gymnosperm plant tissue, the three woody samples came from the coastal ocean while the one non-woody sample was estuarine derived. In 2019, only four samples showed S/V and C/V ratios (Table 7; Figure 16). All four samples have  $S/V$  and  $C/V > 0$ , indicating that these samples are derived from non-woody angiosperm plant tissue. Two of these samples came from the estuary and two came from the coastal ocean.

### 4.2 Acid to Aldehyde Ratios

Acid to aldehyde (Ad/Al) ratios help determine the level of degradation of lignin products (Figure 17). For vanillyl phenols,  $[Ad/Al]_v$ , is the ratio of vanillic acid to vanillin while

the Ad/Al ratio for syringyl phenols,  $[Ad/Al]_s$ , is the ratio of syringic acid to syringaldehyde. Figure 17 shows acid to aldehyde ratios for 2018 and 2019 estuarine and coastal samples. Most samples fall between 0 – 5 on both the  $Ad/Al_v$  and  $Ad/Al_s$  axis, with only four samples, regardless of year or location, falling outside of that range. Higher Ad/Al generally refers to a higher level of sample degradation, while lower Ad/Al, typically  $<0.8$ , indicates fresh plant material (Qiao *et al.*, 2019). The data here suggests that samples were a mix of both fresh and highly degraded plant matter.





## V. DISCUSSION

Storm strength will increase in the future as a function of climate change (IPCC, 2022). Increasing storm strength is commensurate with increase in precipitation and wind speeds, causing excessive amounts of erosion and higher instances of resuspension within coastal systems (Bianucci *et al.*, 2018). This study quantified storm-derived lignin in suspended sediments with the purpose of better understanding the difference in terrestrial input between storm and non-storm periods within both the estuarine system and adjacent coastal ocean. Better understanding of organic inputs caused by a storm period compared to a non-storm quiescent period can shed light on how hurricanes may affect the APES in the future.

### 1. Salinity and Suspended Sediment

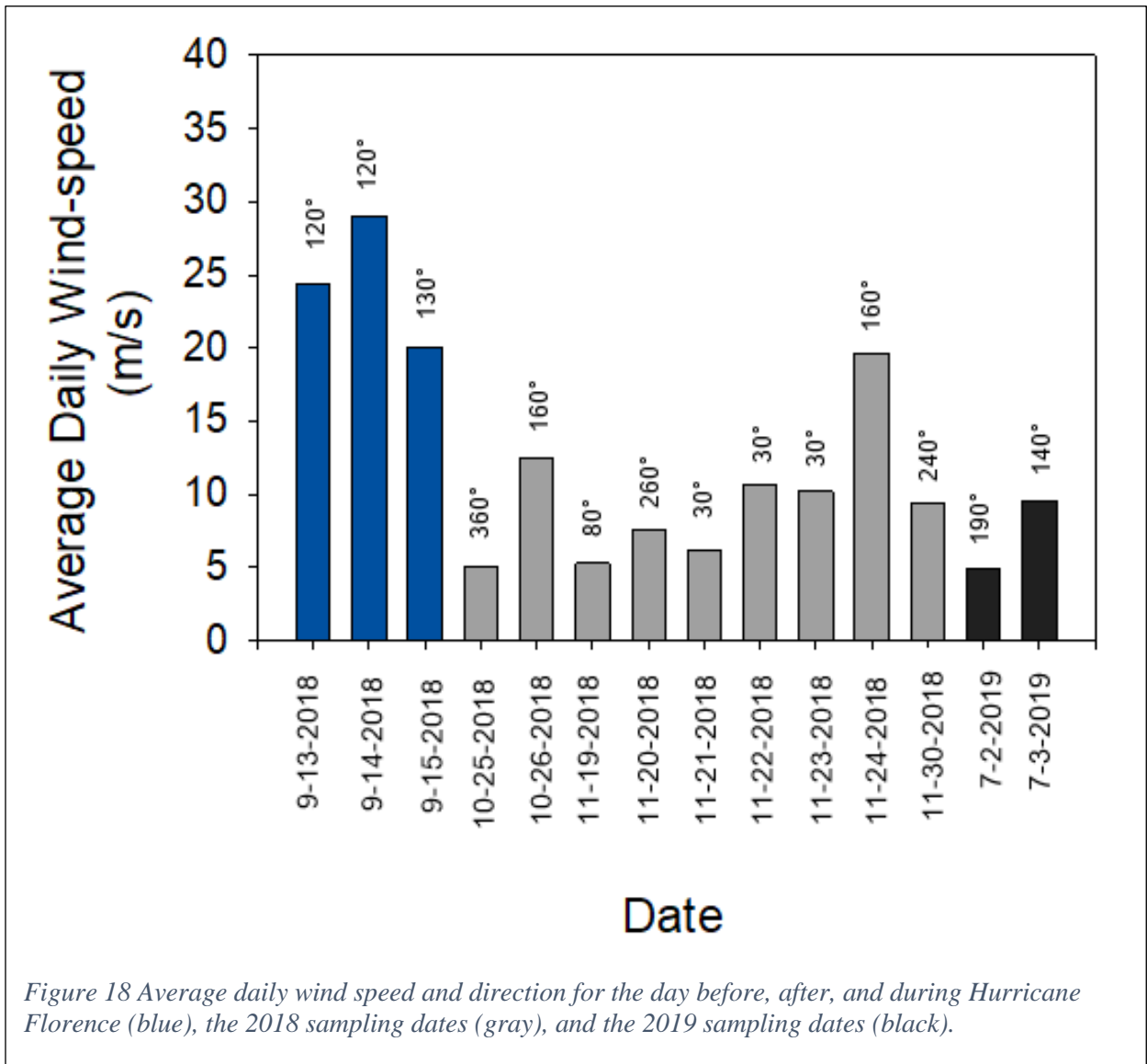
Coastal sea surface salinity is impacted by precipitation, runoff, ocean currents, evaporation, and ice melt (Talley, 2002). Salinity within the APES undergoes spatial and seasonal variation due to differing riverine discharge from season to season (Jia & Li, 2012). Fresh water inflows from riverine sources and salt exchange through the inlets are the primary influencers of salinity, while gravitational force and wind energy are the primary drivers of circulation within the estuarine system (Jia & Li, 2012).

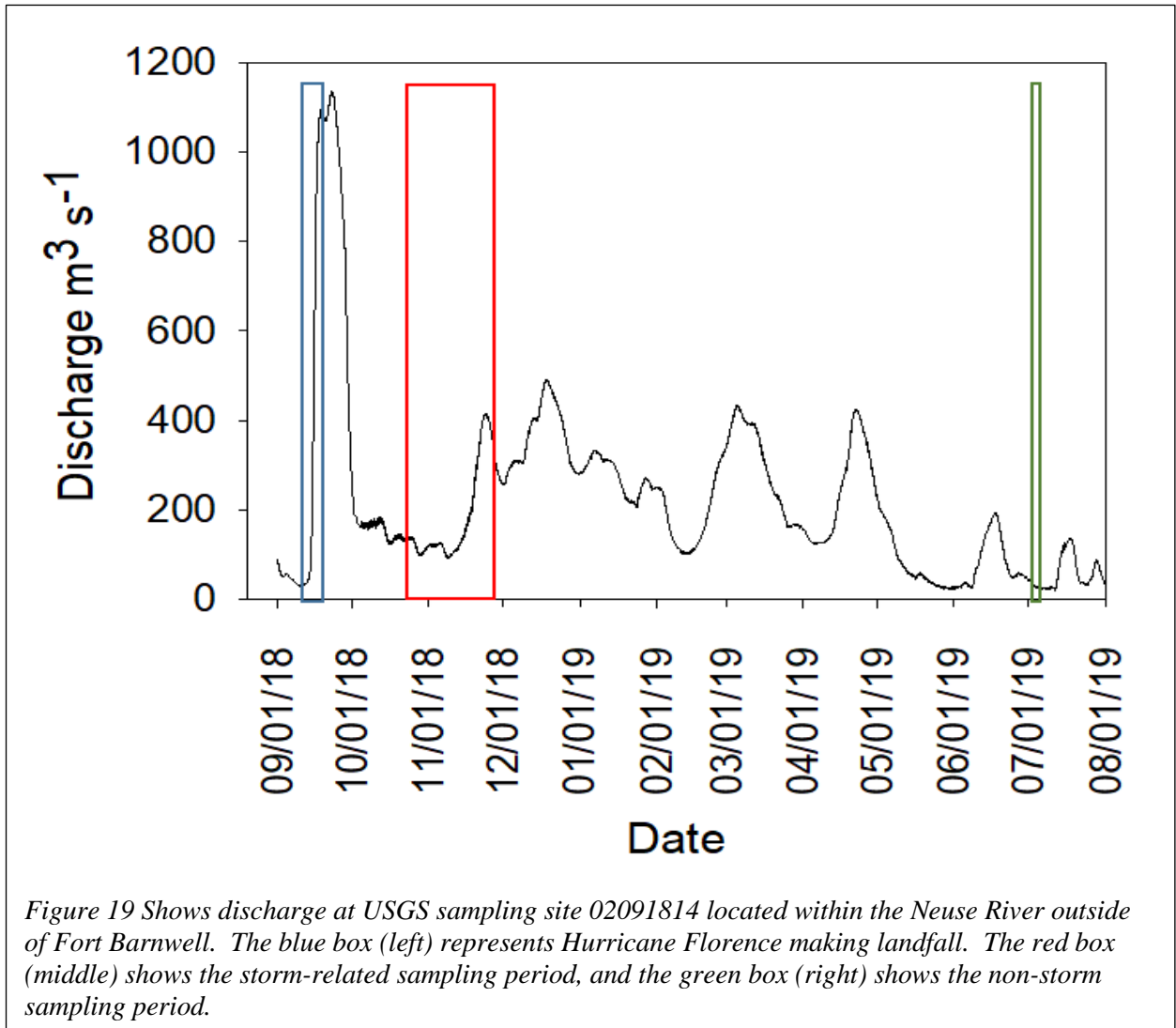
Salinity values measured at 2018 sample stations differ minimally from the salinity values measured at the same stations in 2019, which could be due to the amount of time between the storm and the sampling dates, as well as the location of runoff, with much of the storms-derived runoff coming through the Tar-Pamlico and Neuse Rivers (Stewart & Berg, 2019). It is possible that the freshwater from the storms exited the estuary as a lens on top of the estuarine water prior to our intermittent sampling. It is also possible that the volume of rainwater introduced during the 2018 storm season did not appreciably dilute the salinity in the estuary given its large volume

( $2.6 \times 10^{10} \text{ m}^3$ ; Giese et al., 1979). In general, for both years, lowest salinity values occurred at the stations furthest north of Oregon Inlet. Tidal activity may have affected salinity during our sampling periods. Tide prediction tables suggested tides ranging from 0.73 – 0.86 m would occur between September 10<sup>th</sup> – September 15<sup>th</sup> near Oregon Inlet (NOAA, 2022.), with an actual observed storm tide of ~ 0.7 m at Oregon Inlet on September 13<sup>th</sup> (Stewart & Berg, 2019).

Coastal stations have the least variation in salinity, indicating that, during the time of sampling, precipitation associated with hurricane Florence had little impact to these areas. Estuarine stations had a wider range of salinity, potentially due to varying fresh water and coastal input, as well as varying wind speeds leading to estuarine mixing (Figure 18). The 2018 coastal salinities could be higher than those in 2019 for a variety of reasons including: ocean circulation, wind mixing, or freshwater outflow from the estuary.

Runoff, erosion, and resuspension caused by storms led to a greater quantity of TSS deposition than during a non-storm period. Overall, 2018 estuarine samples had the highest TSS values. The highest 2018 estuarine TSS value ( $70.16 \mu\text{g g}^{-1}$ ) is roughly twice that of the highest 2019 estuarine TSS value ( $35.96 \mu\text{g g}^{-1}$ ). The highest 2018 coastal TSS value ( $39.64 \mu\text{g g}^{-1}$ ) is almost 45% higher than the highest 2019 coastal TSS value ( $22.21 \mu\text{g g}^{-1}$ ). This indicates that heavy rainfall, runoff, and wind-driven erosion associated with the 2018 hurricane season did have an impact on the amount of TSS in both the estuary and the coastal ocean. from the storm Using MODIS-derived TSS maps, Chen *et al.* (2009) described a substantial increase of TSS concentrations in Apalachicola Bay Florida during and directly after Hurricane Frances (Sept. 2004) compared to non-storm conditions indicating that extreme winds from the storm led to sediment resuspension. Cheng *et al.* (2013) found that in 2011, tropical storm Lee caused





flooding of the Susquehanna River which led to 6.7 tons of suspended sediments to be discharged into the Chesapeake Bay. This was equivalent to six years' worth of sediment input in that system. Ward *et al.* (2012) suggest that storms play a crucial role in the mobilization of suspended sediment and found that TSS concentrations were correlated with river discharge for all samples. Apalachicola Bay TSS concentrations ranged from 0.3 – 135 mg L<sup>-1</sup>, while Barataria Bay TSS concentrations ranged from 25 – 165 mg L<sup>-1</sup> (Arellano *et al.*, 2019). Like this study, TSS in Barataria Bay increased during the April storms indicating marsh sediment erosion and resuspension of sediments, while Apalachicola Bay TSS was highest closest to the mouths of the rivers, indicating input of terrestrial derived organic matter coming from the rivers. Hernes *et al.*, (2020) found that TSS was highest in samples taken after a storm period as opposed to samples in the same locations taken during a non-storm period. In some cases, these storm period samples were a full order of magnitude higher than non-storm samples.

North Carolina contains over 23,000 km<sup>2</sup> of wetlands (Vernon Carle, 2011). Wetlands play a role in regulating the fresh water, nutrient, and sediment loading into the estuarine system (Bales & Newcomb, n.d.). Roughly 50% of these wetlands are bottomland hardwood forests, occurring primarily along the Roanoke, Neuse, Tar and Cape Fear rivers, and consisting of cypress, and swamp and black gum in the wettest areas, and red maple, green ash, elm, sycamore, and sweet gum trees in areas that only seasonally flood (Bales & Newcomb, n.d.). Estuarine woody wetlands contain pine, cedars, maples, and sweet gums (NC DEQ, 1997.). Fringe wooded swamps dominate the Albemarle Sound shoreline and present in portions of Pamlico Sound tributaries, consisting primarily of cypress trees. Salt marshes surrounding the APES consist of cord grasses, needlerush and glasswort (Adams, 1963).

Coastal North Carolina contains both woody (oak, eastern redbud), and non-woody (seagrasses, cordgrass, oak leaves, etc.) angiosperms and woody (loblolly pine, cedar, cypress) and non-woody (conifer or pine needles) gymnosperms (Tallamy, 2013), all of which may be contributing to the terrestrial organic matter within the estuary and coastal ocean. Barrier island vegetation zones consist of the oceanfront, dunes, maritime forest, and marsh (Figure 20) that contain mixtures of both angiosperms and gymnosperms. Salt marshes are found on the sound side of the barrier island system are characterized by various marsh grasses (angiosperms) such as salt grass, black needlerush, sea lavender or cordgrass (Burk, 1962.). These areas tend to lack trees. The maritime forests of the Outer Banks are dominated by oaks, cedars, loblolly pines, and various other trees (gymnosperms), and shrubs such as swamp palmettos and holly's (angiosperm) (Bellis, 1995). Dunes contain sea oats, beach grass and switch grasses (angiosperms), while beaches contain little to vegetation (Burk, 1962).

In addition to these stationary sources of enriched organic matter, shorelines throughout the APES are naturally eroding (Cowart *et al.*, 2010) with the highest rates of erosion occurring along sediment banks (Cowart *et al.*, 2011), and an average erosion rate of ~30 cm per year (Corbett *et al.*, 2008). TSS was greater within the APES in samples taken soon after Hurricane Florence.

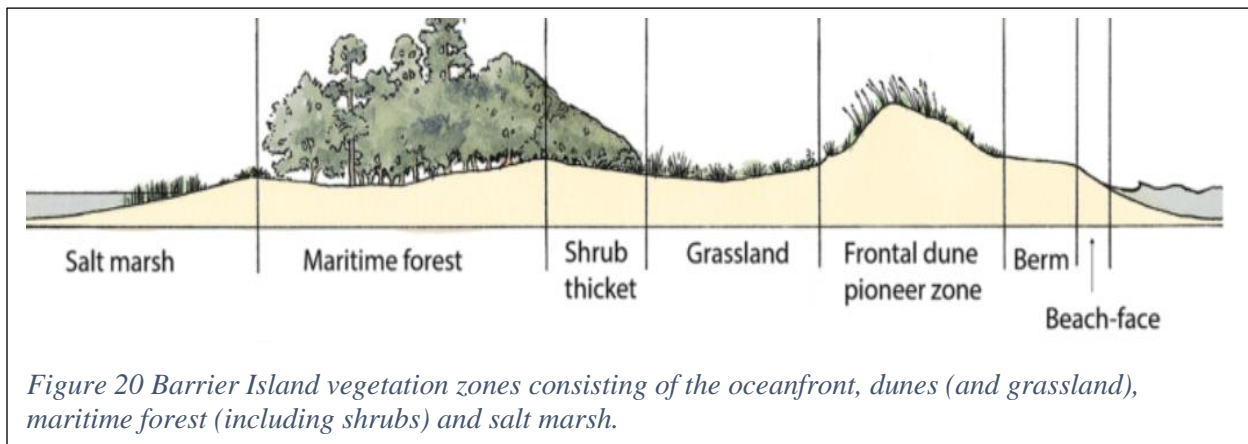


Figure 20 Barrier Island vegetation zones consisting of the oceanfront, dunes (and grassland), maritime forest (including shrubs) and salt marsh.

## 2. Pre- and Post-Storm Lignin Abundances

In the APES,  $L_8$  values vary depending on the year and the location in which they were taken. When comparing the estuary versus coastal ocean for each year, the highest  $L_8$  values occurred primarily within the estuary in both 2018 and 2019. Lignin abundances are higher within the estuary than coastal samples, regardless of year, indicating that the estuarine system receives a greater influx of terrigenous organic matter or experiences greater amounts of resuspension than the coastal ocean. Although salinity did not appear appreciably elevated from 2018 to 2019, the greatest lignin abundances in TSS occur in 2018, indicating that either erosion or resuspension caused wind and rain associated with Hurricane Florence led to higher lignin abundances (Table 6).

Several studies have investigated coastal lignin abundance as a function of storm activity (Table 8). In the Arellano *et al.* (2019) study, Apalachicola Bay and Barataria Bay samples were collected in Spring, Summer and Fall of 2015 and 2016, with an erosion/resuspension event (high wind or high precipitation) occurring in November of 2015 (Apalachicola), and April 2016 (Barataria). Arellano *et al.* (2019) found that the average particulate lignin in Apalachicola Bay didn't vary drastically between dry periods and the period of high precipitation, with averages ranging from  $\sim 7.80 - 13.4 \mu\text{g L}^{-1}$ , with the highest average lignin concentration occurring during a summer dry period. In Barataria Bay, the lignin concentrations were more variable, ranging from  $17.1 - 208 \mu\text{g L}^{-1}$ , with the greatest concentrations occurring during a period of high winds.  $L_8$  and salinity were positively correlated in Apalachicola Bay but not in Barataria Bay. In this APES study, lignin and salinity were not correlated. Overall, the highest lignin values can be found in storm samples taken within the APES and coastal ocean, but when looking at average values, Barataria Bay's erosion/resuspension event has the highest average. Godin *et al.*

(2017) found that their lignin values positively correlated with TSS. The highest lignin concentrations were found in the areas that drain basins with higher quantities of vegetation; a greater concentration of organic material led to a greater  $L_8$  value (Godin *et al.*, 2017). Hernes *et al.* (2020) noted that the highest lignin values were found in samples taken after the precipitation event, and that there was an overall positive correlation between particulate lignin and TSS. In 2018 APES samples, there is no correlation with lignin and TSS, while there is a positive correlation in 2019 estuarine samples. The highest lignin values are found after hurricane Florence, which shows that, similarly to the Godin *et al.* (2017) study, a precipitation event leads to elevated lignin values, but elevated lignin values is not necessarily correlated with TSS. TSS can consist of both organic and inorganic matter (Adawiah *et al.*, 2021). Station samples in the APES and coastal ocean with high TSS and low lignin concentrations could contain a higher quantity of inorganic solids such as sand or silt particles.

Table 8 Shows data like this study from sites throughout North America. Data include site information, salinity, TSS,  $\Sigma_8$  ( $\mu\text{g L}^{-1}$ ), and S/V and C/V ratios as well as the researcher associated with the study. APES and Coastal NC data in this paper thus far has been in  $\text{mg g}^{-1}$ . To better compare these data to similar data,  $\Sigma_8$  was converted to  $\mu\text{g L}^{-1}$ . The Hudson Bay samples focus on riverine input to the Bay; thus, salinity is not included. The Apalachicola Bay and Barataria Bay erosion/resuspension events occurred in November 2015, and April 2016, respectively.

Name	Site Info	Salinity	TSS ( $\text{mg L}^{-1}$ )	$\Sigma_8$ ( $\mu\text{g L}^{-1}$ )			C/V	Range S/V	Citation
	Sample Date			Max.	Min.	Average			
Apalachicola Bay	Mar-15	$16.1 \pm 11.9$	$19.5 \pm 10.3$	22.5	0.380	$7.82 \pm 7.11$			Arellano et al., 2019
	Nov-15	$22.3 \pm 8.70$	$27.4 \pm 14.1$	31.6	0.580	$9.31 \pm 13.6$	0.0500 – 1.31	0.160 – 1.09	
	Jul-16	$19.8 \pm 8.40$	$41.9 \pm 27.9$	91.9	0.320	$13.43 \pm 24.5$			
	Jul-15	$20.5 \pm 4.70$	$70.8 \pm 25.7$	37.5	6.26	$17.1 \pm 8.14$			
Barataria Bay	Apr-16	$13.4 \pm 3.00$	$105 \pm 38.0$	514	29.8	$208 \pm 140.$	0.150 – 0.860	0.270 – 1.43	Arellano et al., 2019
	Oct-16	$16.3 \pm 3.30$	$60.5 \pm 24.1$	134	5.04	$57.7 \pm 38.6$			
San Francisco Bay Estuary	Oct-11 - April-12	$4.00 \pm 4.90$	$44.8 \pm 41.3$	31.56	1.15	$7.20 \pm 7.70$	0.0400 – 1.29	0.0300 – 0.870	Hernes et al., 2020
Hudson Bay	July - Aug. 2010	-	$13.0 \pm 15.5$	9.54	0.260	$2.56 \pm 3.14$	0.0300 – 1.59	0.150 – 1.30	Godin et al., 2017
APES	Oct – Nov 2018	$16.1 \pm 8.90$	$42.3 \pm 17.4$	805	4.55	$185 \pm 265$	0.00 – 2.33	0.00 – 1.09	This study
	July 2019	$15.3 \pm 4.10$	$30.9 \pm 5.60$	42.5	2.76	$13.0 \pm 16.1$	0.00 – 0.690	0.00 – 0.330	
Coastal NC	Oct – Nov 2018	$28.8 \pm 8.30$	$31.9 \pm 7.90$	3620	3.56	$173 \pm 770$	0.00 – 1.73	0.00 – 1.16	This study
	July 2019	$28.7 \pm 1.60$	$21.1 \pm 1.28$	14.6	2.35	$4.38 \pm 5.68$	0.00 – 2.81	0.00 – 0.880	

### **3. Lignin Monomers in Suspended Sediment**

#### **3.1. Monomer Subclasses**

Analysis of lignin monomer subclasses sheds light on specific types of terrestrial organic matter affecting aquatic systems. Although lignin is relatively stable, it has shown degradation potential as it moves through the terrestrial biosphere (Pellerin *et al.*, 2010; Ward *et al.*, 2013). Vanillyl phenols were found during both sampling periods, and in samples taken in both the estuary and coastal ocean. Acetovanillone was only found in two 2019 samples, which could indicate that it had been too heavily degraded to show up in other samples, or that these two samples were anomalous. Vanillin and vanillic acid were both found in most 2018 estuarine samples, more than half of 2018 coastal samples and all 2019 samples. Terrestrial organic matter was found in the system during storm and non-storm periods. Since there was no storm period in 2019, it appears that river input, wind energy, resuspension, and wave energy heavily contribute to the base levels of vanillyl phenols found during dry periods.

Syringyl phenols are found only in woody and non-woody angiosperm tissue. In every instance, phenol concentrations were greater directly after Hurricane Florence. In 2018, the proximity of the sampling station with Oregon Inlet, and the wind direction may have an impact on phenol yields. There were no syringyl phenols being found at three of the stations (6, 7, 8) near the inlet on the Sound side, but phenols were found at Station 51, on the coastal side of the inlet. Stations 6, 7 and 8 were sampled on 10/26/18, while winds were generally blowing in an SSE direction. Sample 51 was taken on 11/30/18, when winds were generally blowing in a WSW direction. Southeastern winds could have potentially pushed suspended solids away from the inlet within the estuary, while southwestern winds could have pushed organic matter along the coast of the Outer Banks towards the sampling location. In general, there were not large

quantities of angiosperm organic matter pulsed out into the ocean after the 2018 storms, most of the angiosperm material was found within the estuary, likely due to the angiosperm dominated swamp forests lining the eastern portion of NC.

Cinnamyl phenols are found in non-woody angiosperm and gymnosperm plant tissue. These phenols are found in 100% of 2019 samples, 80% of 2018 estuarine samples, and only 20% of 2018 coastal samples. Cinnamyl phenol concentrations are present in both coastal and estuarine waters during non-storm periods indicating that non-woody plant matter may always circulate within the system. Non-woody plant matter such as coastal and marsh grasses are abundant along estuarine coasts (Adams, 1963). Cinnamyl phenol quantities are greatest within the estuary (2018) indicating that the hurricane season did cause an increase in the amount of non-woody organic matter either being pulsed into the estuary or resuspended. There was not a high abundance of non-woody organic matter found within the coastal ocean after the storms (aside from Station 11, which is an outlier) indicating that woody material may have been eroded from along the estuarine coasts or the Outer Banks and then pulsed through the Oregon Inlet.

### **3.2 Interclass Ratios**

Based on the lignin interclass ratios of suspended sediments in this study, non-woody angiosperms are the dominant contributor of organic matter to the estuary and coast with 64% of 2018 samples containing non-woody angiosperm plant tissue. Exceptions include three samples containing zero S/V to C/V ratios at Stations 12, 54 and 55 indicative of woody gymnosperm tissue, and Station 8 which contains no syringyl phenols indicating that the organic materials stems from non-woody gymnosperms. The organic material within the estuary is likely coming from nearby coastal grasses, degraded plant litter, or coastal marshes (Adams, 1963). The only lignin marker of woody tissue is found out in the coastal ocean samples. Woody tissue could

either be coming directly from the Outer Banks or could have been pulsed out into the coastal ocean from the estuary.

Acid to aldehyde ratios  $> 0.8$  indicate that the organic material is degraded, with the level of degradation increasing as the ratio increases (Qiao *et al.*, 2019). Ad/Al varied widely within this study. Four 2018 samples had Ad/Al ratios  $< 0.8$  (2 estuary, 2 coastal) while 8 samples had Ad/Al ratios  $> 0.8$  (6 estuary, 2 coastal). This indicates a combination of resuspension of degraded OM and input of fresh material occurred during the storm. The above data confirm that some of the TSS within the estuary and coastal ocean came from erosion and runoff, but much of it was either resuspended or more heavily degraded OM associated from deeper soil depths was eroded into the system.

As noted above, the only stations that contained gymnosperm tissues were post-storm samples taken at Stations 8, 12, 54 and 55 (one estuarine, three coastal). While an acid-aldehyde ratio was not able to be calculated for Station 12, Stations 8, 54, and 55 did have acid-aldehyde ratios  $< 0.8$ , thus indicative of fresh organic matter. The gymnosperm material being introduced into the suspended sediments, post-storm, are fresh while the angiosperm material is more degraded. This suggests that angiosperm-derived organic matter may have originated from resuspension or deep and weathered coastal soils, before being eroded into the system during the storm. In 2019, all lignin was degraded and came from non-woody angiosperm materials meaning that resuspension or other sources of weathered organic matter were introduced into the water column, possibly due to wind driven mixing in shallow areas, or that POM was being washed into the APES from rivers flowing through angiosperm dominated swamp forests.

#### **4. Limitations and Future Directions**

There were a few limitations to this study being able to comprehensively evaluate the immediate impacts of storms on lignin concentrations in the water column. First, due to Hurricane Michael happening so soon following Florence, sample collection didn't begin until ~1.5 months post-storm. While I believe that our current samples are valuable, samples taken directly after the storm would have provided higher temporal resolution related to storm related pulses of lignin. Additional samples would have allowed for a better understanding of the immediate impacts of the storm, which could have been compared to samples taken 1.5 months later, as well as the samples taken during the non-storm period. I believe that sampling location should also have been expanded. Much of the runoff from the storm came from the Neuse and Tar-Pamlico Rivers and flowed into the southern Pamlico Sound and out of the Ocracoke Inlet (Stewart & Berg, 2019). Taking additional samples further south would have allowed for a better understanding of lignin values within the system. Another issue that arose was our inability to acquire bulk carbon and nitrogen data. Typically, lignin abundances are normalized to 100 mg of total organic carbon in a sample, allowing for a lambda index (% of terrestrial organic carbon in a sample), which can provide more insight into the type of plant material found within the system. Portions of some sample filters were sent to UC Davis' Stable Isotope facility, but there was not enough carbon or nitrogen within each subsample to detect organic carbon or nitrogen. We attempted to provide larger portions of replicate GFFs. However, sample size was too large for their elemental analyzer.

## VI. CONCLUSION

The APES is an important resource in North Carolina's economy, playing a huge role in the commercial fishing, tourism, and recreation industries. Furthermore, the APES acts as a nursery to finfish and shellfish. It is an integral part of the coastal North Carolina community. Biogeochemical cycles in estuaries, such as the APES, can be affected by storms. This study suggests that the 2018 storm season affected terrestrial organic matter influx into the water column within the APES and nearby coastal ocean. The time between Hurricane Florence making landfall and the sampling dates may have been too great to gain a meaningful understanding of the storms impacts on salinity within the system. TSS showed no real correlation with salinity in coastal samples, but there was a correlation between the two variables in 2018 estuarine samples. The greatest range and quantity of TSS was found in 2018 estuarine samples, with 2019 coastal samples having the lowest range of TSS. The greatest lignin abundances can be found in both estuarine and coastal 2018 samples, with the highest value occurring in the coastal ocean, although, when excluding this outlying value, the estuarine  $L_8$  average is greater. Moreover, the organic material that comprised the samples was a combination of both relatively fresh and highly degraded lignin. The only fresh lignin came from gymnosperm plant tissue, while the degraded lignin came from non-woody angiosperm plant tissue. Since most samples were degraded, it seems that resuspension and erosion of degraded plant litter played a large role within the system both pre- and post-storm.

Understanding the impact of storms on coastal ecosystems is necessary to determine the fate of organic matter and nutrients, as storms become more severe, and climate change continues to worsen. With estuaries being particularly susceptible to storm impacts, further

research should be done to better understand future implications of increasingly heavy flooding and storms on these systems.

## VII. CITATIONS

- Adams, D. A. (1963). Factors influencing vascular plant zonation in North Carolina Salt Marshes. *Ecology*, 44(3), 445–456. <https://doi.org/10.2307/1932523>
- Adawiah, S. W., Setiawan, K. T., Parwati, E., & Faristyawan, R. (2021). Development of empirical model of total suspended solid (TSS) by using Landsat 8 on the coast of Bekasi Regency. *IOP Conference Series: Earth and Environmental Science*, 750(1), 1–8. <https://doi.org/10.1088/1755-1315/750/1/012039>
- Albemarle Pamlico National Estuary Partnership. (n.d.). *Our Estuary*. APNEP. Retrieved May 3, 2022, from <https://apnep.nc.gov/our-estuary>
- Arellano, A. R., Bianchi, T. S., Osburn, C. L., D'Sa, E. J., Ward, N. D., Oviedo-Vargas, D., Joshi, I. D., Ko, D. S., Shields, M. R., Kurian, G., & Green, J. (2019). Mechanisms of organic matter export in estuaries with contrasting carbon sources. *Journal of Geophysical Research: Biogeosciences*, 124(10), 3168–3188. <https://doi.org/10.1029/2018jg004868>
- Bales, J. D., & Newcomb, D. J. (n.d.). *National water summary wetland resources: North Carolina*. North Carolina Wetland Resources. Retrieved June 18, 2022, from <https://www.fws.gov/wetlands/data/Water-Summary-Reports/National-Water-Summary-Wetland-Resources-North-Carolina.pdf>
- Barbier, E. B., Hacker, S. D., Koch, E. W., Stier, A. C., & Silliman, B. R. (2011). Estuarine and coastal ecosystems and their services. *Treatise on Estuarine and Coastal Science*, 12, 109–127. <https://doi.org/10.1016/b978-0-12-374711-2.01206-7>
- Bauer, J. E., Cai, W., Raymond, P. A., Bianchi, T. S., Hopkinson, C. S., & Regnier, P. A. (2013). The changing carbon cycle of the coastal ocean. *Nature*, 504(7478), 61-70. doi:10.1038/nature12857
- Bellis, V. J. (1995). Ecology of Maritime Forests of the Southern Atlantic Coast: A Community Profile. United States: U.S. Department of the Interior, National Biological Service.
- Bender, M. A., Knutson, T. R., Tuleya, R. E., Sirutis, J. J., Vecchi, G. A., Garner, S. T., & Held, I. M. (2010). Modeled impact of anthropogenic warming on the frequency of intense Atlantic hurricanes. *Science*, 327(5964), 454–458. <https://doi.org/10.1126/science.1180568>
- Bi, W., Wang, J. J., Dodla, S. K., Gaston, L. A., & Delaune, R. D. (2019). Lignin chemistry of wetland soil profiles in two contrasting basins of the Louisiana Gulf coast. *Organic Geochemistry*, 137, 103902. doi:10.1016/j.orggeochem.2019.103902
- Bianchi, T. S. & Bauer, J. E. 2011. in *Treatise on Estuarine and Coastal Science*, Vol. 5 (eds Wolanski, E. & McLusky, D. S.) 69–117 (Academic, 2011).

- Bianchi, T. S., Garcia-Tigreros, F., Yvon-Lewis, S. A., Shields, M., Mills, H. J., Butman, D., Osburn, C., Raymond, P., Shank, G. C., DiMarco, S. F., Walker, N., Reese, B. K., Mullins-Perry, R., Quigg, A., Aiken, G. R., & Grossman, E. L. (2013). Enhanced transfer of terrestrially derived carbon to the atmosphere in a flooding event. *Geophysical Research Letters*, *40*(1), 116–122. <https://doi.org/10.1029/2012gl054145>
- Bianucci, L., Balaguru, K., Smith, R. W., Leung, L. R., & Moriarty, J. M. (2018). Contribution of hurricane-induced sediment resuspension to coastal oxygen dynamics. *Scientific Reports*, *8*(1), 1–10. <https://doi.org/10.1038/s41598-018-33640-3>
- Burk, C. John. (1962) “The North Carolina Outer Banks: A Floristic Interpretation.” *Journal of the Elisha Mitchell Scientific Society*, *78*(1), 21–28. <http://www.jstor.org/stable/24334659>.
- Cai, W.-J. (2011). Estuarine and Coastal Ocean Carbon Paradox: CO<sub>2</sub> Sinks or Sites of Terrestrial Carbon Incineration? *Annual Review of Marine Science*, *3*(1), 123–145. <https://doi.org/10.1146/annurev-marine-120709-142723>
- Cathalot, C., Rabouille, C., Tisnérat-Laborde, N., Toussaint, F., Kerhervé, P., Buscail, R., Loftis, K., Sun, M.-Y., Tronczynski, J., Azoury, S., Lansard, B., Treignier, C., Pastor, L., & Tesi, T. (2013). The fate of river organic carbon in coastal areas: A study in the Rhône River Delta using multiple isotopic ( $\delta^{13}\text{C}$ ,  $\Delta^{14}\text{C}$ ) and organic tracers. *Geochimica Et Cosmochimica Acta*, *118*, 33–55. <https://doi.org/10.1016/j.gca.2013.05.001>
- Chakar, F. S., & Ragauskas, A. J. (2004). Review of current and future softwood Kraft lignin process chemistry. *Industrial Crops and Products*, *20*(2), 131–141. <https://doi.org/10.1016/j.indcrop.2004.04.016>
- Chen, S., Huang, W., Wang, H., & Li, D. (2009). Remote sensing assessment of sediment resuspension during Hurricane Frances in Apalachicola Bay, USA. *Remote Sensing of Environment*, *113*(12), 2670–2681. <https://doi.org/10.1016/j.rse.2009.08.005>
- Cheng, P., Li, M., & Li, Y. (2013). Generation of an estuarine sediment plume by a tropical storm. *Journal of Geophysical Research: Oceans*, *118*(2), 856–868. <https://doi.org/10.1002/jgrc.20070>
- Corbett, D. R., Vance, D., Letrick, E., Mallinson, D., & Culver, S. (2007). Decadal-scale sediment dynamics and environmental change in the Albemarle Estuarine System, North Carolina. *Estuarine, Coastal and Shelf Science*, *71*(3-4), 717–729. <https://doi.org/10.1016/j.ecss.2006.09.024>
- Corbett, D. R., Walsh, J. P., Cowart, L., Riggs, S. R., Ames, D. V., & Culver, S. J., Shoreline change within the Albemarle-Pamlico Estuarine System, North Carolina: A White Paper 1–10 (2008). Greenville, NC, NC; East Carolina University.

- Cowart, L., Walsh, J. P., & Corbett, D. R. (2010). Analyzing estuarine shoreline change: A case study of cedar island, North Carolina. *Journal of Coastal Research*, 265, 817–830. <https://doi.org/10.2112/jcoastres-d-09-00117.1>
- Cowart, L., Corbett, D. R., & Walsh, J. P. (2011). Shoreline change along sheltered coastlines: Insights from the Neuse River Estuary, NC, USA. *Remote Sensing*, 3(7), 1516–1534. <https://doi.org/10.3390/rs3071516>
- Cymbaluk, N. F., & Neudoerffer, T. S. (1970). A quantitative gas-liquid chromatographic determination of aromatic aldehydes and acids from nitrobenzene oxidation of lignin. *Journal of Chromatography A*, 51, 167–174. [https://doi.org/10.1016/s0021-9673\(01\)96851-7](https://doi.org/10.1016/s0021-9673(01)96851-7)
- Deininger, A., & Frigstad, H. (2019). Reevaluating the role of organic matter sources for coastal eutrophication, oligotrophication, and ecosystem health. *Frontiers in Marine Science*, doi:<http://dx.doi.org/10.3389/fmars.2019.00210>
- Droppo, Ian. (2003). A New Definition of Suspended Sediment: Implications for the Measurement and Prediction of Sediment Transport. IAHS-AISH Publication.
- Elsner, James. “Hurricanes and Climate Change.” *Bulletin of the American Meteorological Society*, vol. 89, no. 5, 2009, pp. 677–679., doi:10.1007/978-0-387-09410-6.
- Environmental Protection Agency. (n.d.). *Basic Information about Estuaries*. EPA. Retrieved May 7, 2022, from <https://www.epa.gov/nep/basic-information-about-estuaries>
- Erdman, J., 2018. Florence Sets Preliminary North Carolina and South Carolina Tropical Cyclone Rain Records; Third, Fourth States to Do So in 12 Months [WWW Document]. Weather.com. URL <https://weather.com/storms/hurricane/news/2018-09-15-florence-north-carolina-tropical-rain-record>
- Eulie, D. O., Corbett, D.R., Walsh, J.P. (2018). Shoreline erosion and decadal sediment accumulation in the Tar-Pamlico estuary, North Carolina, USA: A source-to-sink analysis. *Estuarine, Coastal and Shelf Science*, 202(5), 12. <https://doi.org/10.1016/j.ecss.2017.10.011>
- Eulie, D. O., Walsh, J. P., Corbett, D. R., & Mulligan, R. P. (2016). Temporal and spatial dynamics of estuarine shoreline change in the albemarle-pamlico estuarine system, North Carolina, USA. *Estuaries and Coasts*, 40(3), 741–757. <https://doi.org/10.1007/s12237-016-0143-8>
- Giese, G. L., Wilder, H. B., & Parker, G. G. (1979). (rep.). *Hydrology of Major Estuaries and Sounds of North Carolina*. United States Geological Survey. Retrieved May 3, 2022, from <https://pubs.usgs.gov/wri/1979/0046/report.pdf>.

- Giese, G. L. (1985). Hydrology of Major Estuaries and Sounds of North Carolina. United States: U.S. Government Printing Office.
- Green, M. O., & Coco, G. (2014). Review of wave-driven sediment resuspension and transport in estuaries. *Reviews of Geophysics*, 52(1), 77–117. <https://doi.org/10.1002/2013rg000437>
- Godin, P., Macdonald, R. W., Kuzyk, Z. Z., Goñi, M. A., & Stern, G. A. (2017). Organic matter compositions of rivers draining into Hudson Bay: Present-day trends and potential as recorders of future climate change. *Journal of Geophysical Research: Biogeosciences*, 122(7), 1848–1869. <https://doi.org/10.1002/2016jg003569178>, doi:10.1021/ac00239a007.
- Gong, W., & Shen, J. (2009). Response of sediment dynamics in the York River Estuary, USA to tropical cyclone isabel of 2003. *Estuarine, Coastal and Shelf Science*, 84(1), 61–74. <https://doi.org/10.1016/j.ecss.2009.06.004>
- Goñi, Miguel A., and Shelagh Montgomery. “Alkaline CuO Oxidation with a Microwave Digestion System: Lignin Analyses of Geochemical Samples.” *Analytical Chemistry*, vol. 72, no. 14, 2000, pp. 3116–3121., doi:10.1021/ac991316w.
- Hayes, M. O. (1980). General morphology and sediment patterns in tidal inlets. *Sedimentary Geology*, 26(1-3), 139–156. [https://doi.org/10.1016/0037-0738\(80\)90009-3](https://doi.org/10.1016/0037-0738(80)90009-3)
- Hayes, M. O., & FitzGerald, D. M. (2013). Origin, evolution, and classification of tidal inlets. *Journal of Coastal Research*, 69, 14–33. [https://doi.org/10.2112/si\\_69\\_3](https://doi.org/10.2112/si_69_3)
- Hedges, J. I., & Mann, D. C. (1979). The characterization of plant tissues by their lignin oxidation products. *Geochimica Et Cosmochimica Acta*, 43(11), 1803-1807. Doi:10.1016/0016-7037(79)90028-0
- Hedges, J. I., Keil, R. G., and Benner, R. (1997). What happens to terrestrial organic matter in the ocean? *Org. Geochem.* 27, 195–212. doi: 10.1016/S0146-6380(97)00066-1
- Hedges, J.I., Ertel, John. (1982). Characterization of lignin by gas capillary chromatography of cupric oxide oxidation products. *Analytical Chemistry*, 54(2), 5. <https://doi.org/10.1021/ac00239a007>
- Hernes, P. J., Dyda, R. Y., & Bergamaschi, B. A. (2020). Reassessing particulate organic carbon dynamics in the highly disturbed San Francisco Bay Estuary. *Frontiers in Earth Science*, 8. <https://doi.org/10.3389/feart.2020.00185>
- Herrero, A., Vila, J., Eljarrat, E., Ginebreda, A., Sabater, S., Batalla, R. J., & Barceló, D. (2018). Transport of sediment borne contaminants in a Mediterranean river during a high flow event. *Science of The Total Environment*, 633, 1392-1402. doi:10.1016/j.scitotenv.2018.03.205

- Hess, S., Prescott, L. J., Hoey, A. S., McMahon, S. A., Wenger, A. S., & Rummer, J. L. (2017). Species-specific impacts of suspended sediments on gill structure and function in coral reef fishes. *Proceedings of the Royal Society B: Biological Sciences*, 284(1866), 20171279. doi:10.1098/rspb.2017.1279
- “Hurricanes: Statistics.” *North Carolina Climate Office*, 2022, climate.ncsu.edu/climate/hurricanes/landfalling.
- Inman, D. L., & Dolan, R. (1989). The Outer Banks of North Carolina: Budget of Sediment and Inlet Dynamics Along a Migrating Barrier System. *Journal of Coastal Research*, 5(2), 193–237.
- IPCC. (2022). *Climate change 2021: The Physical Science Basis*. IPCC Intergovernmental Panel on Climate Change. Retrieved August 3, 2022, from <https://www.ipcc.ch/report/ar6/wg1/>
- Jarmalavicus, D., Smatas, V., Stankunavicius, G., Pupienis, D., & Zilinskas, G. (2016). Factors controlling coastal erosion during storm events. *Journal of Coastal Research*, Si(75), 1112-1116. doi:<http://dx.doi.org/10.2112/Si75-223.1>
- Jia, P., & Li, M. (2012). Circulation Dynamics and salt balance in a lagoonal estuary. *Journal of Geophysical Research: Oceans*, 117(C1), 1–16. <https://doi.org/10.1029/2011jc007124>
- Jia, P., & Li, M. (2012). Dynamics of wind-driven circulation in a shallow lagoon with strong horizontal density gradient. *Journal of Geophysical Research: Oceans*, 117(C5), 1–14. <https://doi.org/10.1029/2011jc007475>
- Killops, S. D., & Killops, V. J. (2005). Lignins, tannins, and related compounds. In *Introduction to organic geochemistry* (2<sup>nd</sup> ed., pp. 62-64). Malden, MA: Blackwell Pub.
- Katahira, R., Elder, T. J., & Beckham, G. T. (2018). Lignin valorization: Emerging approaches. Chapter 1. A brief introduction to lignin structure. *Energy and Environment Series*, 1–20. <https://doi.org/10.1039/9781788010351-00001>
- Knutson, T. R., Sirutis, J. J., Zhao, M., Tuleya, R. E., Bender, M., Vecchi, G. A., Chavas, D. (2015). Global Projections of Intense Tropical Cyclone Activity for the Late Twenty-First Century from Dynamical Downscaling of CMIP5/RCP4.5 Scenarios. *Journal of Climate*, 28(18), 7203–7224. Doi: 10.1175/jcli-d-15-0129.1
- Kossin, J. P. (2018). A global slowdown of tropical-cyclone translation speed. *Nature*, 558(7708), 104–107. <https://doi.org/10.1038/s41586-018-0158-3>
- Kunkel, Kenneth E., and Sarah M. Champion. “An Assessment of Rainfall from Hurricanes Harvey and Florence Relative to Other Extremely Wet Storms in the United States.” *Geophysical Research Letters*, vol. 46, no. 22, 2019, pp. 13500–13506., doi:10.1029/2019gl085034.

- Laruelle, G. G., Dürr, H. H., Lauerwald, R., Hartmann, J., Slomp, C. P., Goossens, N., & Regnier, P. A. (2013). Global multi-scale segmentation of Continental and coastal waters from the watersheds to the continental margins. *Hydrology and Earth System Sciences*, 17(5), 2029–2051. <https://doi.org/10.5194/hess-17-2029-2013>
- Lehmann, J., Coumou, D., & Frieler, K. (2015). Increased record-breaking precipitation events under Global Warming. *Climatic Change*, 132(4), 501–515. <https://doi.org/10.1007/s10584-015-1434-y>
- Lin, J., Xie, L., Pietrafesa, L.J., Ramus, J.S., Paerl, H.W., 2007. Water quality gradients across Albemarle-Pamlico Estuarine system: seasonal variations and model applications. *Journal of Coastal Research* 23 (1), 213–229
- Liu, Q., Luo, L., & Zheng, L. (2018). Lignins: Biosynthesis and biological functions in plants. *International Journal of Molecular Sciences*, 19(2), 335–351. <https://doi.org/10.3390/ijms19020335>
- Mackenzie, F. T., Andersson, A. J., Lerman, A. & Ver, L. M. in *The Sea* Vol. 13 (eds Robinson, A. R. & Brink, K. H) 193–225 (Harvard Univ. Press, 2005). This is a comprehensive historical description of carbon cycling processes and fluxes through Earth's past, present and future.
- Mallin, M. A., Posey, M. H., Shank, G. C., McIver, M. R., Ensign, S. H., & Alphin, T. D. (1999). Hurricane effects on water quality and benthos in the cape fear watershed: Natural and anthropogenic impacts. *Ecological Applications*, 9(1), 350–362. [https://doi.org/10.1890/1051-0761\(1999\)009\[0350:heowqa\]2.0.co;2](https://doi.org/10.1890/1051-0761(1999)009[0350:heowqa]2.0.co;2)
- Mallinson, D. J., Culver, S. J., Riggs, S. R., Walsh, J. P., Ames, D., & Smith, C. W. (2008). *Past, Present and Future Inlets of the Outer Banks Barrier Islands, North Carolina* (pp. 1–22). Greenville, NC.
- Mallinson, D.J., Smith, C.W., Culver, S.J., Riggs, S.R., and Ames, D., 2010, Geological characteristics and spatial distribution of paleo-inlet channels beneath the Outer Banks barrier islands, North Carolina, USA: *Estuarine, Coastal and Shelf Science*, v. 88, p. 175–189.
- Mallinson, D.J., Smith, C.W., Mahan, S.J., Culver, S.J., McDowell, K., 2011, Barrier island response to late Holocene climate events, North Carolina, USA: *Quaternary Research*, v. 76, p. 46–57
- Mallinson, D., Culver, S., Leorri, E., Mitra, S., Mulligan, R., & Riggs, S. (2018). Barrier Island and estuary co-evolution in response to holocene climate and sea-level change: Pamlico sound and the Outer Banks Barrier Islands, North Carolina, USA. *Barrier Dynamics and Response to Changing Climate*, 91–120. [https://doi.org/10.1007/978-3-319-68086-6\\_3](https://doi.org/10.1007/978-3-319-68086-6_3)

- Mattson, E. A., Brinson, Mark M., Cahoon, D.D., Davis, Graham J. (1983). *Biogeochemistry of the Sediments of the Pamlico and Neuse River Estuaries, North Carolina*  
<https://repository.lib.ncsu.edu/bitstream/handle/1840.4/1621/NC-WRRI-191.pdf?sequence=1>
- Miller, T. L., Morton, R. A., & Sallenger, A. H. (2005). The National Assessment of Shoreline Change: a GIS compilation of vector shorelines and associated shoreline change data for the U.S. Southeast Atlantic Coast. *Open-File Report*. <https://doi.org/10.3133/ofr20051326>
- Moran, M. A., Sheldon, W. M., & Zepp, R. G. (2000). Carbon loss and optical property changes during long-term photochemical and biological degradation of estuarine dissolved organic matter. *Limnology and Oceanography*, 45(6), 1254–1264.  
<https://doi.org/10.4319/lo.2000.45.6.1254>
- Moody, A., 2018. Hurricane Florence: NC rain estimated at 8 trillion gallons | Raleigh News & Observer [WWW Document]. News Obs. URL  
<https://www.newsobserver.com/news/weather/article218273350.html> (accessed 2.6.19).
- Moore, L. J., List, J. H., Williams, S. J., & Stolper, D. (2010). Complexities in barrier island response to sea level rise: Insights from Numerical Model experiments, North Carolina Outer Banks. *Journal of Geophysical Research*, 115(F3), 1–27.  
<https://doi.org/10.1029/2009jf001299>
- NASA. (2018, September 19). *A broad view of flooding in the Carolinas*.  
 earthobservatory.nasa.gov. Retrieved August 1, 2022, from  
<https://earthobservatory.nasa.gov/images/92786/a-broad-view-of-flooding-in-the-carolinas>
- NC DEQ. (n.d.). *Coastal Wetlands*. Estuarine Shorelines - Coastal Management. Retrieved May 20, 2022, from <https://deq.nc.gov/about/divisions/coastal-management/estuarine-shorelines/wetlands/coastal-wetlands>
- NC DEQ. (2015, January). *North Carolina Estuarine Shoreline Mapping Project 2012 Statistical Reports*. NC DEQ. Retrieved August 1, 2022, from  
<https://deq.nc.gov/about/divisions/coastal-management/estuarine-shorelines/wetlands/estuarine-shoreline-mapping-project>
- NC DEQ. (2022, May 20). *The Albemarle-Pamlico Estuarine System: Birds & Habitats*. Retrieved from <https://deq.nc.gov/media/11919/download>
- NC DEQ. (2015, January). *North Carolina Estuarine Shoreline Mapping Project 2012 Statistical Reports*. NC DEQ. Retrieved August 1, 2022, from  
<https://deq.nc.gov/about/divisions/coastal-management/estuarine-shorelines/wetlands/estuarine-shoreline-mapping-project>
- NC DEQ. (1997, August). *Common Wetland Plants of North Carolina*. Raleigh.

- NC Wetlands. (n.d.). *Wetland diversity in North Carolina*. NC Wetlands. Retrieved June 18, 2022, from <https://www.ncwetlands.org/wp-content/uploads/NCWetlands-wetland-types-small-poster.pdf>
- NOAA. (2019, December 5). *Coastal Blue Carbon*. NOAA's National Ocean Service. Retrieved May 8, 2022, from <https://oceanservice.noaa.gov/ecosystems/coastal-blue-carbon/>
- NOAA. (2020, June). *Continental United States Tropical Storms Impacts/Landfalls 1851-1965, 1983-2019*. Atlantic Oceanographic and Meteorological Laboratories. Retrieved October 22, 2021, from <https://www.aoml.noaa.gov/hrd/hurdat/uststorms.html>.
- NOAA. (2021, October 8). *Costliest U.S. Tropical Cyclones*. [ncdc.noaa.gov](https://www.ncdc.noaa.gov/billions/dcmi.pdf). Retrieved October 22, 2021, from <https://www.ncdc.noaa.gov/billions/dcmi.pdf>.
- NOAA. (2021, October 15). *Hurricane Costs*. NOAA Office for Coastal Management. Retrieved October 28, 2021, from <https://coast.noaa.gov/states/fast-facts/hurricane-costs.html>.
- NOAA National Centers for Environmental Information, State of the Climate: Tropical Cyclones for Annual 2018, published online January 2019, retrieved on October 28, 2021, from <https://www.ncdc.noaa.gov/sotc/tropical-cyclones/201813>.
- NOAA's National Weather Service. (2019, May 7). *Hurricane Florence: September 14, 2018*. National Weather Service. Retrieved October 23, 2021, from <https://www.weather.gov/ilm/HurricaneFlorence#:~:text=%20Newspaper%20reports%20claim%20an%20anemometer,Lookout%2C%20NC%3A%20106%20mph>.
- NOAA. (2022). *Tide predictions - NOAA tides & currents*. Tides & Currents. Retrieved June 21, 2022, from <https://tidesandcurrents.noaa.gov/noaatidepredictions.html?id=8652678&units=metric&bdate=20180910&edate=20180918&timezone=LST%2FLDT&clock=12hour&datum=MLLW&interval=hilo&action=dailychart>
- NOAA. (2020). *U.S. Hurricane Strikes by Decade*. U.S. hurricane strikes by decade. Retrieved October 22, 2021, from <https://www.nhc.noaa.gov/pastdec.shtml>.
- North Carolina Department of Environmental Quality. (2015, January). *North Carolina Estuarine Shoreline Mapping Project 2012 Statistical Reports*. NC DEQ. Retrieved August 1, 2022, from <https://deq.nc.gov/about/divisions/coastal-management/estuarine-shorelines/wetlands/estuarine-shoreline-mapping-project>
- Osburn, C. L., Rudolph, J. C., Paerl, H. W., Hounshell, A. G., & Van Dam, B. R. (2019). Lingering carbon cycle effects of hurricane Matthew in North Carolina's Coastal Waters. *Geophysical Research Letters*, *46*(5), 2654–2661. <https://doi.org/10.1029/2019gl082014>
- Otto, A., & Simpson, M. J. (2006). Evaluation of CUO oxidation parameters for determining the source and stage of lignin degradation in Soil. *Biogeochemistry*, *80*(2), 121–142. <https://doi.org/10.1007/s10533-006-9014-x>

- Paerl, H. W., Bales, J. D., Ausley, L. W., Buzzelli, C. P., Crowder, L. B., Eby, L. A., Fear, J. M., Go, M., Peierls, B. L., Richardson, T. L., & Ramus, J. S. (2001). Ecosystem impacts of three sequential hurricanes (Dennis, Floyd, and Irene) on the United States' largest lagoonal estuary, Pamlico Sound, NC. *Proceedings of the National Academy of Sciences*, *98*(10), 5655–5660. <https://doi.org/10.1073/pnas.101097398>
- Paerl, H. W., Hall, N. S., Hounshell, A. G., Luettich, R. A., Rossignol, K. L., Osburn, C. L., & Bales, J. (2019). Recent increase in catastrophic tropical cyclone flooding in coastal North Carolina, USA: Long-term observations suggest a regime shift. *Scientific Reports*, *9*(1). doi:10.1038/s41598-019-46928-9
- Paerl, H. W., Hall, N. S., Hounshell, A. G., Rossignol, K. L., Barnard, M. A., Luettich, R. A., Rudolph, J. C., Osburn, C. L., Bales, J., & Harding, L. W. (2020). Recent increases of rainfall and flooding from tropical cyclones (TCS) in North Carolina (USA): Implications for organic matter and nutrient cycling in coastal watersheds. *Biogeochemistry*, *150*(2), 197–216. <https://doi.org/10.1007/s10533-020-00693-4>
- Paerl, H.W., Valdes, L.M., Joyner, A.R. *et al.* (2006). Ecological response to hurricane events in the Pamlico Sound system, North Carolina, and implications for assessment and management in a regime of increased frequency. *Estuaries and Coasts: JERF* **29**, 1033–1045. <https://doi.org/10.1007/BF02798666>
- Paerl, H. W., Valdes, L. M., Piehler, M. F., & Stow, C. A. (2006). Assessing the Effects of Nutrient Management in an Estuary Experiencing Climatic Change: The Neuse River Estuary, North Carolina. *Environmental Management*, *37*(3), 422-436. doi:10.1007/s00267-004-0034-9
- Paul, S., Ghebreyesus, D., & Sharif, H. (2019). Brief communication: Analysis of the fatalities and socio-economic impacts caused by Hurricane Florence. *Geosciences*, *9*(2). <https://doi.org/10.3390/geosciences9020058>
- Pellerin, B. A., Hernes, P. J., Saraceno, J. F., Spencer, R. G., & Bergamaschi, B. A. (2010). Microbial degradation of plant leachate alters lignin phenols and trihalomethane precursors. *Journal of Environmental Quality*, *39*(3), 946–954. <https://doi.org/10.2134/jeq2009.0487>
- Peng, M., Xie, L., & Pietrafesa, L. J. (2004). A numerical study of storm surge and inundation in the Croatan–albemarle–pamlico estuary system. *Estuarine, Coastal and Shelf Science*, *59*(1), 121–137. <https://doi.org/10.1016/j.ecss.2003.07.010>
- Pew, J. C. (1955). Nitrobenzene oxidation of lignin model compounds, spruce wood and spruce “native lignin.” *Journal of the American Chemical Society*, *77*(10), 2831–2833. <https://doi.org/10.1021/ja01615a048>

- Phillips, J. D. (1999). Event Timing and Sequence in Coastal Shoreline Erosion: Hurricanes Bertha and Fran and the Neuse Estuary. *Journal of Coastal Research*, 15(3), 616–623. <http://www.jstor.org/stable/4298978>
- Prein, A. F., Rasmussen, R. M., Ikeda, K., Liu, C., Clark, M. P., & Holland, G. J. (2016). The future intensification of hourly precipitation extremes. *Nature Climate Change*, 7(1), 48–52. Doi:10.1038/nclimate3168
- Raymond, P. A., & Bauer, J. E. (2001). Use of  $^{14}\text{C}$  and  $^{13}\text{C}$  natural abundances for evaluating riverine, estuarine, and coastal Doc and POC Sources and cycling: A review and synthesis. *Organic Geochemistry*, 32(4), 469–485. [https://doi.org/10.1016/s0146-6380\(00\)00190-x](https://doi.org/10.1016/s0146-6380(00)00190-x)
- Reyna, N. E., Hardison, A. K., & Liu, Z. (2017). Influence of major storm events on the quantity and composition of particulate organic matter and the phytoplankton community in a subtropical estuary, Texas. *Frontiers in Marine Science*, 4. <https://doi.org/10.3389/fmars.2017.00043>
- Riggs, S.R., Bray, J.T., Wyrick, R.A., Klingman, C.R., Ames, D.V., Hamilton, J.C., Lueck, K.L., Watson, J.S., 1993. Heavy metals in organic-rich muds of the Albemarle Sound Estuarine System. Albemarle-Pamlico Estuarine Study. US EPA, National Estuary Program Report No. 93-01.
- Riggs, S. (1996). Sediment Evolution and Habitat Function of Organic-Rich Muds within the Albemarle Estuarine System, North Carolina. *Estuaries*, 19(2), 16. <https://doi.org/10.2307/1352223>
- Roelofs, E. W., Bumpus, D.F. (1953). The Hydrography of Pamlico Sound. *Bulletin of Marine Science*, 3(3), 25.
- Rudolph, J. C., Arendt, C. A., Hounshell, A. G., Paerl, H. W., & Osburn, C. L. (2020). Use of Geospatial, Hydrologic, and Geochemical Modeling to Determine the Influence of Wetland-Derived Organic Matter in Coastal Waters in Response to Extreme Weather Events. *Frontiers in Marine Science*, 7. doi:10.3389/fmars.2020.00018
- Shi, J. Z., Luther, M. E., & Meyers, S. (2006). Modelling of wind wave-induced bottom processes during the slack water periods in Tampa Bay, Florida. *International Journal for Numerical Methods in Fluids*, 52(11), 1277–1292. <https://doi.org/10.1002/fld.1377>
- Sholkovitz, E. R. (1976). Flocculation of dissolved organic and inorganic matter during the mixing of river water and seawater. *Geochimica Et Cosmochimica Acta*, 40(7), 831–845. [https://doi.org/10.1016/0016-7037\(76\)90035-1](https://doi.org/10.1016/0016-7037(76)90035-1)
- Stewart, S. R., & Berg, R. (2019, September 25). *National Hurricane Center Tropical Cyclone Report: Hurricane Florence*. National Hurricane Center. Retrieved from [https://www.nhc.noaa.gov/data/tcr/AL062018\\_Florence.pdf](https://www.nhc.noaa.gov/data/tcr/AL062018_Florence.pdf)

- “Survey of Surface Water Quality Associated with Hurricane Florence, September 2018.” *NC DEQ*, NC Dept. of Environmental Quality, Apr. 2019, [deq.nc.gov/about/divisions/water-resources/water-resources-data/water-sciences-home-page/reports](http://deq.nc.gov/about/divisions/water-resources/water-resources-data/water-sciences-home-page/reports)
- Tallamy, D. (2013). *Native plants for coastal North Carolina landscapes*. Retrieved May 22, 2022, from [http://nc-ipc.weebly.com/uploads/6/8/4/6/6846349/\\_native\\_plants\\_for\\_coastal\\_nc\\_landscapes.pdf](http://nc-ipc.weebly.com/uploads/6/8/4/6/6846349/_native_plants_for_coastal_nc_landscapes.pdf)
- Talley, L. D. (2002). *Salinity patterns in the ocean*. UC San Diego. Retrieved August 10, 2022, from [http://sam.ucsd.edu/ltalley/papers/2000s/wiley\\_talley\\_salinitypatterns.pdf](http://sam.ucsd.edu/ltalley/papers/2000s/wiley_talley_salinitypatterns.pdf)
- Thevenot, M., Dignac, M., & Rumpel, C. (2010). Fate of lignins in soils: A review. *Soil Biology and Biochemistry*, 42(8), 1200-1211. doi:10.1016/j.soilbio.2010.03.017
- Trenberth, K. E., Cheng, L., Jacobs, P., Zhang, Y., & Fasullo, J. (2018). Hurricane Harvey links to Ocean Heat Content and Climate Change Adaptation. *Earth's Future*, 6(5), 730–744. <https://doi.org/10.1029/2018ef000825>
- Tully, L. S. (2004). *Evaluation of sediment dynamics using geochemical tracers in the Pamlico sound estuarine system, North Carolina* (thesis). Greenville.
- Vernon Carle, M. (2011). Estimating wetland losses and gains in coastal North Carolina: 1994–2001. *Wetlands*, 31(6), 1275–1285. <https://doi.org/10.1007/s13157-011-0242-z>
- Ward, N. D., Richey, J. E., & Keil, R. G. (2012). Temporal variation in river nutrient and dissolved lignin phenol concentrations and the impact of storm events on nutrient loading to Hood Canal, Washington, USA. *Biogeochemistry*, 111(1-3), 629–645. <https://doi.org/10.1007/s10533-012-9700-9>
- Ward, N. D., Keil, R. G., Medeiros, P. M., Brito, D. C., Cunha, A. C., Dittmar, T., Yager, P. L., Krusche, A. V., & Richey, J. E. (2013). Degradation of terrestrially derived macromolecules in the amazon river. *Nature Geoscience*, 6(7), 530–533. <https://doi.org/10.1038/ngeo1817>
- Wells, J., Kim, Seok-Yun. (1989). Sedimentation in the Albemarle-Pamlico Lagoonal System: synthesis and hypotheses. *Marine Geology*, 88(3-4), 21.
- World Economic Forum. (2021, January 19). *The global risks report 2021*. WE Forum. Retrieved October 21, 2021, from <https://www.weforum.org/reports/the-global-risks-report-2021>.
- World Meteorological Organization. (2021). *WMO Atlas of Mortality and Economic Losses from Weather, Climate and Water Extremes (1970–2019)*. Library.WMO. Retrieved October 21, 2021, from [https://library.wmo.int/index.php?lvl=notice\\_display&id=21930](https://library.wmo.int/index.php?lvl=notice_display&id=21930).

- Wotton, R. S. (1994). Lignin Oxidation Products. In *The biology of particles in aquatic systems* (2<sup>nd</sup> ed., pp. 63-64). Boca Raton, FL: Lewis.
- Yamamoto, M., Ichikawa, Y., Igarashi, Y., & Oba, T. (2005). Late Quaternary variation of lignin composition in core MD01-2421 off central Japan, NW Pacific. *Palaeogeography, Palaeoclimatology, Palaeoecology*, 229(3), 179-186. Doi:10.1016/j.palaeo.2005.06.021
- Yan, G., Labonté, J.,M., Quigg, A., & Kaiser, K. (2020). Hurricanes accelerate dissolved organic carbon cycling in coastal ecosystems. *Frontiers in Marine Science*, doi:<https://doi.org/10.3389/fmars.2020.00248>
- Xie, X., Li, M., & Ni, W. (2018). Roles of wind-driven currents and surface waves in sediment resuspension and transport during a tropical storm. *Journal of Geophysical Research: Oceans*, 123(11), 8638–8654. <https://doi.org/10.1029/2018jc014104>

## APPENDIX A: L<sub>8</sub>, V, S and C Concentrations

*Mean L<sub>8</sub>, vanillyl, syringyl and cinnamyl phenol concentrations and their standard deviations in 2018 estuarine and coastal stations.*

*n.d. indicates that a phenol is non-detectable, thus there are no possible V, S or C values.*

Station ID	L <sub>8</sub> (mg/g)	V (mg/g)	S (mg/g)	C (mg/g)
GSPS-18 Station 1	(5.94 ± 0.89)	(1.70 ± 0.25)	(1.69 ± 0.25)	(2.55 ± 0.38)
GSPS-18 Station 2	(31.48 ± 4.72)	(10.65 ± 1.60)	(10.81 ± 1.62)	(10.03 ± 1.50)
GSPS-18 Station 3	(25.85 ± 3.88)	(9.32 ± 1.40)	(9.31 ± 1.40)	(7.21 ± 1.08)
GSPS-18 Station 4	(2.49 ± 0.37)	(1.00 ± .015)	(0.71 ± 0.10)	(0.80 ± 0.12)
GSPS-18 Station 5	(11.51 ± 1.73)	(4.51 ± 0.68)	(3.44 ± 0.52)	(3.56 ± 0.53)
GSPS-18 Station 6	<i>n.d.</i>	<i>n.d.</i>	<i>n.d.</i>	<i>n.d.</i>
GSPS-18 Station 7	(0.09 ± 0.01)	(0.09 ± 0.01)	<i>n.d.</i>	<i>n.d.</i>
GSPS-18 Station 8	(0.72 ± 0.11)	(0.55 ± 0.08)	<i>n.d.</i>	(0.17 ± 0.03)
GSPS-18 Station 9	(11.32 ± 1.70)	(5.91 ± 0.89)	(3.57 ± 0.54)	(1.82 ± 0.27)
GSPS-18 Station 10	<i>n.d.</i>	<i>n.d.</i>	<i>n.d.</i>	<i>n.d.</i>
GSPS-18 Station 11	(138.74 ± 20.81)	(35.66 ± 5.35)	(41.23 ± 6.20)	(61.76 ± 9.26)
GSPS-18 Station 12	(0.41 ± 0.06)	(0.41 ± 0.06)	<i>n.d.</i>	<i>n.d.</i>
GSPS-18 Station 13	<i>n.d.</i>	<i>n.d.</i>	<i>n.d.</i>	<i>n.d.</i>
GSPS-18 Station 14	(0.33 ± 0.05)	(0.25 ± 0.04)	(0.08 ± 0.01)	<i>n.d.</i>
GSPS-18 Station 50	(53.23 ± 7.98)	(19.33 ± 2.90)	(15.15 ± 2.27)	(18.75 ± 2.81)
GSPS-18 Station 51	(4.17 ± 0.63)	(2.73 ± 0.41)	(0.24 ± 0.04)	(1.20 ± 0.18)
GSPS-18 Station 52	<i>n.d.</i>	<i>n.d.</i>	<i>n.d.</i>	<i>n.d.</i>
GSPS-18 Station 53	<i>n.d.</i>	<i>n.d.</i>	<i>n.d.</i>	<i>n.d.</i>
GSPS-18 Station 54	(0.29 ± 0.04)	(0.29 ± 0.04)	<i>n.d.</i>	<i>n.d.</i>
GSPS-18 Station 55	(0.27 ± 0.04)	(0.27 ± 0.04)	<i>n.d.</i>	<i>n.d.</i>

*Mean L<sub>8</sub>, vanillyl, syringyl and cinnamyl phenol concentrations and their standard deviations in 2019 estuarine and coastal stations.*

\*Insufficient water available for chemical analyses at Station 103.

Station ID	L <sub>8</sub> (mg/g)	V (mg/g)	S (mg/g)	C (mg/g)
GSPS-19 Station 100	(0.03 ± 0.005)	(0.013 ± 0.00)	(0.009 ± 0.00)	(0.01 ± 0.00)
GSPS-19 Station 101	(0.23 ± 0.034)	(0.15 ± 0.02)	(0.03 ± 0.00)	(0.04 ± 0.01)
GSPS-19 Station 102	(0.17 ± 0.026)	(0.09 ± 0.01)	(0.03 ± 0.00)	(0.05 ± 0.01)
GSPS-19 Station 103*	-	-	-	-
GSPS-19 Station 104	(0.12 ± 0.018)	(0.04 ± 0.01)	(0.04 ± 0.01)	(0.05 ± 0.01)
GSPS-19 Station 105	(0.16 ± 0.02)	(0.06 ± 0.01)	(0.05 ± 0.01)	(0.06 ± 0.01)
GSPS-19 Station 106	(0.61 ± 0.09)	(0.43 ± 0.06)	(0.04 ± 0.01)	(0.14 ± 0.02)
GSPS-19 Station 107	(0.06 ± 0.01)	(0.03 ± 0.00)	(0.01 ± 0.00)	(0.02 ± 0.00)
GSPS-19 Station 108	(0.21 ± 0.03)	(0.10 ± 0.02)	(0.05 ± 0.01)	(0.06 ± 0.01)
GSPS-19 Station 109	(0.60 ± 0.09)	(0.19 ± 0.03)	(0.25 ± 0.04)	(0.16 ± 0.02)
GSPS-19 Station 110	(1.20 ± 0.18)	(0.69 ± 0.10)	(0.27 ± 0.04)	(0.24 ± 0.03)

## APPENDIX B: Sample Filtration Data

*Total suspended sediment mass in 2018 water samples (1.5  $\mu\text{m}$  filter nominal pore size cutoff).*

Station ID	Replicate	Filter Tare Wt. (g)	Volume Filtered (mL)	Total Mass of Filter (g)	Mass of TSS (g)
1	A	0.0968	530	0.1104	0.0136
1	B	0.0982	530	0.1110	0.0128
1	C	0.0964	545	0.1099	0.0135
1	D	0.0962	550	0.1090	0.0128
1	E	0.0969	540	0.1092	0.0123
2	A	0.0978	545	0.1066	0.0088
2	B	0.0971	550	0.1102	0.0131
2	C	0.0987	540	0.1115	0.0128
2	D	0.0983	545	0.1104	0.0121
2	E	0.0956	550	0.1069	0.0113
3	A	0.0971	545	0.1075	0.0104
3	B	0.0967	550	0.1057	0.009
3	C	0.0966	545	0.1046	0.008
3	D	0.0958	550	0.1051	0.0093
3	E	0.0960	545	0.1051	0.0091
4	A	0.0969	545	0.1046	0.0077
4	B	0.096	545	0.1030	0.007
4	C	0.0961	545	0.1035	0.0074
4	D	0.0955	545	0.1036	0.0081
4	E	0.0974	500	0.1052	0.0078
5	A	0.0958	550	0.1089	0.0131
5	B	0.0958	545	0.1077	0.0119
5	C	0.0968	545	0.1097	0.0129
5	D	0.0945	545	0.1058	0.0113
5	E	0.0969	545	0.1094	0.0125
6	A	0.0953	550	0.1101	0.0148
6	B	0.0968	540	0.1125	0.0157
6	C	0.0959	545	0.1118	0.0159
6	D	0.0952	540	0.1109	0.0157
6	E	0.0980	545	0.1133	0.0153
7	A	0.0979	538	0.1198	0.0219
7	B	0.0967	540	0.1168	0.0201
7	C	0.0957	540	0.1147	0.019
7	D	0.0953	545	0.1149	0.0196
7	E	0.0970	548	0.1158	0.0188
8	A	0.0975	535	0.1067	0.0092
8	B	0.0968	540	0.1062	0.0094
8	C	0.0953	545	0.1051	0.0098

8	D	0.0960	545	0.1064	0.0104
8	E	0.0977	542	0.1083	0.0106
9	A	0.0958	540	0.1052	0.0094
9	B	0.0962	542	0.1048	0.0086
9	C	0.0964	545	0.1048	0.0084
9	D	0.0970	540	0.1056	0.0086
9	E	0.0972	540	0.1046	0.0074
10	A	0.0961	1075	0.1132	0.0171
10	B	0.0973	1065	0.1135	0.0162
10	C	0.0966	1070	0.1127	0.0161
10	D	0.0974	1075	0.1142	0.0168
11	A	0.0965	1015	0.1125	0.0160
11	B	0.0961	1067	0.1137	0.0176
11	C	0.0959	1060	0.1125	0.0166
11	D	0.0961	1075	0.1120	0.0159
12	A	0.0971	1075	0.1128	0.0157
12	B	0.0968	1075	0.1152	0.0184
12	C	0.0978	1080	0.1162	0.0184
12	D	0.0973	1065	0.1141	0.0168
13	A	0.0968	1085	0.1136	0.0168
13	B	0.0974	1082	0.1137	0.0163
13	C	0.0982	1090	0.1143	0.0161
13	D	0.0974	1075	0.1132	0.0158
14	A	0.0952	1090	0.1114	0.0162
14	B	0.0951	1080	0.1116	0.0165
14	C	0.0963	1050	0.1133	0.0170
14	D	0.0970	1040	0.1117	0.0147
50	A	0.0956	505	0.1030	0.0074
50	A	0.0958	555	0.1046	0.0088
50	B	0.0976	560	0.1062	0.0086
50	B	0.0990	506	0.1052	0.0062
50	C	0.0970	458	0.1041	0.0071
50	C	0.0971	570	0.1060	0.0089
50	C	0.0977	35	0.1006	0.0029
51	A	0.0965	413	0.1064	0.0099
51	A	0.0966	587	0.1073	0.0107
51	B	0.0957	408	0.1039	0.0082
51	B	0.0974	377	0.1060	0.0086
51	B	0.0973	287	0.1046	0.0073
51	C	0.0978	245	0.1033	0.0055
51	C	0.0978	300	0.1028	0.0050
51	C	0.0978	333	0.1034	0.0056
51	C	0.0976	167	0.1017	0.0041
52	A	0.0973	1567	0.1152	0.0179
52	A	0.0966	360	0.1132	0.0166

52	B	0.0970	2010	0.1131	0.0161
52	C	0.0980	1955	0.1162	0.0182
52	D	0.0964	2085	0.1148	0.0184
53	A	0.0952	2160	0.113	0.0178
53	B	0.0972	2135	0.1151	0.0179
53	C	0.0964	2210	0.1132	0.0168
53	D	0.0968	2160	0.1146	0.0178
54	A	0.0959	1900	0.1125	0.0166
54	B	0.0971	2110	0.1063	0.0092
54	C	0.0966	120	0.1107	0.0141
54	D	0.0968	1760	0.1125	0.0157
55	A	0.0959	1077	0.1046	0.0087
55	B	0.0976	1075	0.1160	0.0184
55	C	0.0967	1070	0.1113	0.0146

---

*Total suspended sediment mass in 2018 water samples (0.7  $\mu\text{m}$  filters).*

Station ID	Replicate	Filter Tare Wt. (g)	Volume Filtered (mL)	Total Mass of Filter (g)	Mass of TSS (g)
1	A	0.1302	505	0.1457	0.0155
1	B	0.1302	505	0.1455	0.0153
1	C	0.1284	510	0.1436	0.0152
1	D	0.1297	505	0.1449	0.0152
1	E	0.1310	510	0.1439	0.0129
2	A	0.1304	502	0.1415	0.0111
2	B	0.1304	503	0.1417	0.0113
2	C	0.1319	505	0.1440	0.0121
2	D	0.1319	497	0.1436	0.0117
2	E	0.1334	500	0.1468	0.0134
3	A	0.1296	505	0.1368	0.0072
3	B	0.1302	505	0.1377	0.0075
3	C	0.1287	460	0.1370	0.0083
3	D	0.1302	520	0.1368	0.0066
3	E	0.1301	504	0.1383	0.0082
4	A	0.1314	512	0.1408	0.0094
4	B	0.1324	505	0.1416	0.0092
4	C	0.1304	518	0.1391	0.0087
4	D	0.1298	504	0.1385	0.0087
4	E	0.1289	510	0.1371	0.0082
5	A	0.1312	520	0.1462	0.0150
5	B	0.1321	515	0.1467	0.0146
5	C	0.1312	517	0.1433	0.0121
5	D	0.1295	513	0.1412	0.0117
5	E	0.1327	518	0.1470	0.0143
6	A	0.1306	510	0.1472	0.0166
6	B	0.1309	510	0.1486	0.0177
6	C	0.1297	500	0.1485	0.0188
6	D	0.1306	504	0.1515	0.0209
6	E	0.1308	515	0.1534	0.0226
7	A	0.1306	502	0.1484	0.0178
7	B	0.1291	500	0.1466	0.0175
7	C	0.1301	520	0.1477	0.0176
7	D	0.1297	540	0.1467	0.0170
7	E	0.1306	525	0.1472	0.0166
8	A	0.1287	503	0.1374	0.0087
8	B	0.1273	508	0.1358	0.0085
8	C	0.1252	512	0.1332	0.0080
8	D	0.1256	512	0.1344	0.0088
8	E	0.1248	511	0.1327	0.0079
9	A	0.1283	499	0.1326	0.0043

9	B	0.1272	480	0.1316	0.0044
9	C	0.1276	511	0.1314	0.0038
9	D	0.1269	500	0.1309	0.004
9	E	0.1283	513	0.132	0.0037
10	A	0.1295	1040	0.1498	0.0203
10	B	0.1309	1040	0.1513	0.0204
10	C	0.1296	1030	0.1532	0.0236
10	D	0.1327	1035	0.1573	0.0246
11	A	0.1298	1010	0.1534	0.0236
11	B	0.1333	1015	0.1586	0.0253
11	C	0.1322	1030	0.1573	0.0251
11	D	0.1346	1040	0.1586	0.024
12	A	0.1305	1035	0.1572	0.0267
12	B	0.1297	1040	0.1527	0.023
12	C	0.1295	1020	0.1534	0.0239
12	D	0.1314	1040	0.155	0.0236
13	A	0.1311	1045	0.1549	0.0238
13	B	0.1306	1035	0.1536	0.023
13	C	0.1301	1060	0.151	0.0209
13	D	0.1308	1050	0.1535	0.0227
14	A	0.1308	995	0.1501	0.0193
14	B	0.1308	1030	0.1567	0.0259
50	A	0.1293	1040	0.1332	0.0039
50	B	0.1313	1045	0.1348	0.0035
50	C	0.132	1040	0.1351	0.0031
51	A	0.1315	1040	0.1361	0.0046
51	B	0.1292	1030	0.1345	0.0053
51	C	0.1290	1040	0.1335	0.0045
52	A	0.1327	1927	0.1606	0.0279
52	B	0.1314	1867	0.1586	0.0272
52	C	0.1298	1890	0.1548	0.025
52	D	0.1291	2050	0.1546	0.0255
53	A	0.1306	2130	0.1559	0.0253
53	B	0.1318	2070	0.1567	0.0249
53	C	0.1329	2120	0.159	0.0261
53	D	0.1309	2055	0.1572	0.0263
54	A	0.1343	1775	0.1613	0.027
54	B	0.1311	2020	0.1541	0.023
54	C	0.1305	77	0.1444	0.0139
54	D	0.1327	1682	0.1562	0.0235
55	A	0.1323	1040	0.1535	0.0212
55	B	0.1298	1030	0.1478	0.018
55	C	0.1357	1030	0.1540	0.0183

---

*Total suspended sediment mass in 2019 water samples (0.7  $\mu\text{m}$  filters).*

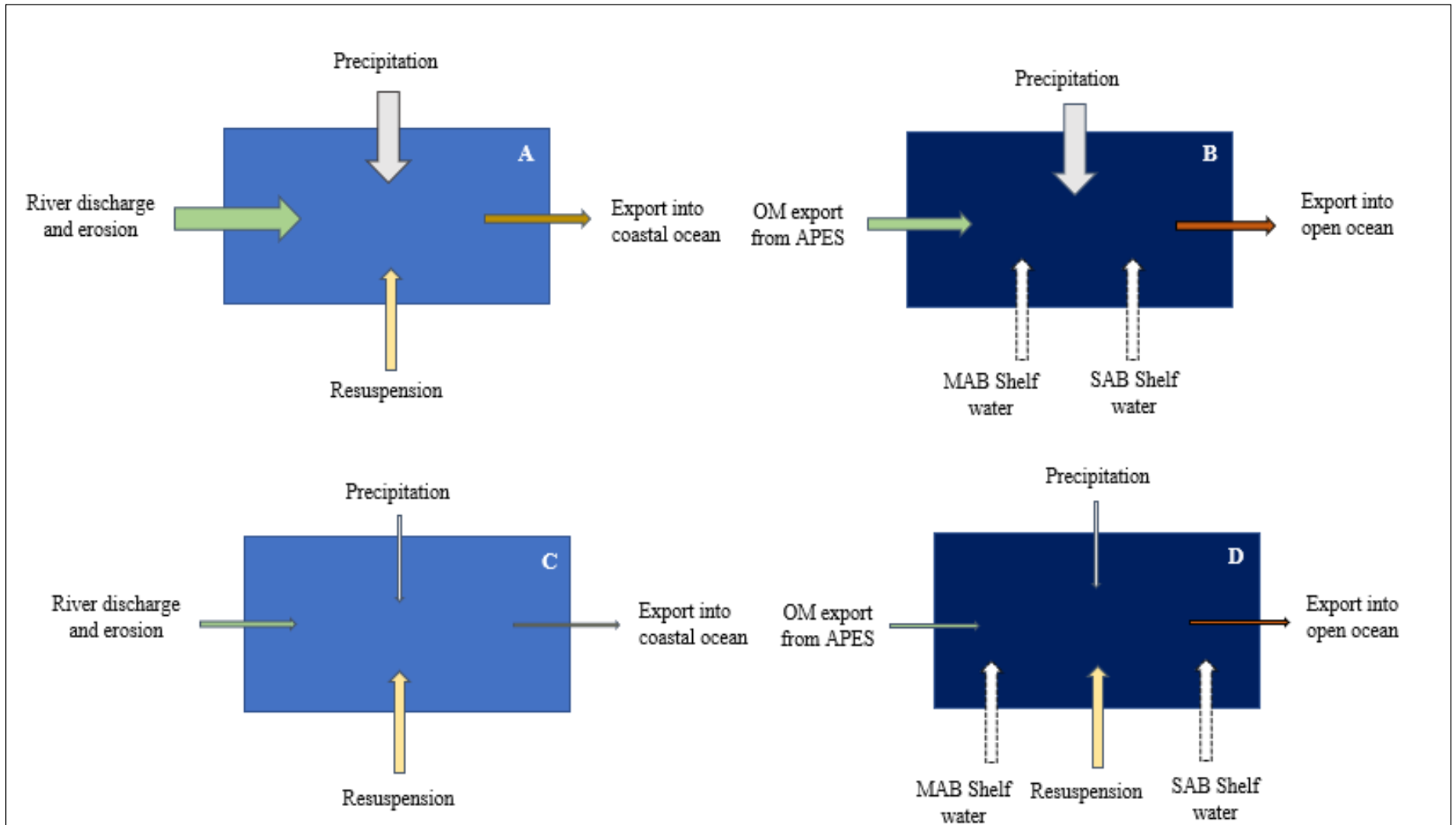
Station ID	Replicate	Filter Tare Wt. (g)	Volume Filtered (mL)	Total Mass of Filter (g)	Mass of TSS (g)
100	A	0.1305	1160	0.1549	0.0244
100	B	0.1282	1035	0.1513	0.0231
101	A	0.1319	975	0.1568	0.0249
101	B	0.1293	985	0.1479	0.0186
102	A	0.1305	1125	0.1544	0.0239
102	B	0.1300	1210	0.1509	0.0209
104	A	0.1310	1040	0.1514	0.0204
104	B	0.1306	1030	0.1538	0.0232
105	A	0.1311	675	0.1487	0.0176
105	A	0.1325	355	0.1475	0.01500
105	B	0.1316	500	0.1446	0.01300
105	B	0.1305	340	0.1448	0.0143
106	A	0.1298	900	0.1493	0.0195
106	B	0.1299	530	0.1481	0.0182
106	B	0.1307	610	0.1508	0.0201
107	A	0.1307	500	0.1451	0.0144
107	A	0.1312	575	0.1463	0.0151
107	B	0.1278	500	0.1421	0.0143
107	B	0.1314	570	0.1476	0.0162
108	A	0.1332	525	0.1458	0.0126
108	A	0.1312	705	0.1455	0.0143
108	B	0.1312	550	0.1427	0.0115
108	B	0.1302	690	0.1450	0.0148
109	A	0.1307	400	0.1439	0.0132
109	A	0.1312	430	0.1437	0.0125
109	A	0.1311	285	0.1441	0.0130
110	A	0.1322	285	0.1471	0.0149
110	A	0.1305	380	0.1405	0.0100
110	A	0.1301	345	0.1417	0.0116
110	B	0.1319	315	0.1417	0.0098
110	B	0.1301	270	0.1392	0.0091
110	B	0.1313	250	0.1402	0.0089
110	B	0.1311	225	0.1399	0.0088

## APPENDIX C: Percent Difference in Similar Stations

*The percent difference between salinity and TSS in 2018 and 2019 stations in similar locations. See Figure 8 for station locations.*

Nearby Stations		Salinity			TSS		
2018	2019	2018	2019	Percent Difference	2018	2019	Percent Difference
2	106	16.9	18.7	-10.9	45.1	29.7	34.2
3	107	11.7	15.9	-35.9	32.0	28.0	12.4
6	109	29.9	14.0	53.2	66.5	35.9	46.0
9	110	5.79	8.50	-46.8	23.8	36.0	-51.4
52	100	33.5	29.9	10.8	22.8	21.7	5.00
53	101	32.4	29.7	8.28	20.4	22.2	-9.03
54	102	31.4	29.8	5.16	20.9	19.3	7.67

## APPENDIX D: Conceptual Model



A conceptual model of the 2018 estuarine (A) and coastal (B) systems, and the 2019 estuarine (C) and coastal (D) systems. The 2018 samples are taken during a period of increased precipitation, whereas 2019 samples are taken during a relatively dry period. Discharge and erosion experienced during a storm are higher than during a dry period. The 2018 estuarine system had the highest lignin concentration, leaving more material available for export into the coastal ocean. The 2019 estuarine system had lower lignin concentrations leaving less material available for export. There are three instances of  $Ad/Al > 5$ , in image A, C and ending to possible resuspension of sediments. Mid- and South-Atlantic Bight waters may contribute to organic matter in coastal systems.

